2019 | VOLUME 46

Structural Integrity Associates, Inc.®

NEWS & VIEWS

1-877-4SI-POWER www.structint.com

Multi-discipline Solution for Pressure Vessel Asset Management 52

PlantTrack™
Engineering Insight Through Data

Plant Integrity Assistant – There's an App for That! 4

Delivering Value: Modernization of Plant Automation Controls 31

In-line Inspection Performance Validation Pipe Experiment 63

President's Corner

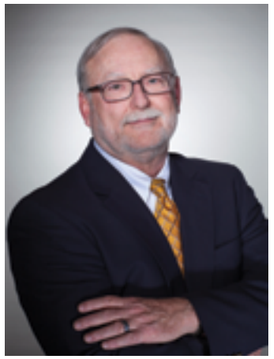

LANEY BISBEE
lbisbee@structint.com

After a significant number of Pres Corners, I sit here and wonder "what should I write about?" Which topics excite you? There is a lot happening in the world; more geopolitics and macro-economics than I care to elaborate on here. Technology is still changing so rapidly – smart watches, autonomous cars, rockets that go into space and return to earth landing upright (sometimes), folding money (as my father called it) or credit cards (my preferred payment method) are no longer required, just pass your watch over this; I love it, it's like being a character in the Jetsons! There's also a lot happening in our primary industry – electric utilities. And, there is a lot happening here at SI. All of these will or have the potential to have a huge impact on our personal and professional lives.

There's more than enough to write about but what is of most interest to our News & Views readers? Are you interested in learning more about --

- Our market and the impact of cheap world energy prices, increasingly more stringent environmental regulations, will solar and wind capacity continue to increase?
- Whether Yucca Mountain will reopen as our nuclear waste repository?
- Will SMRs get the same subsidies that wind and solar enjoyed?
- Will internet companies and distributed power models replace investor-owned and co-operative electric utilities?
- Will there be more nuclear plant shutdowns or more new nuclear construction projects once nuclear is deemed the penultimate carbon-free, renewable energy source?
- What's going to provide our base-load generation and what's going to cycle – nuclear, coal, HRSGs, renewables?
- What's the next industry generic issue – waste (nuclear, coal ash, emissions), concrete life predictions and optimization, critical structures' resiliency and integrity, or that cyber-security becomes so overwhelming that we go back to using rotary phones and typewriters with carbon paper (oops there's that bad word – carbon)?

Or are you more interested in what's happening at SI? Maybe you'd like to know more about our new integrated digital marketing capability or about our latest acquisition (a creep testing laboratory), new NDE testing technologies we've added, or that we have new leadership (welcome Darren Gale, new VP of our Nuclear operations). Maybe it's that we're the first to ever receive accreditation to provide seismic, wind, and blast certifications. It could be about our integrated digital solutions and technologies around sensors, monitoring, and test informed modeling. Or that you can now go to the Apple App store and download the SI PlantTrack application for free.

So much to choose! I welcome your feedback on what you are interested in and which subject(s) would be of most interest to you -- what would make you want to read the President's Corner as well as the rest of News & Views? It's hard for me to know what is on our readers' minds; however, from all the above, you can see some of what is on mine.

In this Issue

Plant Integrity Assistant – There's an App for That!

PlantTrack App now available

MATT FREEMAN
mfreeman@structint.com

Plant engineers must often answer 'what damage is this piece of equipment susceptible to, and what can we do about it?' or 'how much longer can this component continue operating'? A free app is now available in both the Google Play store and the Apple App store to help answer these and other equipment integrity questions (see figure 1).

The PlantTrack App is a plant integrity assistant that provides life calculators, damage mechanism guides, technical articles, lab sample submittal form, and other functions relevant for plant engineers. While it is geared towards fossil (both coal and gas) power plants, it has applicability for equipment at other plants as well. For subscribers to the PlantTrack web application, the mobile app also provides a dashboard view of inspection history, action items, damage tracking results, etc. Users of the PlantTrack software will recognize some of the features from the 'PlantTrack Tools' that have previously been available through a web browser.

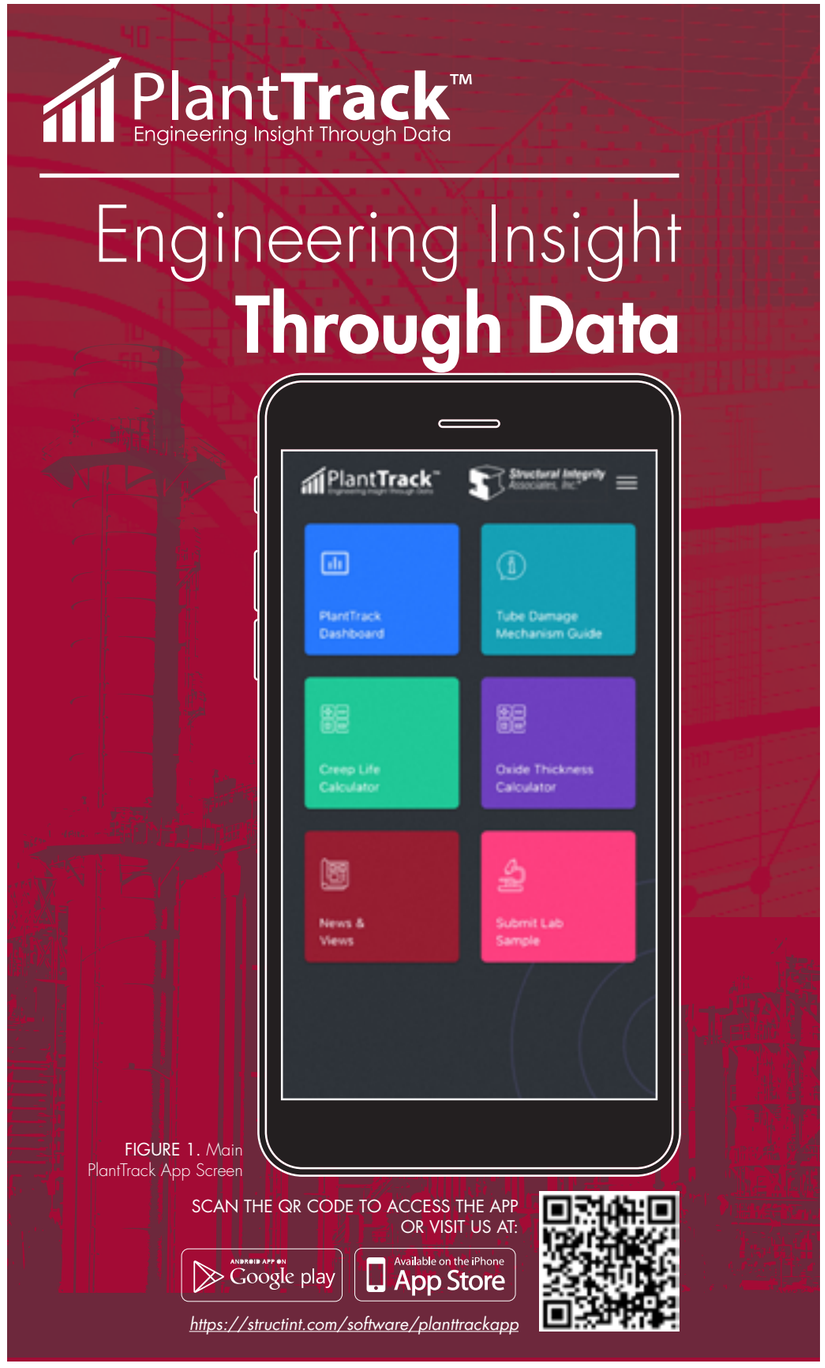

FIGURE 1. Main PlantTrack App Screen

Damage Mechanism Guide

The Tube Damage Mechanism Guide shown in figure 2 helps users identify what damage mechanisms are relevant for various components and materials and aids in identifying which damage mechanism may have caused a failure. Several early users of the application have commented this is a useful training tool for engineers and technicians to learn where and why various damage mechanisms occur, and what can be done to mitigate them. In this area of the app, the user is prompted to enter boiler type (e.g. HRSG or Conventional Boiler), fuel being burned, region of boiler/HRSG, metallurgy, and failure feature (e.g. pin hole, fishmouth, etc.). Based on the input, the app narrows the list of damage mechanisms to only display those that are relevant. The user can then select any of the remaining mechanisms to learn more about what it is caused by, where and when it is most likely to occur, and what corrective actions can be taken. Sample images are provided as well.

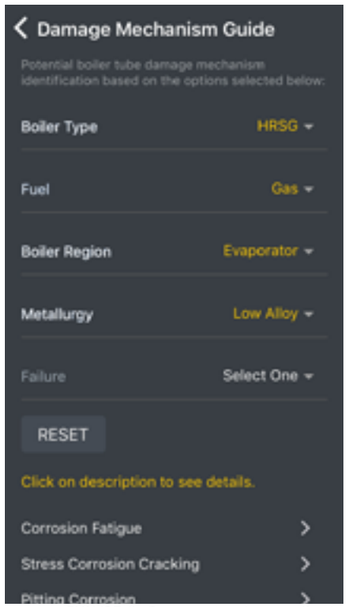

FIGURE 2. Damage Mechanism Guide

Use the PlantTrack app to request a lab analysis and receive a free tumbler! Submit photos and details of desired analysis through the app and if SI is awarded the analysis work, we'll send an SI branded Tumbler (or similar) with the analysis results. Quantities are limited, but anticipated to last through September 2019.

Calculators

Two calculators are included in the initial release of the app: Creep Life, and Oxide to Temperature, and are shown in figure 3. The creep life calculator works for tubes and pipes and the user must choose the material and enter diameter, wall thickness, pressure, and temperature. The result will be an estimated number of hours of remaining life assuming that all parameters remain constant. The calculation is based on typical hoop stress, and while heat flux and oxide are not considered, the calculator still provides a rough approximation of the number of hours the component can be expected to remain in service or provide a relative value to be used in planning inspections.

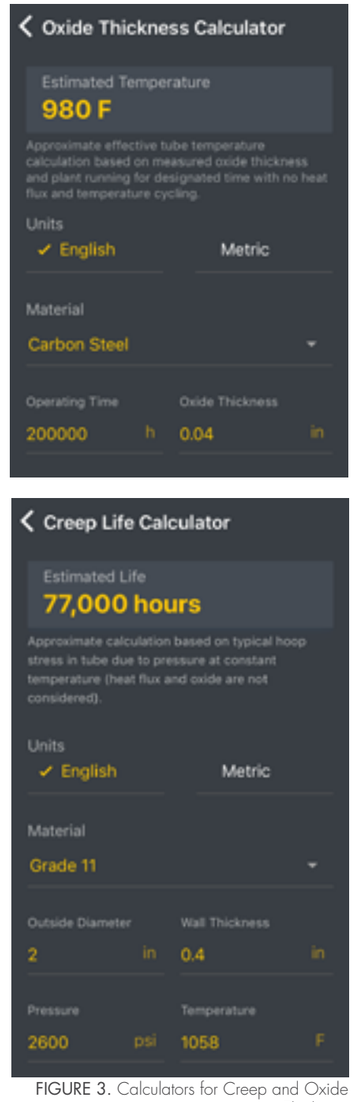

FIGURE 3. Calculators for Creep and Oxide Thickness

Continued on next page

The Oxide to Temperature calculator provides an approximate effective tube temperature based on oxide thickness measurements. The user must choose the material, enter the number of hours the tube has been in service and the oxide scale measurement. The calculator then outputs the estimated temperature the tube has been operating at for the oxides to achieve the thickness specified. This is beneficial for predicting tube failures and/or identifying where design or operating changes may be warranted.

Lab Sample Submittal

The app also facilitates transmitting information to SI's metallurgical lab when a lab analysis is needed. As shown in figure 4, The user inputs the plant, unit, component, and other information that may be known as well as details on whether a failure analysis or condition assessment is needed. Photos can be taken directly from the phone/tablet and files attached as well. When the user is ready, a click of a button sends all the relevant information to the lab as an email. The lab personnel then have details necessary to provide a consultation, a proposal, and/or prepare for receipt of a sample for analysis.

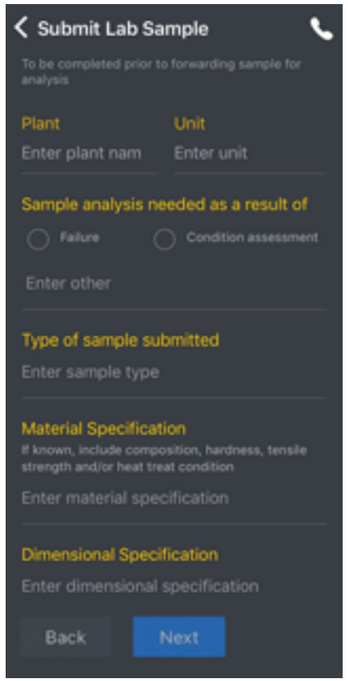

FIGURE 4. Lab Sample Submittal Form

PlantTrack Dashboard

Subscribers to the PlantTrack web application can also use the app to access a dashboard displaying information regarding equipment inspections (both planned and completed), online continuous life calculators, and design information. As shown in figure 5, Some of the information is presented in tiles showing the number of items that require action in the short and long term. The user can then select the tile of interest to drill down to access more details. Alerts are shown for any locations being monitored that have exceeded a user-defined threshold, such as rate of life consumption or number of impingement/pooling events caused by the attemperator.

News and Views

Twice a year, Structural Integrity highlights significant energy industry experience, developments and breakthroughs in the News & Views newsletter. These articles provide technical details for many of the issues that impact the lifecycle of equipment and are often provided as case studies. The app provides a link to articles in the most recent issue, and from there the user can search for older articles as well.

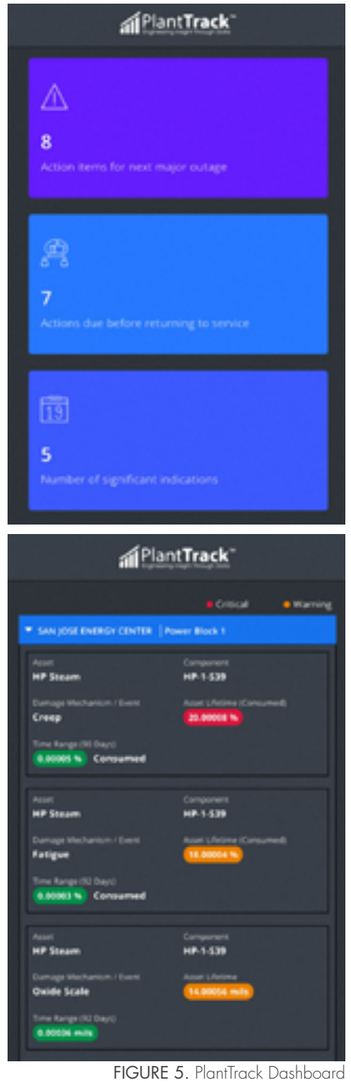

FIGURE 5. PlantTrack Dashboard

Hydrogen Fueling Structural Integrity into New Markets

DANIEL PETERS
dpeters@structint.com

MYLES PARR
mparr@structint.com

Energy sources that don't have carbon emissions are rapidly developing in the country and around the world today. The use of renewable energy sources such as wind, hydro, and solar is becoming increasingly common. One area that is also changing is in the automotive arena. The use of alternative fuels in the transportation sector, such as natural gas and hydrogen, has been under development for many years. Natural gas is quite common today in the public transportation sector in many cities for fueling buses in cities.

Development of hydrogen fuel cell automobiles increased significantly around the turn of the century and recently has gained increasing popularity. Many hurdles have been considered and needed to be overcome to make this a practical reality. Issues such as reliability of components used in cars, risks of fires due to leaks, and sources of hydrogen needed for those cars are just a few of them.

Certain parts of the US are encouraging the use of hydrogen fuel cell cars. In January 2004, the governor of the State of California made a recommendation in the Governor's State of the Union address that State funding be made available for fueling stations and vehicle incentives. California passed a bill in February of 2018 to allocate $20 million annually until there are at least 100 publicly available hydrogen-fueling stations in the state. The intent of this would be to have a complete infrastructure of fueling stations in place by 2020.

Companies have been developing various concepts for the manufacturing of ground storage steel pressure vessels designed to approximately 15,000 psi. One of the key concepts in their manufacture includes maximizing the life of the vessels using some traditional pre-stressing techniques such as autofrettage. Some companies have been attempting to sell vessels in this market using ASME Section VIII Division 1 design standards and stating that the potential for fatigue failure is negligible. Currently, ASME Section VIII Division 3 (ASME VIII-3) is the only pressure vessel construction Code within ASME to include rules for construction in hydrogen environments.

Rules were added to the ASME VIII-3 code to describe the additional testing that would be required for the manufacture of these vessels. This included testing to validate information such as the crack growth rate in a hydrogen environment for materials used in manufacture of the vessels. It was determined that additional testing should be performed for the threshold stress intensity above which time dependent crack growth would occur in a hydrogen environment (K_{IH}). This type of testing is extremely specialized and takes a significant amount of time to perform. Testing has been performed by several US National Laboratories and internationally by several steel companies.

Continued on next page

This data has been compiled and has established the basis for the recently approved ASME Code Case 2938 for use with ASME VIII-3.

Issues with the Cylinders

The main concern with the cylinders centers around the cyclic life of the cylinders. Traditionally, many natural gas cylinders operate at pressures considered to be below the "endurance limit" for the cylinders giving them theoretically infinite life.

In contrast, hydrogen storage cylinders operate at high enough pressures that infinite life is impossible to achieve. ASME VIII-3 requires that the cylinders be designed using fracture mechanics-based life assessment. Additionally, ASME requires that testing be performed for use of specific grades and alloys of materials for use in high pressure hydrogen environments. This includes testing for increased cyclic crack growth rates due to the hydrogen, and testing for the limit above which time dependent crack growth due to exposure to hydrogen will occur. The design will then use the crack growth rates in a life assessment to determine the life of the equipment, which will be limited to prevent any time dependent crack growth.

The testing in high pressure hydrogen is very expensive and there are only a limited number of labs around the world that can perform this type of testing. ASME was able to leverage testing done to date to develop Code Case 2938 for hydrogen crack growth for common materials. Figure 1 shows a comparison of the rate of crack growth in hydrogen versus the traditional air curves. It which shows that the rate of crack growth in hydrogen is greatly accelerated compared to that in air. Additionally, the "R" ratio, shows the effect of the "mean" or average stress within a cyclic range. In other words, the rate of crack growth increases significantly as the mean stress increases.

SI has been able to work in designing cylinders to improve the life of the cylinders based on these effects for many of our clients. The one effect that is leveraged is to lower the mean stress using techniques such as autofrettage. Autofrettage is a technique that induces favorable residual stresses into a component to extend the life of the component. In pressure vessels, this is commonly achieved using pressurization to extreme pressures to cause plasticity in the bore of cylinders. Figure 2A shows the resultant residual stresses in a cylinder after such a procedure. The "hoop" stress at the bore is left in a compressive residual stress state after yielding. The operational pressure stress in the wall (Figure 2B), when added to the residual "hoop" stress will result in the same "range" of pressure ($\Delta\sigma$) but with a lower mean stress. In doing so, the life will be increased because part of the crack growth life calculated will have the crack in compression.

Ground storage tanks for automotive fueling do not return to ambient pressure frequently. Cars generally have onboard fueling tanks that have pressure ranges between 5,000 and 8,000 psi. The ground storage tanks for fueling are typically around 13,000 psi when full and emptied to around 8,000 to 10,000 psi during operation. This varies based on many factors.

The lives of these vessels, as discussed previously are very dependent on the pressure range that the vessels cycle between, and the level of autofrettage in the vessel. Figure 3 shows a comparison of a typical autofrettaged vessel when cycled between a "full" condition and a lower pressure (shown as a % of the design pressure). It is typically expected that the larger the range, the lower the cycle life, even in autofrettaged cylinders. This is not entirely the case when calculating the life in a hydrogen environment. The test data, which was for tests performed in hydrogen, did not include any data where the flaws are in compression. Due to that fact, if a vessel can be designed for hydrogen with as much of the range as possible in the compressive regime, significant advantages in life can be achieved as shown in Figure 4.

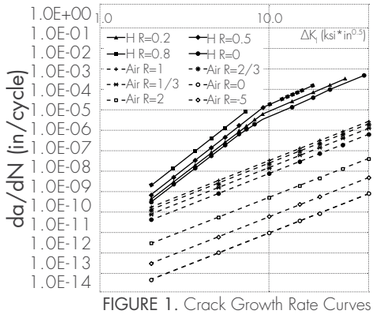

FIGURE 1. Crack Growth Rate Curves

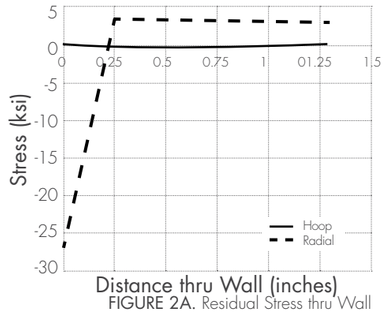

FIGURE 2A. Residual Stress thru Wall

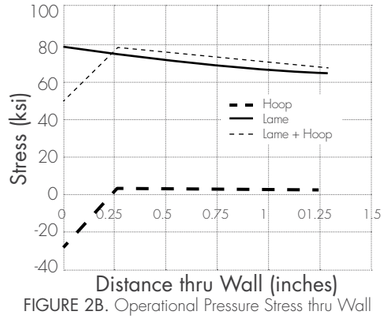

FIGURE 2B. Operational Pressure Stress thru Wall

Additionally, the life predictions show that when the lower end of the pressure cycle for this cylinder is below 40%, the life is constant. This is due to an incomplete data set upon which the Code Case was based. The cyclic ranges were not performed considering the cracks in the compressive regime. SI continues to work through ASME with the national laboratories to encourage more testing in this regime, which could give more realistic predictions on life and maximize the time between in-service inspections.

Performing autofrettage involves significantly high pressures and can result in degraded material properties due to issues such as the Bauschinger effect. Some designs attempt to achieve similar results by other means.

SI has worked with many cylinder manufacturers both in hydrogen and other industries to maximize the life of high-pressure cylinders and other equipment for many years by designing using autofrettage. Maximizing the predicted life in cylinders is a function not only of the autofrettage pressure, prestress conditions in the vessel, material properties, degradation effects due to hydrogen or other contained fluids and gases, but also involves a complete understanding of the interaction of these properties to get the most out of a design. Structural Integrity has a team focused on maximizing the life of your equipment and stretching those in-service expenses.

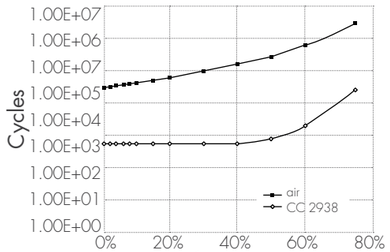

FIGURE 3. Cycles per Design Pressure Range IN Air and Hydrogen

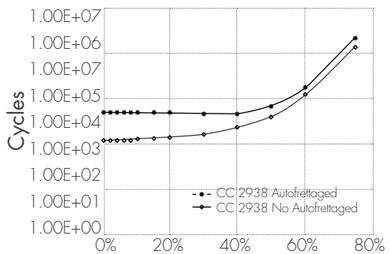

FIGURE 4. Cycles per Design Pressure Range in Hydrogen with and without Autofrettage

NDE Best Practices for Generator Rotors

PAUL ZAYICEK
pzayicek@structint.com

Three factors typically drive inspection intervals of generator rotors:

1. a timeframe recommended by the insurance carrier or OEM
2. an engineering evaluation that supports a different inspection interval due to service operation events or existing rotor damage
3. industry best practices

Drivers from the OEM include issues defined in service bulletins or technical information letters that pertain to the entire fleet or some subset of the population. Intervals based on engineering evaluations can be derived from an identified damage mechanism with the rotor or with a critical component. An engineering evaluation can also provide for extended inspection intervals in situations where the generator has no inherent material issues, has a clean inspection record, and sees limited operational stress such as in a base-load unit. Regardless of the approach followed, one of the inputs for determining generator rotor operability and inspection interval is a comprehensive nondestructive examination (NDE). The objective of NDE is to identify the state of current damage in the component, which then informs future actions such as inspection intervals, repairs, and replacements.

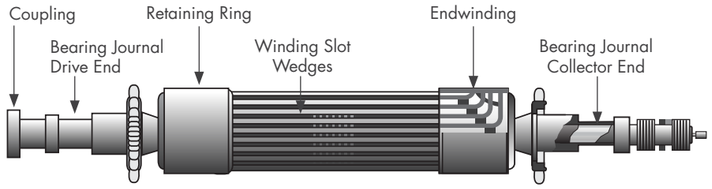

FIGURE 1. Major area of interest for generator rotor inspection

The objective of NDE is to identify the state of current damage in the component, which then informs future actions such as inspection intervals, repairs, and replacements.

For generator rotors, NDE is performed in several critical areas prone to various damage mechanisms, as shown in Figure 1. The following sections highlight several damage mechanisms and the NDE techniques used to inspect for the presence of damage.

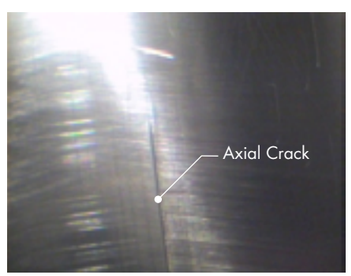

FIGURE 2. Rotor Bore Radial-Axial Crack

Rotor Forging

The rotor forging is inspected during major outages with the rotor out of the stator. Generator rotors with a central bore hole undergo a boresonic inspection for the detection of surface flaws on the main bore and subsurface flaws in the near bore region. Primary flaws of interest in the bore are radial axial in orientation, due to bore stress, and material manufacturing inclusions.

The main bore surface is inspected with eddy current probes, with coincident inspection of the near bore region with multiple ultrasonic probes. Radial-axial flaws (Figure 2) are detected with probes oriented in the clockwise and counterclockwise

Continued on next page

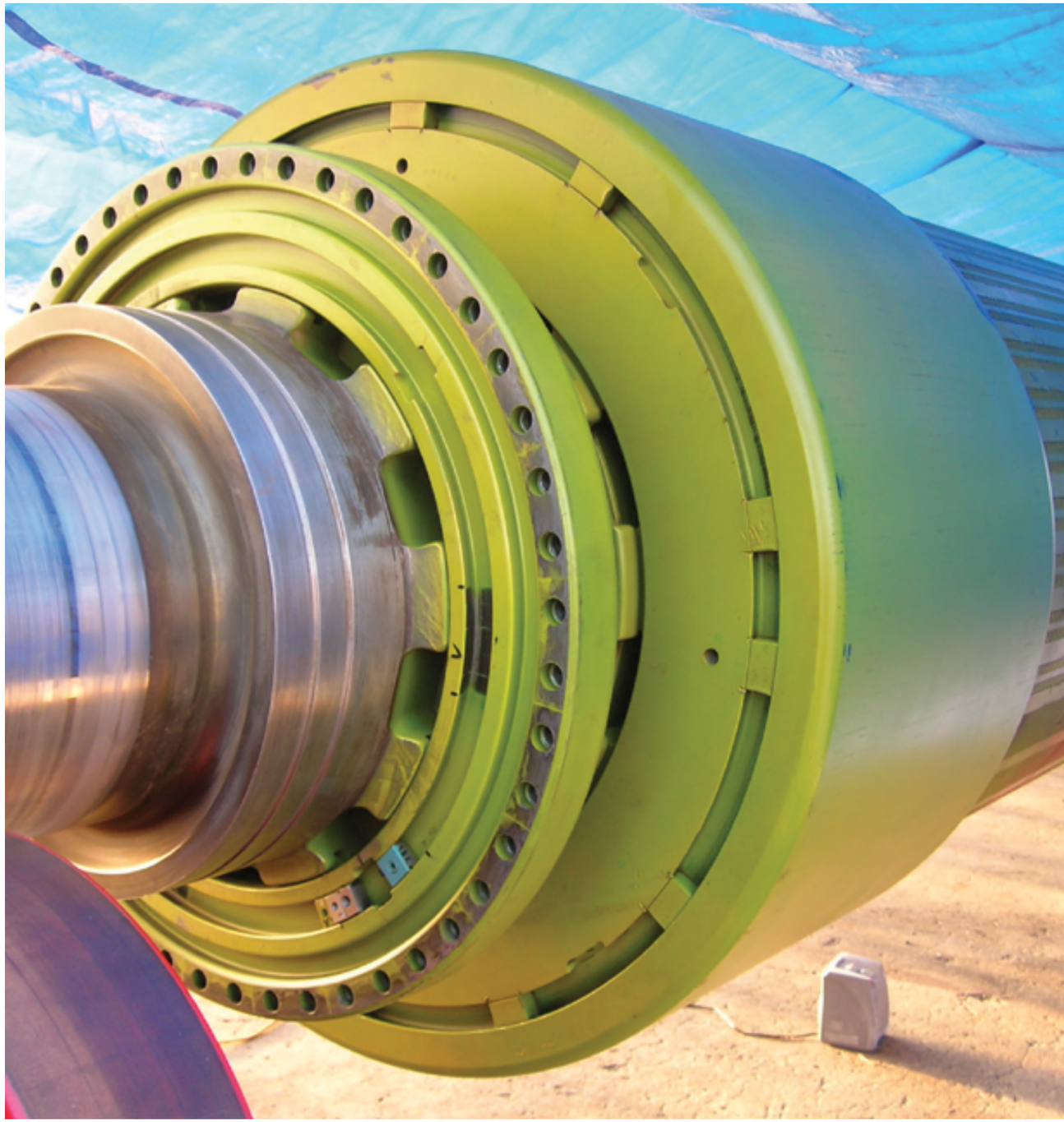

directions. A probe looking in the radial direction identifies nonmetallic material inclusions from the manufacturing process.

After the boresonic inspection (Figure 3), the inspector will run a "link-up," or similar algorithm, of the boresonic indications to see if there is potential for flaws to linkup in the radial-axial plane. This information **becomes one of the inputs for a rotor engineering assessment using EPRI SAFER-PC or other similar analysis packages.**

As in the main bore, we also want to detect/size radial-axial flaws and nonmetallic inclusions in the collector bore. Unlike the main bore, the collector bore contains electrical components, including radial leads and bore copper that must be removed to allow access for honing and inspection. At the completion of the ultrasonic and eddy current inspection of the collector bore, the electrical components are re-installed. Since the collector section of the rotor is much smaller in diameter than the main body of the rotor, it is also feasible to perform a volumetric inspection from the OD surface due to the relatively short metal path. Being able to inspect from the OD surface means that the electrical components in the collector bore do not need to be removed, as would be required for an inspection from the collector bore surface, saving the owner time and money. Also, the collector bore, due to its smaller diameter, is at much lower stress (minimal loading) resulting in critical crack sizes much deeper and longer than those in the main bore, making detection/sizing of the significant collector bore flaws from the OD surface even more feasible/justifiable. **Flaws that "linkup" in the radial-axial plane in the collector near-bore become one of the inputs for a rotor engineering assessment using EPRI SAFER-PC or other similar analysis packages.**

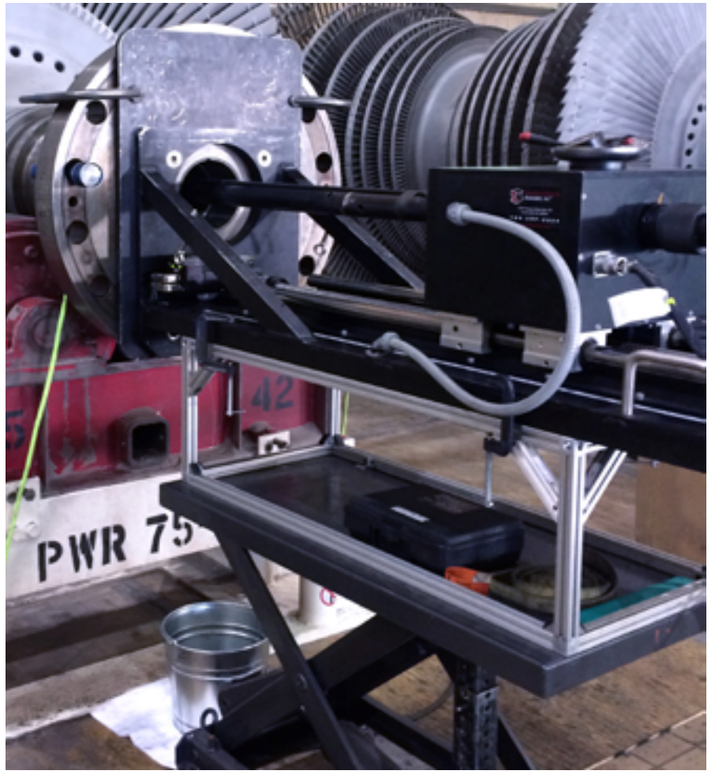

FIGURE 3. Boresonic inspection system mounted to the rotor for inspection of bore surface and near bore regions

Retaining Rings

Retaining rings are high strength ring forgings, typically a nonmagnetic 18Mn5Cr or 18Mn18Cr material, installed at either end of the generator rotor main body to support the rotor end turn windings, as shown in Figure 4. The retaining rings are installed on the rotor by an interference fit to the rotor body and with a crucial circumferential assembly at or near the interference fit region to prevent axial movement of the ring.

The 18Mn5Cr rings are susceptible to stress corrosion cracking. These rings are much less vulnerable to stress corrosion cracking but can still be damaged by grid events that result in arcing damage between the ring and rotor body or amortisseur winding, or, from fretting damage resulting from relative motion between the ring and the mating shrink-fit surface as a result of frequent load fluctuation/torsional oscillations. Arcing and fretting damage can initiate micro-cracking.

Retaining rings can be inspected with the rotor in the stator (with some disassembly of the stator housing) using a low-profile scanner with the rotor out of the stator on stands or power rollers. With the retaining rings fitted to the rotor, a Visual Inspection or Remote Visual Inspection of the ring OD surface and accessible ID surface areas identifies surface anomalies including corrosion. Ultrasonic inspections from the OD surface, in circumferential and axial directions, are used to interrogate the critical ID surfaces of the rings. The OD surface of the ring is also inspected with eddy current or with fluorescent liquid penetrant.

Basic ultrasonic detection scans are performed using a conventional, contact shear wave (S-wave) technique, implemented via a fully automated scanning and data acquisition system, as shown in Figure 5. This inspection provides four channels of pulse-echo S-wave interrogations (CW, CCW, axial fore, and axial aft) plus a 0-degree (radial) longitudinal wave inspection. While the pulse-echo tests are sufficient for the detection of cracks at the inner surface, many geometric reflectors are also detected in the shrink-fit region, and it can be difficult to positively discriminate between the two, depending upon the proximity of the flaw to geometric reflectors.

Time-of-flight diffraction (TOFD) a dual transducer ultrasonic technique that is used as a supplement to the pulse echo tests for positive discrimination between geometric reflectors and real flaws. TOFD is implemented as the second standard technique to improve detection reliability and enhance sizing accuracy, but not as a stand-alone inspection technique. Mode converted longitudinal wave inspection is applied as needed for characterization of flaws. **Other techniques, such as, linear and annular phased array ultrasonic techniques, can be implemented as needed to aid in flaw discrimination and proper classification.**

Retaining rings that are inspected while installed on the rotor are in tensile stress (shrink-fit). In this state, surface cracks are open, allowing detection with ultrasonic inspection or penetrant inspection. Retaining rings can also be inspected with the rings removed from the rotor. However, free-standing rings revert to a compressive residual stress condition allowing cracks to close. Ultrasonic inspection becomes less effective as energy passes across the gap, decreasing the detectability of the crack. Penetrant inspection becomes less effective as the crack closes, inhibiting capillary action of the penetrant, resulting in a lack of sensitivity and low reliability. Eddy current inspection relies on changes in magnetic permeability and/or conductivity to detect flaws. Even with the ring in a compressive state, oxide on crack surfaces is detectable with eddy current, making it the preferred inspection technique of ID and OD surfaces of the rings when rings are removed from the rotor.

Continued on next page

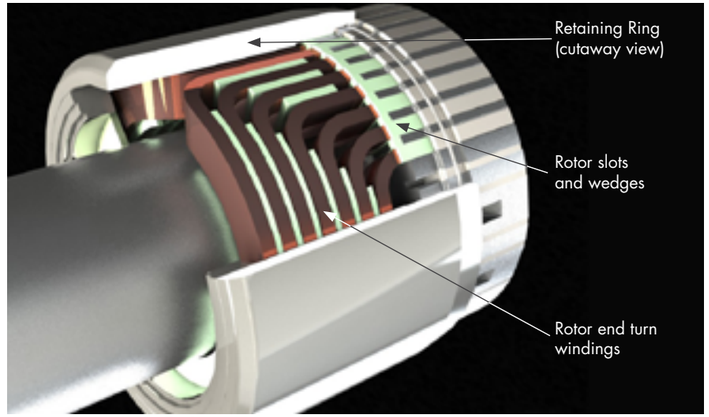

FIGURE 4. Schematic of retaining ring showing rotor end turn windings contained by the retaining ring as they emerge from the slots of the main body.

FIGURE 5. BELOW Automated scanner with ultrasonic inspection of the retaining ring with the rotor removed from the stator.

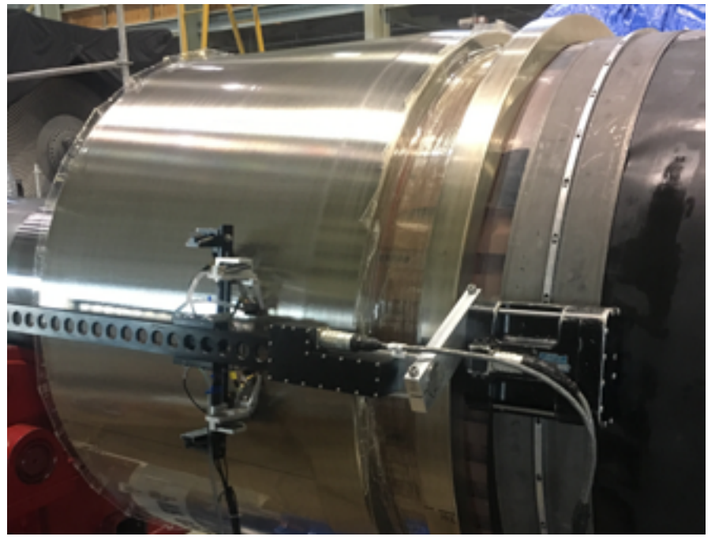

FIGURE 6. Scanning fixture and probe for eddy current inspection of dovetail crush surface with wedges removed

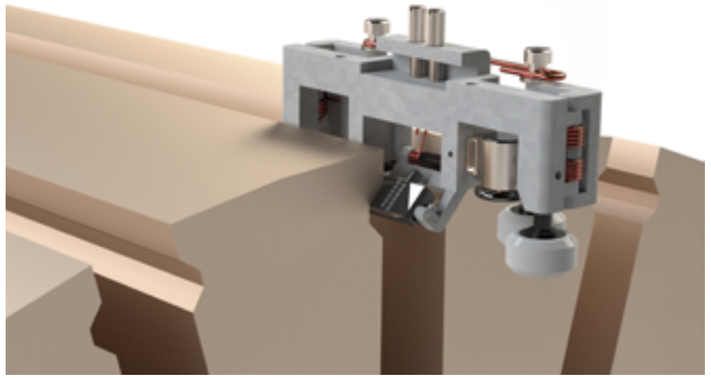

Generator Rotor Dovetails

The copper rotor windings are positioned over the length of the rotor body in axial slots machined into the rotor body. The material remaining between the slots has a dovetail geometry machined near the OD surface for fitment of wedges that retain the rotor windings along the length of the rotor body against centrifugal loads. The need for inspection of the wedge/dovetail mating surface, or crush surface, is driven by the possibility of two damage mechanisms that can result in crack initiation; fretting and electrical arcing.

Fretting damage is the result of the relative movement of the steel wedges against the steel dovetail during operation. During low-speed operation, relative movement between the wedges and crush surface is significant, but the load bearing from the rotor windings on the wedges is not sufficient to cause fretting. At synchronous speed, the bearing load of the rotor windings is sufficient to lock the wedges to the rotor. With no relative motion, fretting cannot occur. However, at intermediate speeds, the right combination of relative movement and bearing load occurs to cause fretting. Therefore, fretting damage is a function of the start/stop cycles.

Generator rotors can also experience stray currents from electrical phase imbalance or other electrical anomalies. The stray currents tend to travel down the wedges and then arc to the rotor at the end of the wedge and then arc back to the next wedge leading to localized heating and causing surface damage. Subsequent cooling results in brittle untempered martensite that is prone to cracking.

In both cases, the cracks are oriented in a circumferential-radial plane, subject to one-per-revolution bending, potentially resulting in high cycle fatigue. The goal of the inspection is to detect and size dovetail cracking. An inspection can be done using eddy current or linear phased array (LPA) ultrasonic techniques.

The eddy current technique is most easily applied to rotors that are stripped for rewind, as shown in Figure 6. This inspection is implemented with eddy current probes placed directly on the crush surface at the wedge/dovetail interface for the detection of cracking. The eddy current technique can also be applied to rotors not being rewound but requires removal of at least one retaining ring to facilitate wedge removal for direct access to the crush surface. Eddy current provides suitable detection capabilities but not crack depth sizing.

The LPA technique uses a compound wedge multi-element search unit positioned either on the adjoining pole face or slot tooth at each wedge butt joint and directed at the turbine end and collector ends as shown in Figure 7. The compound

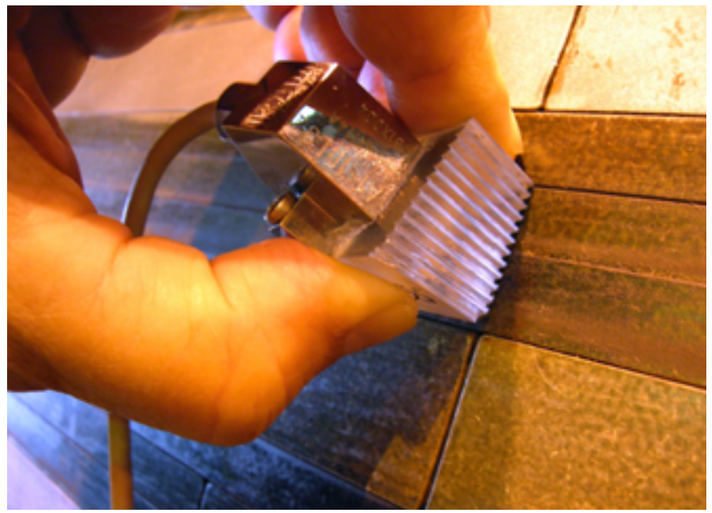

FIGURE 7. Manual LPA inspection of crush surface at the wedge butt joints with wedges installed.

wedge provides for the correct skew angle for interrogating the dovetail contact surface. The dovetail contact surface at each wedge butt joint is scanned by electronically steering the ultrasonic beam through a wide beam angle range in small incremental angles with the beam focused at the intended flaw plane. The swept beam is set for angular increments not to exceed 1°. The examination is typically performed with the rotor on power rollers. The linear phased array inspection process has been demonstrated to offer detection and sizing capabilities of flaws without the need to remove wedges.

Rotor Couplings

Generator shaft keyway cracking is an issue with some large, vintage, four-pole generator rotors using shrunk-on couplings that are typically in nuclear plants. The couplings are shrunk-fit to the rotor shaft, and anti-rotation keys are fitted to keyways machined into the coupling and the rotor shaft. Generator rotors subjected to torsional perturbations from the grid can experience keyway fretting as a result of the key movement against the machined keyway. The crack initiation site is on the loaded side of the keyway at the inboard edge of key contact. The crack propagates along the shaft in a spiral direction as a result of torsional forces, as shown in Figure 8. The initial discovery of this damage mechanism resulted in instructions from the OEM to remove the coupling from the rotor shaft and perform a surface inspection for detection of cracking. The removal of the coupling was a cost and time-intensive task. Alternatively, a phased array ultrasonic inspection technique, shown in Figure 9, allows for inspection of the keyway, without removal of the coupling, has been proven effective for crack detection.

Structural Integrity offers comprehensive inspection and engineering analysis of critical turbine and generator components. Like other critical components in the power plant, generator rotors suffer in-service damage that can be detected through non-destructive examinations. By detecting damage early, actions can be taken to repair or replace affected components before failure occurs, or perform analysis to justify continued operation. Deciding when and where to perform examinations is determined by OEM or insurance carrier requirements, engineering evaluations, or by industry best practices. The inspection processes described above provide critical inputs for engineering assessments of critical generator rotor components used in establishing appropriate inspection intervals.

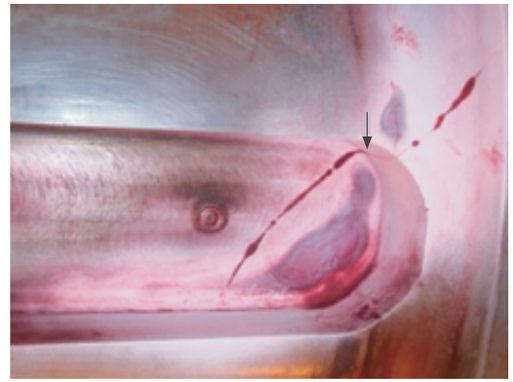

FIGURE 8. Crack initiation site on the loaded side of the keyway at the inboard edge of key contact, progressing in a spiral direction along the shaft.

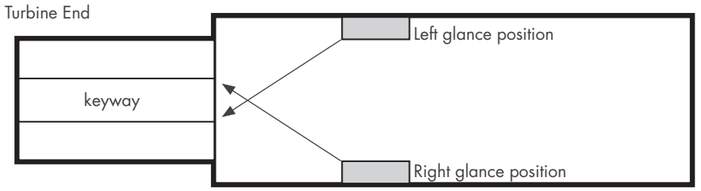

FIGURE 9. Ultrasonic probe positioning for inspection of generator keyway shaft cracking

The Newest Phased Array Ultrasonic Technique: Full Matrix Capture

JEFF MILLIGAN
jmilligan@structint.com

STEVE GRESSLER
sgressler@structint.com

ALLEN PORTER
aporter@structint.com

Full Matrix Capture (FMC) and Total Focusing Method (TFM) have evolved over the past few years into NDE buzz words that warrant explanation and context for their proper and successful application. Structural Integrity (SI) is well vested and engaged in FMC and actively exploring the use of this technology where it enhances ultrasonic sensitivity and characterization to bring added value to our clients. An explanation of these technologies and what they mean to the future of ultrasonic inspection follows.

Phased Array Ultrasonic Testing (PAUT) has evolved significantly over the last 20+ years, with improvements and innovations in sensor design, signal processing, and data interpretation; however, the method by which PAUT is applied has remained relatively unchanged: Excite an array of transducer elements with predetermined time delays, called focal laws, and receive resulting reflections with the array of transducer elements, illustrated in Figure 1. SI regularly performs this "traditional" PAUT inspection technique with a variety of probe configurations: linear phased array (LPA), annular phased array (APA), matrix and dual-matrix phased arrays, to name a few. Focal laws are created for specific focusing (e.g., projection, depth, or half-path) and specific beam steering, depending on the inspection component geometry and expected flaw location or orientation.

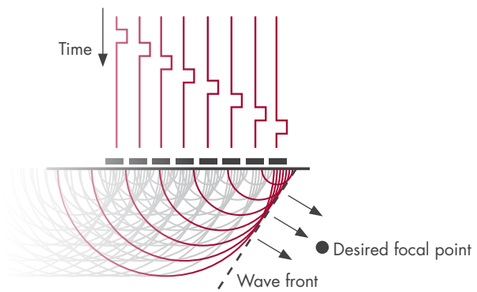

FIGURE 1. Illustration showing how eight transducer elements can be pulsed with different time delay focal laws to produce a transmitted wave front that can be steered and focused.

Full Matrix Capture is a step-change in how PAUT is applied. With FMC, each transducer element in the array is individually pulsed one at a time and all array elements are used as receivers creating a matrix of signal data. For an n-element probe, a total of n^2 individual data sets are acquired. Figure 2 illustrates this concept showing four elements of a linear phased array probe. It should be noted that the term, "Matrix," in, "Full Matrix Capture," does not imply the use of a Matrix Phased Array (MPA) probe; it is merely a reference to the process illustrated in Figure 2.

Focusing is then applied to the matrix of A-Scan data collected via post-processing algorithms to reconstruct a focused result for many points in the inspection volume. Total Focusing Method (TFM), Sectorial Total Focusing (STF), and Inverse Wavefield Extrapolation (IWEX) are a few processing methods found in the industry. The potential advantages of any of these FMC techniques are improved resolution over a larger area of focused data, improved sensitivity to small defects, and enhanced flaw characterization. For example, an FMC/TFM display may focus at 1,024 locations (32 x 32 data points), while standard PAUT may only focus at 80 locations (40° beam sweep x 0.5° angular resolution). Another benefit is the same probes used for standard PAUT can be utilized for FMC. Due to continually improving equipment capabilities, larger aperture probes (i.e., 64 elements) can be used to further enhance focusing and resolution.

Some limitations of FMC include significantly larger data file sizes, slower scanning speeds, and reduced signal-to-noise ratio (SNR) because the data is being collected after pulsing only one element at a time. FMC equipment manufacturers have ways of getting around some of these limitations, like only collecting half-matrix data, or not saving all raw A-Scan data, so the TFM image is saved without the ability to reprocess the data. The different processing techniques, and even new phasing techniques, such as plane wave imaging (PWI), allow for an improvement in the SNR issues. It is important to remember that FMC techniques do not change the laws of physics and are subject to the same focalization limitations as standard PAUT. For example, like standard PAUT, focusing is limited to the near field of the probe. As with most NDE methods, compromise is required to provide the most effective solution.

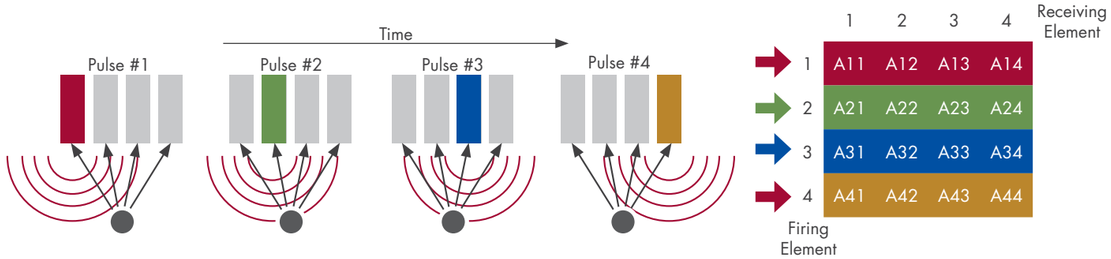

FIGURE 2. Illustration showing how each of four transducer elements are pulsed individually with FMC and a resulting matrix of results are collected.

Another current limitation to FMC is with Codes and Standards, which are traditionally slow to develop for new NDE technology. ASME Code rules for "traditional" PAUT have been in place for a few years. However they do not support the calibration and implementation of FMC techniques. While these issues may currently preclude the use of FMC techniques for Code weld acceptance, FMC techniques are still a viable option for detecting and characterizing service damage. Additionally, an industry-accepted vocabulary for terms used to describe the full matrix capture method is being discussed, as often the name "FMC/TFM" is seen in literature since TFM has become the most common focusing algorithm to date.

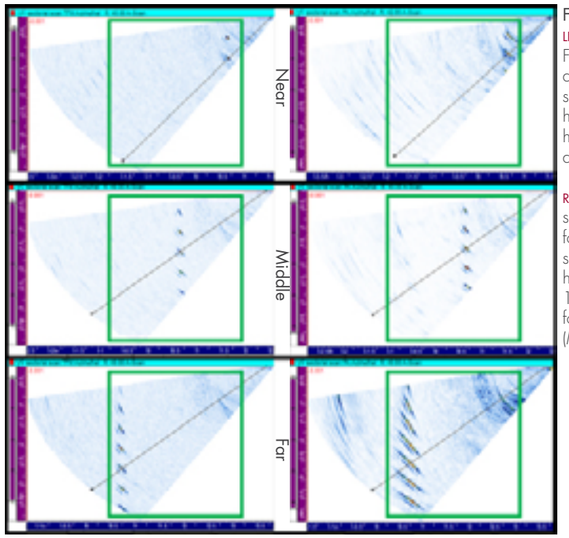

FIGURE 3.
LEFT Images of FMC/STF show a focused vertical stack of side drilled holes throughout highlighted focus area (boxed);

RIGHT Images of standard PAUT show focused vertical stack of side drilled holes at prescribed 1.0 inch projection focus area only (Middle).

Conclusions

FMC is a phased array technique that has received increased attention in the NDE community. While it can enhance images over standard PAUT, certain limitations and trade-offs must be evaluated to optimize its use. For instance, even though FMC can provide a larger volume of focused data (Figure 3), the resulting signal quality remains dependent on variables that affect ultrasonic sound propagation for all techniques (e.g., grain morphology, homogeneity, surface condition, geometry, expected damage locations, etc.). Therefore, the best FMC applications are those where SI's team of NDE experts, engineers, and metallurgists pinpoint the highest risk positions, expected damage morphologies, and required sensitivities.

FMC is just one of the many advanced tools in our NDE arsenal, and we selectively deploy the technology where we believe it adds value to our clients. In this regard, SI's experts are available to discuss how FMC and other advanced technologies can be integrated into multi-disciplined approaches that solve your inspection challenges.

Adding Value Through Test Informed Modeling: Hydro Structures

ERIC KJOLSING, Ph.D., PE
ekjolsing@structint.com

DAN PARKER, PE
dparker@structint.com

In 2018, Structural Integrity Associates (SI) supported a utility in the structural assessment of a submerged concrete intake tower. The tower is nearly a century old and was investigated as part of the utility's periodic maintenance program.

The assessment required the generation of an analysis model that accounted for both the structure and the surrounding water. When accounting for fluid effects, a typical analysis approach is to develop a fluid-structure interaction (FSI) model that explicitly accounts for the interaction between the surrounding water and concrete tower. However, this modeling approach is expensive both in terms of (a) cost, due to the increased effort needed in generating the model and (b) schedule, due to the increased analysis run time. In lieu of developing an FSI model, SI implemented an alternative numerical approach to model the effects of the water and justified the approach through physical testing of the in-situ structure.

SI developed a finite element model of the concrete structure and incorporated the numerical representation of the surrounding water. An eigenvalue analysis was performed to obtain the first five natural frequencies of the submerged structure (four flexural modes and one torsional mode). SI engineers then traveled to the site and used impact testing and ambient excitation sources, along with proprietary signal processing software, to non-destructively characterize the dynamic behavior of the submerged structure. The first five natural frequencies of the physical structure were found to be within several percent of those predicted by SIs eigenvalue analysis, giving confidence in the modeling approach.

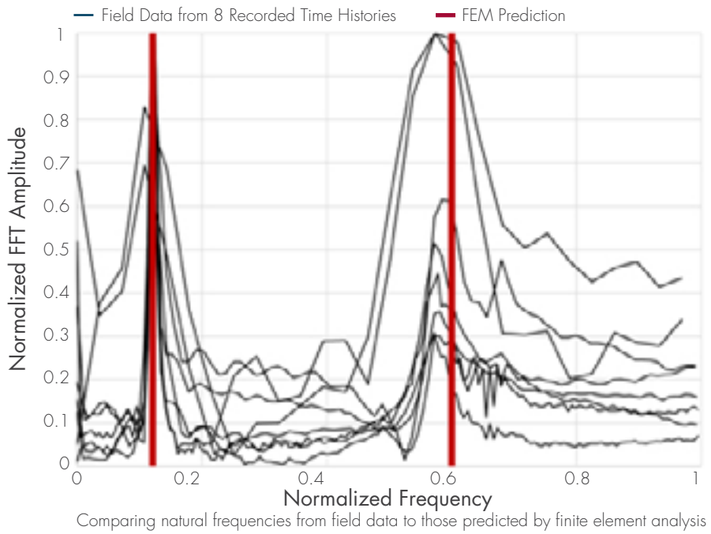

Comparing natural frequencies from field data to those predicted by finite element analysis

Structural Integrity's alternative numerical approach to modeling the effects of water provided a reduced cost and timeline for the structural assessment, while SI's in-field testing provided a tangible demonstration that the model accurately represented the physical structure.

SI's alternative numerical approach to modeling the effects of water provided a reduced cost and timeline for the structural assessment, while the in-field testing provided a tangible demonstration that the model accurately represented the physical structure.

Please contact Eric Kjolsing, Ph.D., PE if you are interested in learning more about test informed modeling or how SI can help you in the evaluation of existing infrastructure.

The concrete tower just after construction (photo courtesy of facility owner)

Acoustic and Blowdown Load Calculations for Reactor Internals

MATTHEW WALTER
mwalter@structint.com

As part of the general design criteria for nuclear power plants, the primary structures and systems of the plant must be designed to handle postulated accident events, including the dynamic effects of postulated pipe ruptures. For a Boiling Water Reactor, analyzed events include various accident conditions in the recirculation piping, including a Loss of Coolant Accident (LOCA). One postulated LOCA event is assumed to be an instantaneous double-ended guillotine break of the recirculation line. This event causes several loads to be imparted on the reactor vessel, attached piping, and reactor internal components. [Some loads such as jet impingement, annulus pressurization, and pipe whip impart loads on the outside of the reactor vessel and the attached piping.][Other loads, including flow-induced drag and acoustic loads, transmit loads inside the vessel on critical components such as jet pumps, core shroud, and the shroud support structure.] Figure 1 shows the pipe and resulting loads.

Over a decade ago, the NSSS vendor identified numerous errors in computer codes and methods used to calculate some of these loads, including drag loads and acoustic loads on the reactor vessel internals. These errors created a significant problem for utilities that needed to perform structural evaluations and determine the operability of critical plant components, most notably reactor internal components such as the jet pumps and core shroud. These components are essential for the plant to maintain safe operating and shutdown conditions. Furthermore, several plants have known flaws in these components and require evaluations to justify continued operation and determine appropriate reinspection intervals.

The postulated LOCA event causes various phenomena to occur in the reactor vessel. First, due to the sudden depressurization of the recirculation pipe, a shock wave develops at the pipe break location that travels into the vessel. This wave travels at the speed of sound; thus, it is called an acoustic load. This load acts directly on the core shroud, shroud support, access hole covers and jet pumps as a complex pressure distribution. After the acoustic pressure wave passes through the vessel, the other phenomena that occur are the sudden discharge of fluid from the vessel. This event causes drag loads to occur on the same components as the fluid rushes out of the vessel at the break location, commonly referred to as blowdown.

FIGURE 1. Examples of good and bad loads on the outside of the reactor vessel and the attached piping.

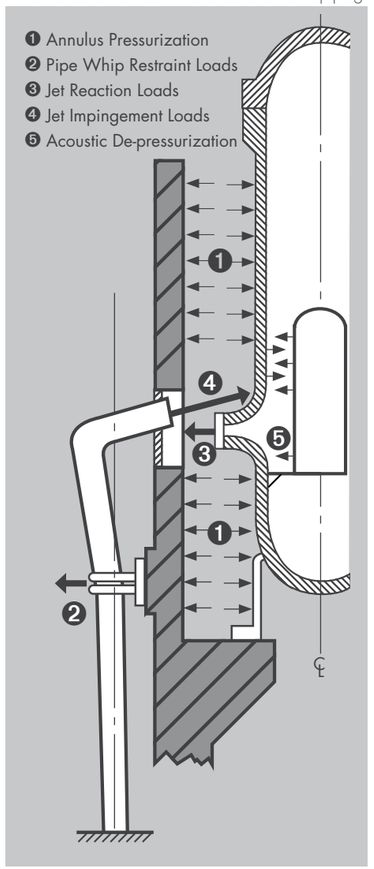

Structural Integrity Associates (SI) has developed methods for calculating blowdown and acoustic loads. These methods are independent of the errors identified by the NSSS vendor and use a 1-millisecond break opening time methodology, which is accepted by the US NRC. SI has been using these methods since 2009, and multiple independent consultants have verified the methodology. SI has also published numerous publicly available papers on this topic[1].

To calculate blowdown and drag loads, SI developed a unique solution that can use off-the-shelf finite element software rather than vendor-specific computer codes. In short, the drag load is determined using the Laplace equation for potential flow, assuming an ideal fluid. The same equation is used to solve steady-state heat transfer problems, using temperature instead of velocity potential. Using the analogous heat transfer terms for the Laplace equations, ANSYS can be used to determine the fluid velocity and, in turn, blowdown drag loads, providing the advantage of being able to use complex three-dimensional (3D) geometry and commercially available software. Figure 2 shows the blowdown load analysis.

For acoustic loads, ANSYS is also utilized. A 3D model of the key vessel and internal components is used to simulate the wave propagation around the annular region. A transient pressure analysis is performed using a one millisecond break time, consistent with the US NRC Standard Review Plan. This methodology is benchmarked against experimental data[2].

The acoustic wave imparts on internal structures, to account for dynamic effects, dynamic load factors are applied to appropriate components. This methodology is independent of the vendor-specific thermal-hydraulic codes that have been used in the past and are the subject of the NSSS errors. The acoustic load pressure results are shown at three different time steps in Figure 3 as the waves travel through the annular region of the reactor vessel.

For over a decade, SI has been calculating blowdown and acoustic loads for nuclear utilities in need of accurate loads for reactor internals evaluations. SI provides a unique alternative for reactor owners of all types for providing loads using non-proprietary methods and software while ensuring regulatory compliance and component integrity.

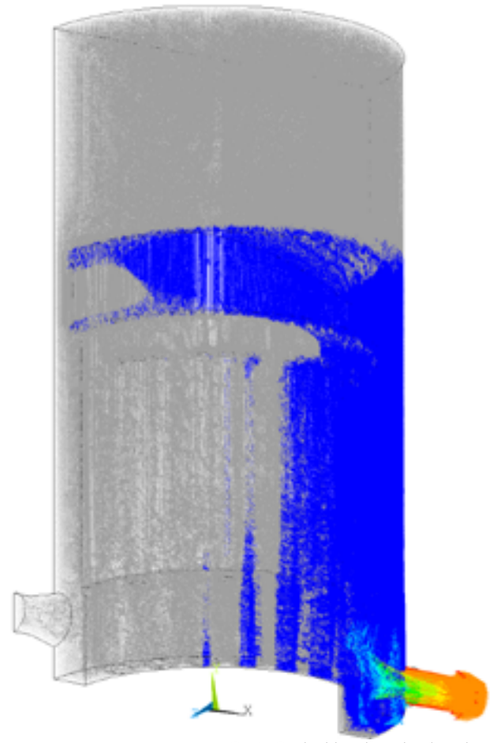

FIGURE 2. The blowdown load analysis

References

[1] Publicly available papers include PVP2010-25866, PVP2010-25865, PVP2011-57743, PVP2013-97728, PVP2015-45769 and PVP2016-63091

[2] See PVP2010-25865: Benchmark of an Application of Acoustic FEA for Light Water Reactor Loss of Coolant Accident Acoustic Loads

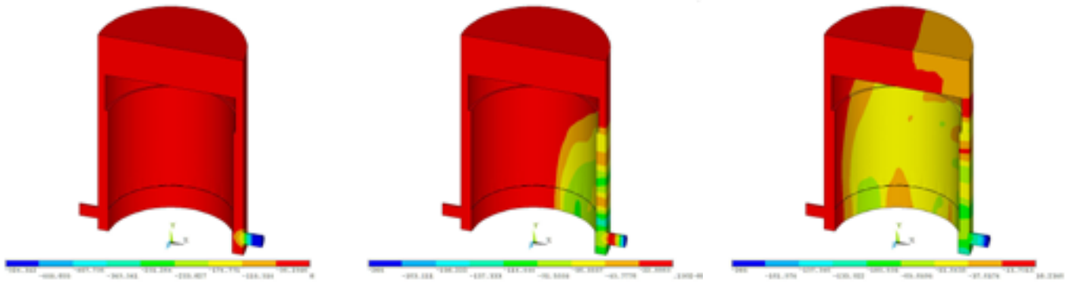

FIGURE 3. The acoustic load pressure results shown at three different time steps as the waves travels through the annular region of the reactor vessel.

Strategies, Projects and Technologies to Help Improve NDE Reliability in the Pipeline Industry

SCOTT RICCARDELLA
sriccardella@structint.com

JASON VAN VELSOR
jvanvelsor@structint.com

ROGER ROYER
rroyer@structint.com

Pipeline operators face a multitude of threats, including service, environmental, or operational induced degradation to pipelines and related facilities. Non-Destructive Examination (NDE) is often used to characterize the nature and extent of this degradation. Thus, there is a critical need for reliable NDE as pipeline operators rely extensively on NDE as the basis for validating In-Line Inspection (ILI) results, determining fitness for service, and making repair and other operational decisions. Erroneous or inaccurate characterization of these defects can lead to unexpected leaks or failures, unnecessary and costly repairs, the establishment of an incorrect remaining life or re-assessment interval, and inaccurate (in)validation of ILI results.

A significant industry need has been identified to reduce the variability and improve the performance associated with NDE technologies along with personnel and training for implementing these NDE techniques. Thus, Structural Integrity (SI) has established a significant initiative to help improve NDE performance with internally funded development projects, advanced research projects with select partners and research institutes, and specific NDE training programs focused on this objective. Several projects have either recently been completed or are in progress to help improve NDE performance across the pipeline industry. These projects include:

NDE Performance Characterizing Crack Defects

Over the last four years, two significant projects have been completed, with another underway, to quantify the performance of emerging and commonly employed NDE technologies. The research was conducted on behalf of the Pipeline Research Council International (PRCI), the pipeline industry's leading research institute. The objective of these projects was to gain a better understanding of NDE performance by developing and implementing a process to evaluate the applicability, accuracy, and sensitivity of different NDE methodologies for sizing Stress Corrosion Cracking (SCC) anomalies, Electric Resistance Weld (ERW) seam defects, and other forms of cracking. The evaluation included state-of-the-art ultrasonic testing (UT) and electromagnetic NDE techniques.

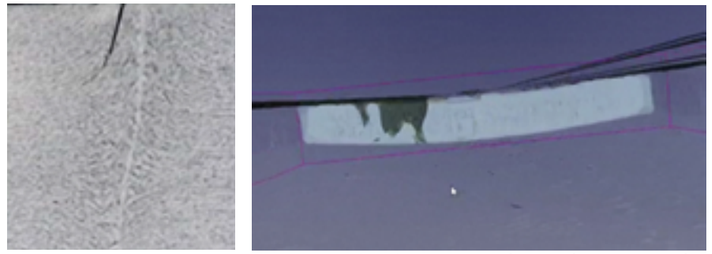

FIGURE 1. Micrograph and XRCT From Verification of ERW Seam Defect

Following the NDE evaluation and consolidation of results, designated test samples were verified using a combination of X-Ray Computed Tomography (XRCT) on cutouts and metallography on cross-sections. The XRCT served as a useful complement to metallography as it allowed 3-Dimensional representation and viewing of flaws (Figure 1) and helped guide the location of and increments between cross-sections. Comparing the NDE results to the metallography, several analytical and statistical metrics were then analyzed to assess and compare NDE performance.

NDE Modeling

As a separate phase to the NDE performance evaluation, SI developed a software interface application that allowed for the quick and efficient configuration of Phased Array Ultrasonic Testing (PAUT) test parameters, component and flaws for input into commercial Finite Element Analysis (FEA) software. Post-processing algorithms were then used to process and present the FEA results in the same way as a PAUT instrument. The results provided insight into the behavior of the ultrasound interacting with the component and flaws and generated results that mirrored closely what is observed in-ditch on actual PAUT equipment. Figure 2 provides an example of the model results, showing a merged view of PAUT sectorial scans from two sides of a crack cluster.

As part of a new continuation project, the modeling is currently being expanded to incorporate Full Matrix Capture UT techniques as well as evaluating various crack configurations, pipe dimensions, and other added complexities (such as laminations and

Continued on next page

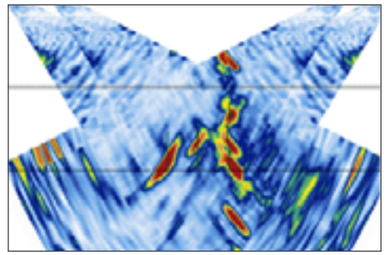

FIGURE 2. Example FEA modeling results showing a merged sectorial scan from a simulated dual-sided PAUT examination of a crack cluster

surface corrosion) to gain better understanding in terms of how these factors influence NDE (UT) performance.

Study on Human Performance Factors

Human factors have long been identified to have one of the most significant impacts on overall NDE performance. SI recently concluded a research project that investigated the effects of human performance factors on NDE performance for conducting Magnetic Particle Inspections (MPI) and Ultrasonic Thickness Testing (UT) on pipeline components.

The project involved a round-robin type study, where service providers conducted MPI and UT examinations on blind samples with known defects. Ultimately, several human performance factors observed during the round robin were compared with the accuracy of the NDE results, to conclude the impact of the human factors on the NDE performance.

SCC NDE Recommended Practices

Taking lessons learned from NDE performance studies and advanced modeling, SI is leading a project to develop a state-of-the-art Recommended Practice (RP) document for assessing SCC. Input from industry leading NDE service providers, equipment manufacturers, and pipeline operators will be considered in the preparation of the RP to ensure practical guidance and application. The RP will summarize guidance in the following areas:

- Component and Equipment Preparation
- Technique Applicability for Varying Configurations
- Technology Limitations
- Equipment Settings
- Calibration (Samples and Process)
- Data Collection Process
- Supplemental Data Collection
- Analysis and Reporting Requirements

Taking lessons learned from NDE performance studies and advanced modeling, Structural Integrity is leading a project to develop a state-of-the-art Recommended Practice (RP) document for assessing SCC.

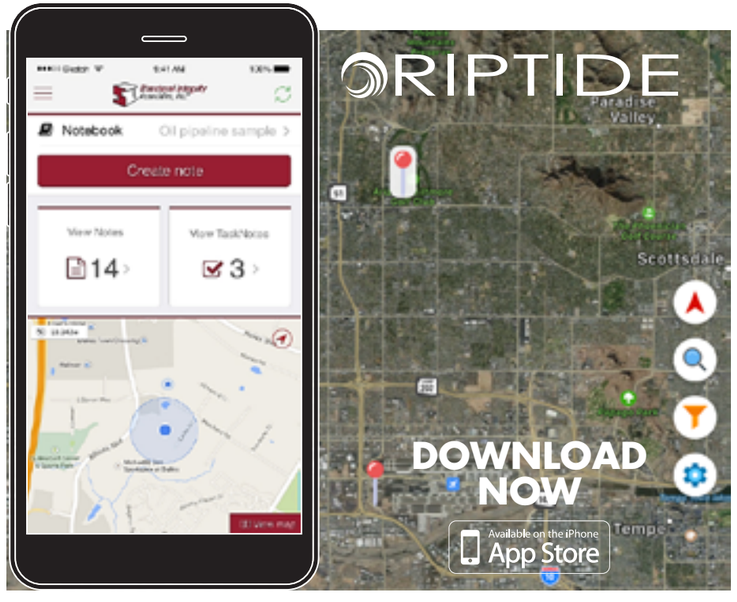

RIPTIDE™

Recognizing that data is a critical component of pipeline integrity management that impacts all aspects of operations. Collecting and integrating reliable field inspection data poses a wide range of challenges. These challenges include having consistency in how field data is collected and reported, maintaining a consolidated database system able to integrate with other data sources and policies, and ensuring data collection and reporting is completed in a timely manner and consistent format. From a recent research study conducted on Human Performance factors, inaccurate and inconsistent reporting is one of the most significant Human Performance errors in NDE.

To help address some of these issues, SI developed a cloud-based field data acquisition and reporting solution named RIPTIDE. RIPTIDE provides the following advantages:

- Uses a tablet/mobile application to guide and facilitate the collection of all primary field data required during a pipeline integrity inspection.
- Utilizes intuitive conditional electronic forms to collect the right data, the first time.
- Automatically imports and integrates field inspection data into a cloud-based database system with an ability to integrate with a Geographic Information System.
- Enables real-time data synchronization when connected to a network and remote off-line data collection and subsequent automatic synchronization when there is no available network.
- Cloud-based data synchronization and automated report generation facilitate expedited reporting.

Advanced NDE Technologies

SI continually evaluates, implements, and even develops new NDE technologies that have the potential to improve the accuracy and reliability of pipeline assessments and to provide inspection solutions in situations where the pipe surface cannot be directly accessed. Some examples of the advanced solutions that SI offers are as follows:

- **Corrosion Mapping with LATITUDE™:** High-resolution encoded PAUT thickness data obtained using SI's patent-pending non-mechanized NDE data encoding technology, LATITUDE, provides the highest quality thickness data for pipeline assessment while eliminating the time and expense associated with complicated automated scanning equipment (See, Turnkey Rapid-Response Plant Support page 49).
- **Full Matrix Capture (FMC) PAUT:** The latest adaptation of PAUT technology that uses wave focusing algorithms in post-processing to provide notable improvements in resolution and sensitivity, FMC has shown potential for improved assessment of SCC and seam weld anomalies. (See, The Newest Phased Array Ultrasonic Technique -Full Matrix Capture (FMC) page 16).
- **Inspection through Coatings with SIPEC™:** Measuring wall thickness through thick internal liners or external coatings using SI's patented dynamic pulsed eddy-current technology, SIPEC, can provide critical thickness data in situations where coating removal is undesirable or not possible or when internal liners or fouling prevent the use of traditional inspection technologies. SI has partnered with Qi2 to deliver robotic in-line inspections with SIPEC.
- **Short-Range Guided Wave Testing (SR-GWT):** Deploying the latest in SR-GWT technology using magnetostrictive sensors, SI assesses localized areas with obstructions, such as the areas under pipe clamps and supports, or at ground and wall penetrations with significantly enhanced signal-to-noise ratios and directional wave control to identify areas of hidden wall loss.

References

[1] Pipeline and Hazardous Materials Safety Administration (PHMSA) sponsored, comprehensive research study [US Department of Transportation, PHMSA, "Long Seam ERW R&D PHMSA Update"] researchers identified in-the-ditch nondestructive examination (NDE) techniques as requiring improvement in anomaly identification, false call rates, defect depth and length sizing, and in general consistency and standardization of NDE practices.

Assessing Prestress Losses in a Nuclear Containment Structure for License Renewal

ERIC KJOLSING, Ph.D., PE
ekjolsing@structint.com

INTRODUCTION

Nuclear power plants around the world are approaching the end of their original 40-year design life. Efforts are underway to extend the operating license for these plants to 60 years or beyond. As part of the license extension, it must be demonstrated that the reactor containment building remains able to safely perform its intended functions for the extended duration of operation. Many of these containment buildings utilize a post-tensioned concrete design where the tendons are grouted after tensioning. Since these grouted tendons cannot be re-tensioned, an assessment for the loss in prestress beyond the original design life must be performed.

This article describes a methodology to assess the structural performance of a containment structure over time as a function of confidence in the tendon losses and is split into three parts:

1. A description of the methodology
2. A representative probabilistic assessment
3. Representative analysis results

The methodology presented herein can be used by the plant owner to demonstrate sufficient structural capacity beyond the design life or help guide future analyses of containment performance utilizing best estimate (i.e. less conservative) prestress losses.

METHODOLOGY

Consider a containment structure with grouted post-tensioning that is approaching the end of its licensed 40-year design life. To demonstrate additional useful life, it must be shown that the containment structure remains able to safely perform its intended design functions past the original 40-year design life. This can be demonstrated by showing (a) that the prestress values are still greater than the design specified minimum value so that the containment remains within the design basis, or if the prestress value is shown to drop below the specified design minimum, (b) that the containment still has sufficient margin above the design pressure. Unfortunately for grouted tendons, the identification of in-situ prestress values is difficult as directly measured tendon losses are generally unavailable. However, secondary measurements of prestress, such as displacements or strains recorded during structural tests, are usually available and can be used to estimate time-dependent prestress values.

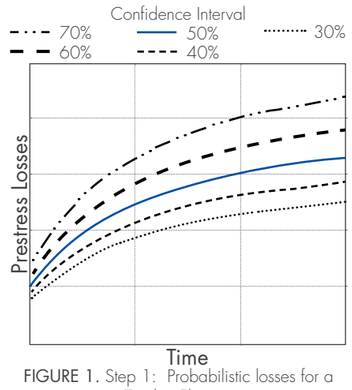

FIGURE 1. Step 1: Probabilistic losses for a Tendon Element

The methodology proposed in this article is described by the following steps.

Step 1. Perform a probabilistic assessment using design code methods and structure-specific inputs to calculate prestress losses based on variations of concrete creep, concrete shrinkage, and tendon relaxation. The results of this assessment are time-dependent cumulative distribution functions that define relationships between tendon losses and confidence (likelihood) of those losses. For a specific tendon element and at discrete confidence intervals, these results take the time-dependent form shown in Figure 1.

Step 2. Develop a finite element model (FEM) of the structure that includes the expected tendon losses (50% confidence) from Step 1. Using finite element analyses (FEA), recreate past structural tests (e.g., structural integrity tests) and iterate the tendon prestress values until agreement is reached between secondary measurements (e.g., structural displacements and strains) recorded in the field and those predicted by the FEA. The results of this step are estimates of tendon prestress values at specific instances in time, as shown in Figure 2.

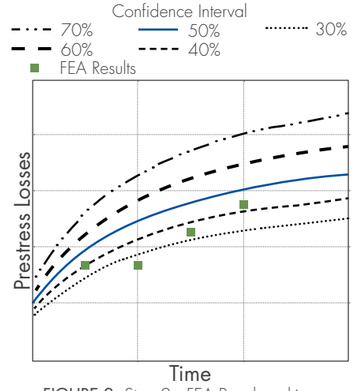

FIGURE 2. Step 2: FEA Benchmarking

Step 3. Identify the prestress loss curve that bounds the FEA output, as shown in Figure 3.

Continued on next page

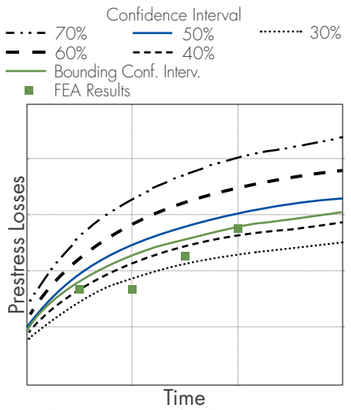

FIGURE 3. Step 3: Bounding Prestress Loss Curve

Step 4. Compare the design allowable prestress values to projected prestress estimates (which utilize the bounding confidence interval losses from step 3). Ideally, this comparison will show that the containment prestress value is greater than the design specified minimum value so that the containment remains within the design basis. If the prestress value is less than the specified design minimum, then projected prestress losses from the bounding confidence interval (see Figure 4) can be used in predictive FEAs to demonstrate that the containment still has sufficient margin above the design pressure.

REPRESENTATIVE CONTAINMENT STRUCTURE

A representative containment structure is chosen in this study to demonstrate aspects of this methodology. A cross section is shown in Figure 5 and utilizes dimensions typical for this type of design. Four external buttresses are located at 90° intervals along the circumference of the structure. Hoop tendons are anchored in these buttresses with each tendon wrapping around the entire circumference of the structure.

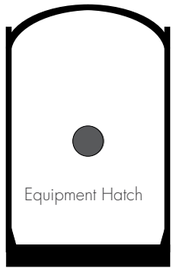

FIGURE 5. Representative Containment Structure Cross Section

Vertical tendons are anchored at the bottom of the base mat and at the wall-dome junction. The wall-dome junction also anchors sets of dome tendons oriented at 120° from each other. The structure contains hoop, vertical, and dome tendons typical for this type of design. The example structure contains various penetrations including an equipment hatch located near mid-height of the structure and centered on one of the buttresses.

REPRESENTATIVE PROBABALISTIC ASSESSMENT OF TENDON LOSSES (Demonstration Step 1)

A study is performed to estimate time-dependent prestress losses over 60 years using design code methods. These methods, used in design basis calculations, are primarily functions of the concrete creep, concrete shrinkage, and tendon relaxation characteristics. The assessment utilizes assumed probabilistic distributions for the calculation inputs in a Monte Carlo simulation. Cumulative distributions are developed from the simulation results for the hoop, vertical, and dome tendons at various instances in time. These distributions relate prestress losses and cumulative probability for various tendon elements along the tendon length. Representative distributions at one instance in time for the hoop tendons are shown in Figure 6. Multiple cumulative distributions can be used to develop element-specific output akin to that shown in Figure 1.

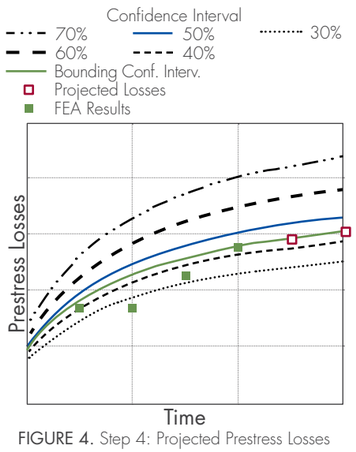

FIGURE 4. Step 4: Projected Prestress Losses

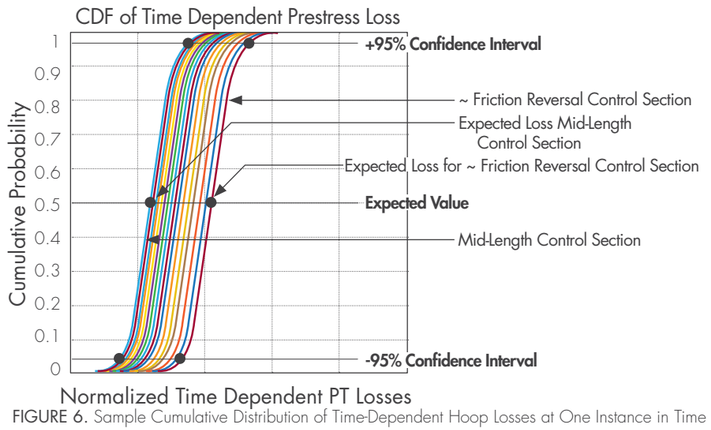

FIGURE 6. Sample Cumulative Distribution of Time-Dependent Hoop Losses at One Instance in Time

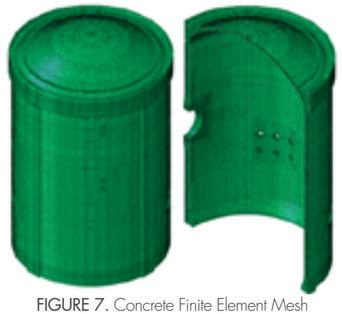

FIGURE 7. Concrete Finite Element Mesh

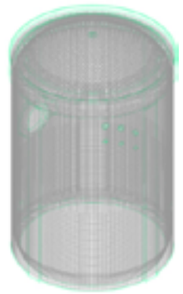

FIGURE 8. Rebar Finite Element Mesh

FIGURE 9. Hoop Interior LEFT and Exterior RIGHT Tendon Finite Element Meshes

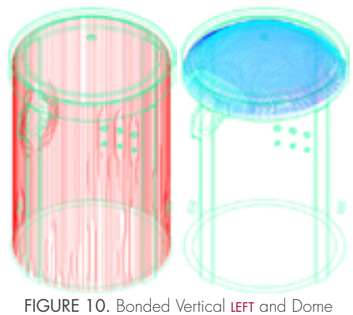

FIGURE 10. Bonded Vertical LEFT and Dome Tendon RIGHT Finite Element Meshes

REPRESENTATIVE FINITE ELEMENT ANALYSIS (Demonstration Step 4)

Assume that the bounding confidence interval results in projected prestress levels that are lower than the design minimum. In Step 4, tendon-specific prestress values at specific instances in time are used in finite element analyses of the structure to demonstrate that the containment still has sufficient margin above the design pressure. Prestress losses corresponding to a 95% confidence interval are used in this article for demonstration.

Finite Element Model

This section describes the finite element model of the representative structure. The model includes a full containment structure less the base mat. Large penetrations, reinforcement, and tendons are explicitly modeled.

Concrete

The concrete finite element mesh is shown in Figure 7. An equipment hatch, personnel airlocks, and pipe penetrations are explicitly modeled. ANACAP, a proprietary Structural Integrity Associates, Inc. concrete constitutive model, is used in the finite element analyses. Among other capabilities, the ANACAP model can capture multi-axial tensile cracking, compressive crushing with strain softening, and crack dependent shear stiffness. It has been successfully utilized in blind predictive studies and nuclear related work and is further described by others [1-3].

Reinforcement

The rebar finite element mesh is shown in Figure 8. The reinforcement includes all major vertical and hoop reinforcement in the containment wall and dome section.

Tendons

The finite element meshes for the interior and exterior hoop tendons are shown in Figure 9. The finite element meshes for the bonded vertical and dome tendons are shown in Figure 10. Each tendon is individually modeled.

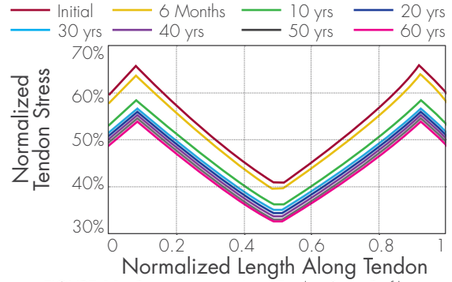

FIGURE 11. Representative Hoop Tendon Stress Profile

Tendon Stress Profiles

For each tendon group (hoop, vertical, and dome), a spatially dependent tendon stress profile is developed for various instances in time. The tendon stress profiles incorporate tendon losses calculated from the probabilistic assessment and are based on a 95% confidence interval for this demonstration; the bounding confidence interval (Figure 4) would be used in a structure-specific analysis. Representative profiles for the hoop tendons are shown in Figure 11.

Continued on next page

Representative Finite Element Analysis Results

Finite element analyses are performed with tendon stress profiles utilizing 95% confidence losses 60 years after stressing. The analysis model is subjected to both structural integrity test (SIT) pressure/time histories as well as beyond-design basis pressure load scenarios. Representative results are presented here for the two tests to demonstrate outputs useful in assessing structural performance. The specific results shown here utilize high-confidence loss estimates for demonstration purposes.

Simulated SIT Results

An analysis model utilizing prestress losses 60 years after initial stressing is subjected to simulated SIT loading. Figure 12 shows the tensile strain in the bonded tendons at the maximum applied internal pressure. The legend is normalized to the yield strain of the embedded rebar (ε_{ry}). Figure 13 shows the maximum principal strain in the concrete around the equipment hatch at the maximum applied internal pressure. The legend is normalized to 10 times the concrete tensile strain (ε_{ct}) where light grey areas indicate significant concrete cracking.

Estimating Containment Capacity

An analysis model utilizing prestress losses 60 years after initial stressing is subjected to beyond-design basis pressure loading. This analysis is performed to demonstrate the limiting capacity of the representative containment structure. Because such an assessment is beyond a design basis, the pressure capacity will depend on best estimate failure criteria rather than code-based allowable values and will also depend on elevated temperatures associated with the source of pressure. However, the following example results are provided to indicate analysis output valuable in structural evaluations. As an example, Figure 14 shows the maximum principal strain in the concrete around the equipment hatch under a beyond-design basis pressurization. The legend is normalized to the concrete cracking strain where light grey areas indicate concrete cracking.

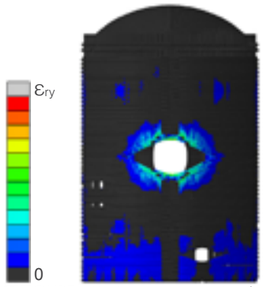

FIGURE 12. Representative Bonded Tendon Strain Around Equipment Hatch; Peak SIT Test Pressure; 60 Year Losses

FIGURE 13. Representative Max Principal Concrete Strain Around Equipment Hatch; Peak SIT Test Pressure; 60 Year Losses

FIGURE 14. Representative Max Principal Concrete Strain; Beyond-Design Pressure; 60 Year Losses

SUMMARY

In order to extend a nuclear plant's operating license, the required additional useful life of the containment structure must be assessed. Sufficient structural capacity must be demonstrated so as to meet established design requirements, such as elevated pressures and temperatures for a loss-of-coolant accident. For concrete containment structures with grouted post-tensioning tendons that cannot be re-tensioned, the accumulated concrete creep, shrinkage, and tendon relaxation at times beyond the original design life are important as they may result in concrete prestress below the design allowable.

The methodology presented herein can be used by the plant owner to demonstrate sufficient structural capacity beyond the design life or help guide future analyses of containment performance utilizing best estimate (i.e. less conservative) prestress losses.

More details can be found in a recent ASME publication[4] or can be discussed directly with Eric Kjolsing at ekjolsing@structint.com.

References

[1] Dameron, Robert; Dunham, Robert; Rashid, Joe; and, Sullaway, Mike. "Pretest Predictions Report for the Sandia 1:6 Scale Reinforced Concrete Containment," *Transactions of SMiRT9*. pp.221-226, Lausanne, August, 1987.

[2] Rashid, Joe and Dunham, Robert. "Development of a General Three-Dimensional UMAT Model for Concrete Considering Aging, Viscoplasticity and Cracking," ANATECH Report ANA-85-P-0041, to Waterways Experiment Station, U. S. Army Corps of Engineers, December 1985

[3] Rashid, Joseph; James, Randy; and Dunham, Robert. "Modeling and analysis of aging behavior of concrete structures in nuclear power plants." *Proceedings of Fontevraud 7 International Symposium*. A088 T10: pp.115-126. Avignon, France, September 26-30, 2010.

[4] Kjolsing, Eric; James, Randy; Kubischta, Keith; and Parker, Dan. "Assessing prestress losses in a nuclear containment structure for license renewal." Proceedings of the ASME 2019 Power Conference. POWER2019-1842. Snowbird, Utah, July 14-18, 2019.

Delivering Value:

Modernization of Plant Automation Controls

GERRY DAVINA
gdavina@structint.com

The modernization of plant automation controls represents a step change in performance that optimizes Operations and Maintenance resources, shifting their focus to performance maintenance and plant monitoring and away from inefficient corrective maintenance and troubleshooting.

FIGURE 1. Condensate Demineralizer Panel at a BWR (Front Panel Face)

According to the U.S. Energy Information Administration, the average age of the U.S.-based nuclear power plant is approximately 38 years old. Three of the "youngest" plants (Watts Bar, Nine Mile Point 2 and River Bend) all began construction in the mid-1970's with their designs approved years earlier. In terms of industrial control systems, this means that most, if not all, of the plants in the U.S. nuclear fleet, continue to operate with 1970s in automation equipment and technology. Although it can be argued that the equipment and technology have proven to stand the test of time, the reality of the digital age, with low cost and high-powered processors, is that relay-based control systems are long-obsolete and no longer practical for any automation system that requires more than a handful of relays and switches. In an industry that has publicly advocated a commitment to improved reliability and efficiency, ironically, the most evident impact for any plant with the continued use of 40-year-old automation equipment and technology is poor system reliability and inefficiency burdening both Operations and Maintenance resources.

Continued on next page

FIGURE 2. Condensate Demineralizer Panel at a BWR (Inside View)

A tour of almost any of these plants will, undoubtedly, bring you past an array of relay-based control systems (Figures 1 and 2) still in operation but either stripped down to their bare essentials or labeled with long-standing deficiency tags, mainly due to the characteristic maintenance issues (bad relay and switch contacts, burned-out pilot lights, etc.) that are compounded by the unavailability of replacement parts. Additionally, the complexity of modifying their hard-wired design for even the most basic process control improvement perpetuates operational inflexibility, and they are often thrust into the "if it is not broke" abyss. These systems are frozen in time from the day they left the manufacturer's facility decades earlier. Not surprisingly, most utilities have been slow to modernize these systems.

Although the advent of the programmable logic controller (PLC) in the 1960s ushered in an alternative to the relay-based control system, the prominence of the PLC with automation system designers did not take hold until well after the designs for most of the U.S. nuclear fleet were already complete and well into the construction phase or beyond. However, most plants have implemented some form of digital automation control upgrades over the years, but these upgrades have typically been associated with information systems or distributed control systems (DCS) for overall plant operations, not the autonomous sub-systems that contain the bulk of the obsolete automation equipment and technology of the 1970s.

With the rapidly expanding growth of computing power and communication speeds in the 1990s, the industry was keenly aware of the need to modernize with digital automation control systems to operate both more safely and efficiently. Despite this fact, many plant engineers did not have a sufficient knowledge base for processor-based automation controls and were wary of championing system upgrades with this technology. Also, many veteran plant operators and maintenance personnel did not fully understand or trust the modern equipment. Aside from a computer screen, none of the equipment was standard panel-mount equipment the operators were accustomed to working. Switches, pushbuttons, and pilot-lights were replaced with computer graphics; the turning of a switch was replaced with the click of a mouse button. Maintenance had no relays to replace or wires to trace; troubleshooting now involved a laptop rather than a multimeter. At that time, the most likely way for a processor-based controller to find its way onto the plant floor was by default, procured by the plant as part of a more extensive system the manufacturer had already standardized with PLC automation, not by plant-driven modernization initiatives. Implementation of PLC-based automation control modernization was and remained a challenge.

Fast-forwarding to 2018, Structural Integrity's Chemistry and Materials Group was contracted by Exelon to implement a full, PLC-based upgrade of the Reactor Water Cleanup (RWCU) filter-demineralizer (F/D) control system at the James A. FitzPatrick (JAF) Nuclear Power Plant during their fall 2018 refueling outage (RFO-23). The original relay-based system, supplied by DeLaval around 1971 (Figure 3), had been in operation for over 40 years.

In the mid to late 1990s, JAF installed an Alternative Decay Heat Removal (ADHR) system adjacent to the first RWCU F/D control panel which resulted in high personnel radiation exposure for plant operators while manipulating the RWCU F/D control

FIGURE 3. Original RWCU F/D Control Panel at James A. FitzPatrick NPP

system. Operational dose rates, along with component obsolescence and system reliability issues, drove the station to finally implement a modernization upgrade. The modification provided an opportunity for the station, at the recommendation of the Structural Integrity Chemistry and Materials Group, to implement specific control enhancements in the system. Eliminating the possibility of powdered resin intrusions from the RWCU F/Ds into the reactor vessel and thus, reduce the risk of intergranular stress corrosion cracking of reactor internal materials of construction was a major driver. A long-standing industry recommendation from 1976 was to modify the control system to reduce the possibility of powdered resin intrusions, but these recommendations could not be practically implemented, due in part to the complexity of modifying the original relay-based control system.

The replacement control system supplied by Structural Integrity was designed with a state-of-the-art automation system utilizing the Allen-Bradley ControlLogix PLC platform (Figure 4) in combination with dual, Allen-Bradley Human Machine Interface (HMI) industrial workstations operating in the Windows® environment (Figure 5). For the remote field signals, an in-cabinet modular design using the Allen-Bradley Flex I/O line (Figure 6) was chosen to provide the appropriate mix of digital and analog input/output (I/O) hardware for the associated field equipment and instrumentation signals.

The associated HMI graphics application programs and PLC ladder logic (Figures 7 and 8) were both developed in-house by SI. Utilizing the Chemistry and Materials Group's extensive experience with filter demineralizer backwash and precoat (powdered resin) systems, process improvements to the backwash and precoat sequences were layered into the automation software design. Also, the design incorporated operator feedback with regards to expanded operational control features, including the ability for Operations' supervisors to fine-tune the control system configuration through the HMI workstation.

Continued on next page

FIGURE 4. Allen-Bradley PLC (ControlLogix Platform)

FIGURE 5. Allen-Bradley HMI Industrial Computer (750R)

FIGURE 6. Allen-Bradley PLC (Flex I/O Modules)

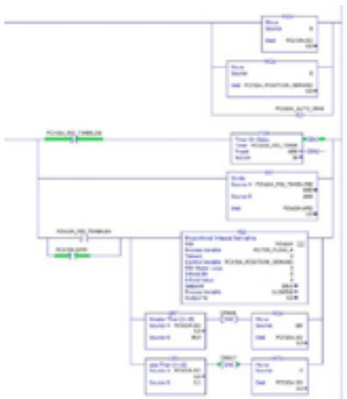

FIGURE 7. AF RWCU F/D Control System - PLC Ladder Logic

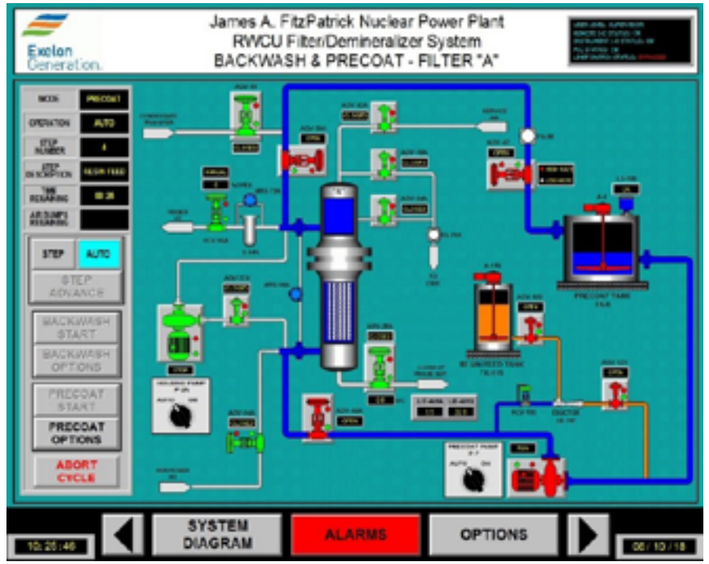

FIGURE 8. JAF RWCU F/D Control System - HMI Software Application Graphics

The original RWCU, F/D control system, not only required access to the ADHR's high dose field near the control panel but also needed access to the adjacent RWCU, F/D instrument rack to monitor process conditions and manipulate the system's rack-mounted flow controllers. The new RWCU, F/D control system, was arranged to eliminate all operations near the ADHR system, addressing the dose issue (Figure 9). A new Operator Control Panel, where Operations performs system operations, was installed in a low dose ALARA area away from the ADHR system and included the ability for the operator to access and control a dedicated instrument rack camera for remote monitoring. The original control panel was replaced with an I/O panel housing the mix of I/O hardware for the associated field equipment signal wiring and a third panel was placed adjacent to the RWCU, F/D instrument rack housing the mix of I/O hardware for the associated instrumentation signal wiring. The incorporation of the instrument panel into the design allowed the original system's rack-mounted flow controllers to be removed and replaced with virtual flow controllers at the Operator Control Panel and houses sufficient I/O hardware in the event the station decides to modernize the instrument rack in the future. The three new control system panels were interconnected with a fiber optic communication cable (TCP/IP protocol).

FIGURE 10. JAF RWCU F/D Control System Simulator

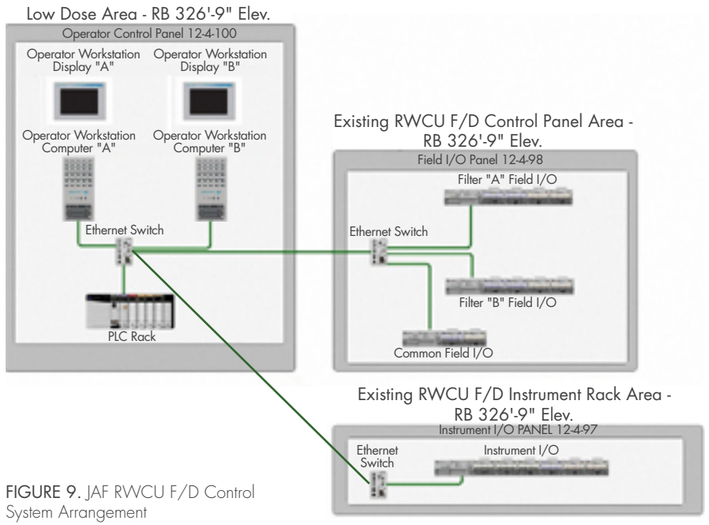

FIGURE 9. JAF RWCU F/D Control System Arrangement

The outage work for the RWCU F/D control system at JAF included complete removal of the original DeLaval system and installation of the Structural Integrity system followed by a fully functional/startup test. Since the RWCU F/D system is required to be in service before reactor startup to achieve industry chemistry goals, any delays in the installation and testing schedule due to poor system design would have resulted in startup delays and would have placed the RWCU F/D control system modification on the critical path. Therefore, Structural Integrity ensured during the design phase that the re-landing of the approximately 200 field wires would mesh seamlessly with each of the new control panels' field wire terminals, avoiding time-consuming field splices as well as optimizing installation time. Additionally, to verify that the supplied automation control system would work as designed with minimal field revisions, Structural Integrity built a hard-wired simulation system (Figure 10) that duplicated all of the RWCU F/D instrumentation and equipment. The simulator was utilized by Structural Integrity to develop and challenge the PLC and HMI software applications. JAF personnel further used the simulator during both factory and site acceptance testing to ensure that all design requirements were met and that operators were proficient with the new automation control system before startup. The JAF engineering department was also able to utilize the simulator to aid in the development of the installation/startup test procedure as well as identify improvements to the plant operating procedure.

With Structural Integrity engineers providing round-the-clock site support, critical path impacts were avoided as the installation/startup testing (Figure 11) was completed in approximately four days – well within the anticipated contingency timeframe and more than one week before reactor startup demonstrating the quality and value that Structural Integrity delivers. The success of the JAF RWCU F/D control system upgrade has had a positive impact within Exelon as Nine Mile Point (NMP) contracted Structural Integrity immediately after the JAF startup to design, fabricate and deliver a simulator system earlier this year for their Unit 2 Reactor Water Cleanup system upgrade. Fabrication and testing of the NMP simulator unit were completed, and the simulator was shipped to NMP's training facility in April 2019. Additional stations have inquired about an upgrade to their Fuel Pool Filter/Demineralizer control systems and are currently working through the budget approval process. The modernization of plant automation controls represents a step change in performance that optimizes Operations and Maintenance resources, shifting their focus to performance maintenance and plant monitoring and away from inefficient corrective maintenance and troubleshooting.

FIGURE 11. JAF RWCU F/D Control System Startup Testing

Metallurgical Lab Featured Damage Mechanism:

Waterwall Fireside Corrosion (WFSC) in Conventional Boilers

WENDY WEISS
wweiss@structint.com

Thin edged rupture due to fire side corrosion

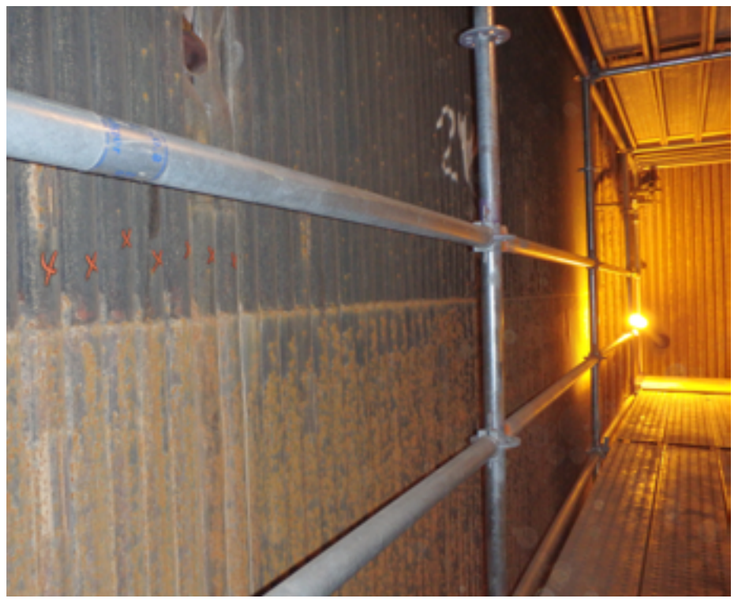

Industry experience shows that waterwall tubing in conventional boilers can be susceptible to fireside corrosion, depending on fuel type, firing practice, etc. In boilers where fireside corrosion has been identified as a maintenance issue, wastage rates of 5 to 25 mils/year are not uncommon. Since the mid 1990s, the installation of low NOx burner systems designed to lower NOx emissions has significantly increased the wastage rates in some boilers. Operators of subcritical boilers have reported wastage rates as high as 30 mils/year, while those operating supercritical boilers have reported rates exceeding 100 mils/year in the worst cases. These higher damage rates have resulted in an increase in tube failures, and operators have struggled to accurately define the extent of the damage and install the appropriate mitigating technologies.

Mechanism

Fireside corrosion is an extraordinarily complex phenomenon due to the number of chemical and physical reactions that influence the damage process. Two important contributors to the damage are corrosive species in the fuel, such as

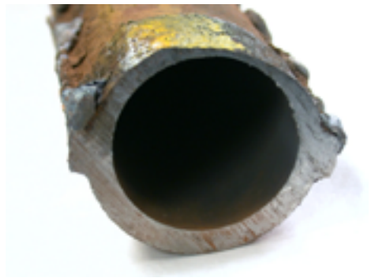

Tube section showing OD wastage

sulfur and chlorine, and the local furnace environment, including the composition of the furnace gases, the composition of the slags that form on the walls as a by-product of combustion, and the tube metal temperatures.

There are three primary mechanisms for fireside corrosion: sulfidation by iron sulfides (pyrites), gaseous corrosion by hydrogen sulfide, and corrosion by alkali chlorides that are produced from gaseous hydrogen chloride. All of these occur in reducing or alternating reducing/oxidizing conditions. Unburned carbon, iron oxide and iron sulfide found in scale overlaid by sintered deposits are typical signs of "poor combustion" and locally reducing environments. Low NOx firing technologies (burners and staged air), by design, stage combustion and create a reducing environment in the lower furnace.

The corrosion rates vary widely as each mechanism is influenced by elemental concentrations and temperature. Tube failures due to fireside corrosion are the direct result of loss of wall thickness, which causes an increase in the hoop stress of the thinned tubes, usually culminating in a longitudinally-oriented thin-lip rupture.

Typical Locations

Due to the influence of the local environment on the extent and severity of the corrosion, the location of damage can vary significantly depending on boiler type and firing system design. Fuel and air nozzle position and condition, coal particle size, and the location of the areas of highest heat flux all are variables that can determine where corrosion occurs and how severe the rate of attack will be.

- Wall fired boiler: the damage usually is concentrated on the side walls from mid burner elevation upward. Front and rear walls may also exhibit corrosion, but usually the wastage rates are much lower.
- Tangentially fired boiler: the greatest wastage rates are typically on the front and rear walls, with the side walls showing much lower rates of attack. The most severe damage often is found from the upper burner elevations into the separated overfired air ports and generally is more predominant in the "hot corners".

Features

- The wastage often is most severe at the crown of the tube, but damage can extend to the entire fireside surface of the tube and the adjoining membrane, if present.
- Tubes that have suffered severe attack will often be covered by a deposit with a hard, dense black layer at the tube metal interface and a layer of soft, loose ash on the outside.
- The external surface usually exhibits an irregular surface beneath the deposits that have a dimpled or "alligator hide" appearance.

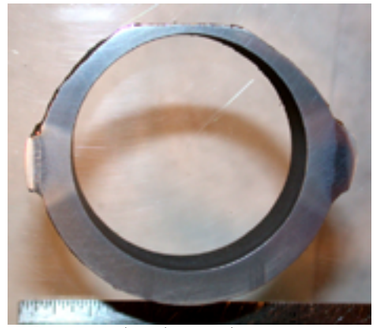

Ring section through area adjacent to rupture showing external wastage around hot side of tube with most severe wastage at crown of tube

SEM

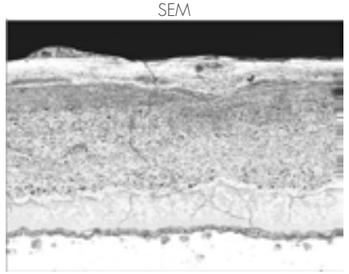

S

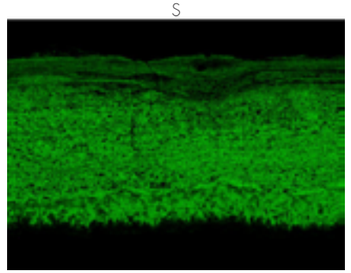

C

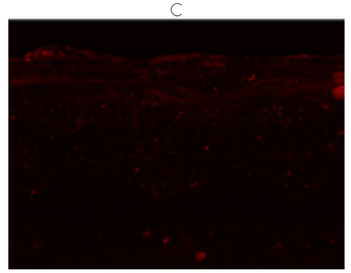

LP economizer tube from an HRSG showing dewpoint corrosion.

Delivering Medical Devices to Market Faster Using Finite Element Analysis

DOUG FANKELL
dfankell@structint.com

In any industry, the time to bring a product to market costs a significant amount of capital. This is especially true in the medical device design world. With the advent of advanced computational modeling techniques, including the non-linear finite element analysis capabilities of Structural Integrity Associates (SI), medical device designers now possess a tool to bring their products to market much more quickly, resulting in lower costs and faster revenue generation.

According to Makeover et. it costs an average of $31 Million to bring a 510k medical device, and $94 Million to bring a PMA medical device from its initial proof of concept through FDA clearance [1]. Sources of this cost include spending significant time and resources on the concept development phases as well as the clinical study phases. Delays in these areas can be extremely costly. Sheldon et. estimated in 2014, that an 8 week delay can cost a 30 person company $1.8 Million in lost time and revenue [2]. If an additional 20 animal clinical study is required or 100 patient clinical study is required, a company should expect to see an estimated cost of $5.5 Million and $10.8 Million respectively [2]. SI uses computational modeling to supplement the design iteration process and help reduce these costs in three primary ways:

1. Speeding up the design process.
2. Predicting potential errors early when they cost much less to fix.
3. Limiting and improving costly experimental testing.

The Design Process

Though the design cycle and process of medical devices can vary significantly in time and complexity, design teams nearly always follow the same general blueprint for taking a device from an idea through to a finished product. The gray boxes shown in Figure 2 show the typical design cycle for a medical device design team. To begin, a team identifies a need in the industry, for example, surgeons constantly ask for "a separate tool to seal vessels in young children". Once a need is identified, the team begins the ideation process. The ideation process involves brainstorming and establishing a potential solution to address the need developed in step one. Often many ideas are chosen and taken to the next step, prototyping the design. During the prototype design phase, the engineering team develops a design of their initial protype or prototypes often using Computer Aided Drafting (CAD). These prototypes are then fabricated and evaluated for their ability to address the need established in the initial step. From the protype tests, new needs or different needs often arise, or the prototype does not perform as expected and the whole process begins again. Once the prototype is deemed to address the need at hand, clinical tests are designed and conducted and FDA approval is sought. Often, over the life of a project, engineering teams may traverse this design loop tens or even hundreds of times, testing multiple prototypes and refining their devices

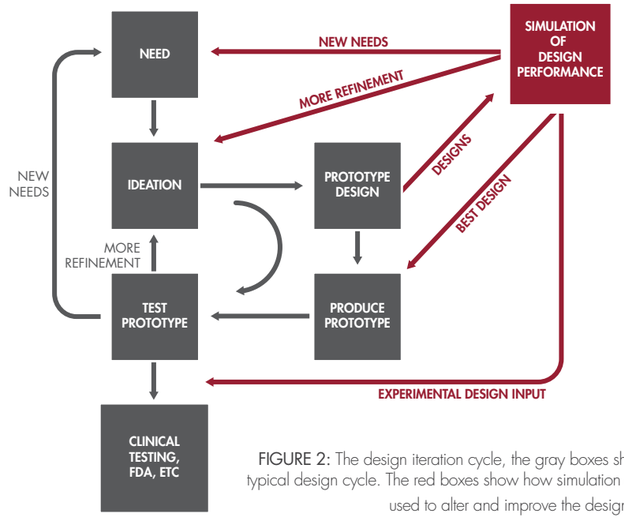

FIGURE 2: The design iteration cycle, the gray boxes show the typical design cycle. The red boxes show how simulation can be used to alter and improve the design cycle.

over time. Depending on the complexity of the device, it can take companies weeks or months just to produce and test one prototype. SI seeks to significantly change this process by using computational modeling to speed up the design iteration process, catch potential errors early in the process ,and limit and improve experimental testing.

Speeding up the Design Process

As mentioned earlier, the design and testing of one physical prototype can take a significant amount of time and be costly. Typically, companies must develop several physical prototypes to arrive at a solution and often could benefit from even more iteration if time and money allowed. Computational simulation allows for design teams to speed up the design process in two primary ways. First, it allows designers to test prototypes virtually, eliminating the need of producing costly physical prototypes and conducting expensive tests. Secondly, it allows designers to converge on the optimal design much more quickly by providing a platform for testing immense numbers of prototypes through optimization schemes and parametric analysis.

It can often take several weeks or months and significant financial resources to procure materials, machine parts, and assemble a prototype. Frequently, all of this is done just to discover the device does not work as intended or tweaks need to be made; thus, another device must be built. With computational modeling, engineers can replace the prototype production and physical testing phases with computational models that often take hours and at most days or a couple of weeks to set up and run. Thus, engineers can gain significant insight into their design in an order of magnitude less time than it would take to build and test a full device, saving them essential time and reaching market (and revenue) much more quickly.

Continued on next page

FIGURE 1: Cost of delays in bringing a medical device to market for a 30 person company [2].

The second benefit of computational modeling's speed is that it allows for many more design iterations to be examined and improved. For example, if a client is iterating in the design process to determine the optimal carbon fiber orientation in a device, it takes them 6 weeks to produce and test a prototype. After 3 prototypes and 18 weeks, they have discovered a workable solution but have not found what they deem to be the optimal solution. They must move forward because they have run out of time and money. To develop a computational model of the device would have taken 2 weeks, and each simulation 3 hours to run. Thus, in the 18 weeks it took to examine 3 prototypes, 128 different simulations and carbon fiber orientations could have been examined, allowing for significant improvement of the device and convergence on an optimal solution.

Predicting Potential Unforeseen Errors

Not only does "virtual prototyping" or computational modeling allow for increased design cycle time, it allows engineering teams to discover potential errors in their device design by allowing them to examine scenarios not possible to reproduce using bench testing. Thus, many errors in device performance are not discovered until in-vivo clinical testing which occurs late in the product development phase. Changes to a device during or after clinical testing are an order of magnitude more expensive than changes during the design iteration phase of product development. Computational models allow for simulations to be conducted representing in-situ conditions before a prototype has even been built, allowing engineers to discover errors that prototype testing would not have caught and doing so when design changes are inexpensive to make.

Limiting and Improving Experimental Testing

Expanding on the benefits laid out in the previous section, computational modeling enables teams to conduct fewer experimental tests and informs the teams of what types of clinical tests will provide the most useful information. For example, a team is looking to examine a vessel sealing device's impact on surrounding tissues. It is not possible to examine the thermal spread to surrounding tissue and organs during an arterial fusion with ex-vivo bench tests, so they must conduct expensive in-vivo animal tests. Additionally, the team is unsure if the in-vivo test will even produce the phenomena they desire to examine. By conducting computational simulations of the tests before performing any experimental tests, the team is able to examine if any damage will occur to the surrounding tissues due to thermal spread, providing the team with an answer to their question without going through the expensive process of a full animal study. Secondly, by conducting the simulations before testing, the scientists will gain insight into what the tests will likely produce, allowing them to make changes to the test, or examine if an alternative testing method would be more beneficial. Therefore, the team can optimize their financial and temporal resources and ensure that their clinical testing produces the desired results.

The Future of Computational Modeling in the Medical Device World

In this work, three arguments have been laid out demonstrating SI's ability to drastically impact a design team's process through the use of finite element modeling and computational simulation. With SI's capabilities, engineers can reduce the time to market of their product, catch unforeseen errors, and improve their experimental testing process, enabling them to get better products to market faster, less expensively. Additionally, the cutting-edge work and research being done at SI is at the forefront of a surge of what may soon become commonplace in the medical device world, for "The FDA also believes that computational modeling is poised to become a critical tool for accelerating regulatory decision making. Continued adoption will be essential for advancing the FDA's mission" [3].

References

[1] Makower, J., Meer, A. Denend, L., "FDA Impact on U.S. Medical Technology Innovation", 2010

[2] Sheldon, M. "Accelerating Medical Device Innovation in the U.S." The National Acadamies Innovation Policy Forum, 2014

[3] Morrison, T.M., Pathmananthan, P., Adwan, M., Margerrison, E., "Advancing Regulatory Science with Computational Modeling for Medical Devices at the FDA's Office of Science and Engineering Laboratories,", Frontiers in Medicine, 2018

TRU Compliance Achieves Accreditation as a Product Certification Body

ANDY COUGHLIN
acoughlin@structint.com

TRU Compliance, a division of Structural Integrity Associates, announced in March the achievement of accreditation from the International Accreditation Service (IAS) as a product certification body for seismic, wind, and blast/physical security performance of nonstructural components. According to the International Accreditation Service, TRU Compliance is the second company to be certified for Seismic performance of non-structural components and the first company to be certified for Wind and Blast/Physical Security performance.

"This is a significant milestone for Structural Integrity and our certification agency, TRU Compliance," Chris Larsen, Vice President of Critical Structures at Structural Integrity comments. "The accreditation further validates our robust program as well as our comprehensive approach, which not only meets the stringent guidelines of the ISO standards but offers our customers a full scope solution for product certification".

TRU Compliance is contracted by domestic and international manufacturers whose products and equipment are required to achieve high performance during and after earthquakes, high wind events, terrorist attacks, and accidental explosions. "This accreditation is critically important for our clients," says TRU Compliance Director Andy Coughlin, "It sets the TRU Compliance certification on a higher plane and paves the way for unified acceptance across hundreds of jurisdictions." The certification process involves subjecting products to activities such as seismic shake table runs, cyclic load tests, simulated wind events, blast testing, vehicle ramming, and engineering analysis simulating these extreme environments in accordance with recognized standards. "Our process is rigorous by design. The products we certify have an independent and verifiable performance during extreme events, meaning you can depend on them to perform when they are most needed," mentions Coughlin.

TRU Compliance's clients are worldwide leaders in the manufacturing and distribution of products for electrical distribution, HVAC, power production, medical diagnostic, life safety, water treatment, building material, and perimeter security. Products achieving the rigorous TRU Compliance standard may bear the TRU Compliance logo and achieve a certification listing on trucompliance.com. Once listed, surveillance and sampling confirm ongoing production continues to create products meeting compliance requirements. Jurisdictions across the United States and Canada have accepted TRU certification for essential facilities such as hospitals, police and fire stations, emergency operations centers, power production and distribution centers, and mission-critical military facilities.

Effective March 17, 2019, the accreditation confirms TRU Compliance conforms to ISO/IEC 17065:2012, the standard governing product certification bodies worldwide. The International Accreditation Service (IAS) maintains an online list of accredited companies at www.iasonline.org.

Metallurgical Lab Case Study:

Cracking of Grade 23 Steel Furnace Wall Tubes

TERRY TOTEMEIER, Ph.D.
ttotemeier@structint.com

Grade 23 is a creep strength enhanced ferritic (CSEF) steel that was designed to offer similar creep strength to Grade 91 but with lower Cr content and, in the original concept, fabrication without pre- and post-weld heat treatment making the material attractive for the furnace wall tubes of ultra-supercritical coal plants where T12 has insufficient strength and T91 would be too complex to fabricate. Experience gained with T23 has shown that pre-heat is necessary and that post-weld heat treatment should also be performed when the material is employed in "high restraint" applications such as furnace wall tubes. Like other CSEF steels, T23 is very sensitive to heat treatment, and care must be taken to ensure that hard, brittle microstructures do not enter service – particularly in high restraint applications such as furnace wall tubes.

More generally, T23 has been employed in some superheater and reheater tubes of coal-fired boilers and HRSGs. In these loose tube applications (low restraint), the experience with the material has been much better (fewer failures), but occasional issues can occur. Most notably, several HRSGs have experienced T23 tube failures at the tube to header connections due to the combination of local bending loads and carbon migration associated with welding to a higher chromium content material.

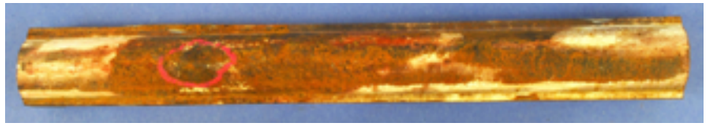

FIGURE 1. Furnace side of the as-received T23 furnace wall tubes. The leak areas are marked with red circles. TOP Tube A BOTTOM Tube B

This article explores a recent tube failure in an ultra-supercritical boiler with T23 furnace wall tubes. Leaks were found on two membrane-welded furnace wall tubes after approximately 37,000 hours of service. Sections of the two tubes containing the leaks were removed and sent to SI's Materials Science Center for metallurgical analysis to determine the cause of the leaks.

Visual Examination

Overviews of the furnace sides of the two as-received tubes (Tube A and Tube B) are shown in Figure 1. The plant had circled the location of a leak on each tube. There were no other indications of mechanical or corrosion damage on either tube; the original paint was still present in many areas.

The tubes were split longitudinally along the furnace membrane weld to reveal the tube inner surfaces. Figure 2 and Figure 3 show close views of the leak areas as seen on the outer and inner tube surfaces. An axially oriented crack was present at the leak area along with the furnace side tube crown in each tube. The cracks were approximately 0.5 inches long. The appearance of the cracks on the two tubes was similar: the crack lengths were more significant on the inner tube surface than on the outer surface, and the cracks were tight, relatively straight, and unbranched. There was no evidence of abnormal corrosion associated with the cracks on either the outer or inner tube surface, although an oxide nodule covered the crack on the inner surface of Tube B (Figure 3).

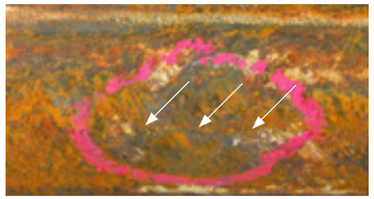

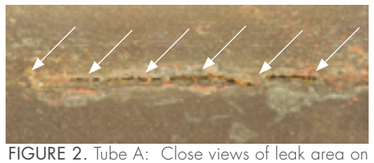

FIGURE 2. Tube A: Close views of leak area on the tube outer TOP and inner BOTTOM surfaces. An axially-oriented through-wall crack was present (arrowed).

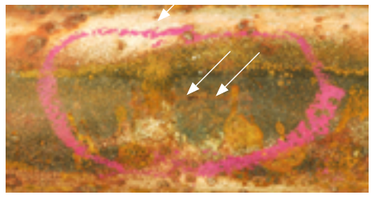

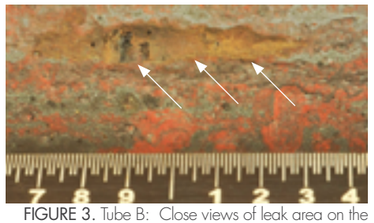

FIGURE 3. Tube B: Close views of leak area on the tube outer TOP and inner BOTTOM surfaces. An axially-oriented through-wall crack was present (arrowed). In Tube B the crack was covered by an oxide/deposit crust on the inner tube surface.

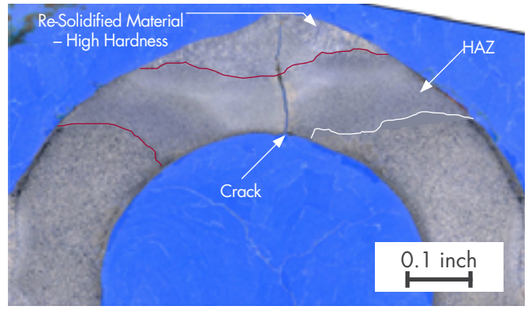

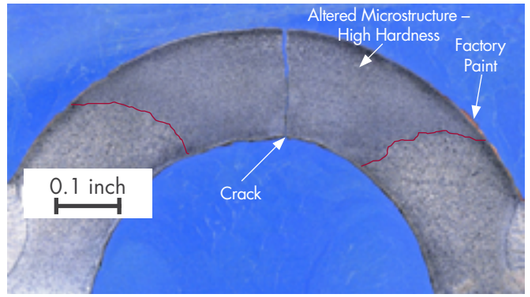

FIGURE 4. Macroscopic overviews of the prepared transverse metallographic cross-sections through the cracks on Tube A TOP and Tube B BOTTOM. Both cracks were associated with a local zone of altered microstructure with relatively high hardness (325 to 340 HV); in Tube A local melting appeared to have occurred. Vilella's etch.

Metallographic Examination

A transverse metallographic section was prepared through each tube at the center of the visible crack. Figure 4 shows macro views of the furnace side of the tubes. In both tubes, the crack was found to run relatively straight through the tube wall with no branching, and there was a large zone of altered microstructure, centered on the tube crown outer surface, in which the crack was present.

In Tube A, the outer tube wall at the crown had a columnar grain structure, and the profile of the outer tube surface was irregular, indicating that local melting had occurred. The heat-affected zone (HAZ) associated with the melting extended through the tube wall. The crack itself was more open on the inner half of the tube and tighter on the outer half of the tube; the transition points roughly corresponded to the transition from the HAZ to a re-melted structure. As shown in Figure 5, the inner length of crack was significantly oxidized, whereas there was very little visible oxidation on the outer length of the crack. The thickness of the oxide in the crack was approximately the same as found along the inner tube surface.

There were no microstructural features or significant corrosion attack observed at the tube inner or outer surfaces which might have led to the cracking, other than the gross microstructural alteration created by the melting. Figure 6 compares the typical columnar grained, bainitic microstructure found in the melted zone with the equiaxed, tempered bainite structure found on the casing side of the

Continued on next page

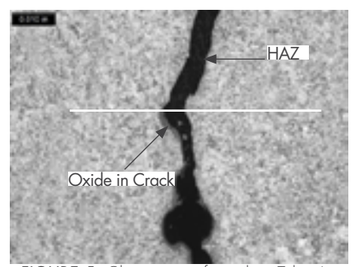

FIGURE 5. Close view of crack in Tube A at approximately the mid-wall location, showing the transition from the being oxidized toward the ID TO BOTTOM to being unoxidized toward the OD TO TOP.

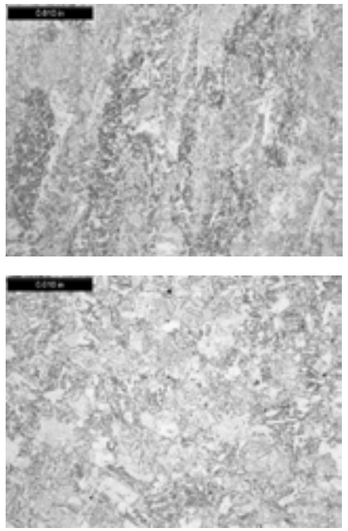

FIGURE 6. Comparison of the columnar-grain, re-solidified microstructure near the OD of Tube A TOP with the normal tempered bainite T23 microstructure observed on casing side of Tube A BOTTOM. Vilella's etch.

tube, typical of non-affected areas in both tubes and normal for Grade 23 material.

Similar microstructural features and cracking morphology were observed in Tube B. One difference was that in Tube B there were no indications of local melting, but rather the region of altered microstructure consisted of untempered bainite, indicating heating above the lower critical temperature. There was also an area where the original factory paint was present over the altered microstructure, as shown in Figure 4.

Two additional transverse sections were prepared from each tube to determine if the altered microstructure was localized or present over a large area. None of the other sections showed evidence of alteration, so the altered microstructures appear to be localized to the areas of the cracks.

Hardness, Dimensional Measurements, and Chemical Analysis

The Vickers hardness was measured in the microstructurally altered areas and at a mid-wall location on the casing side of the tubes. The average hardness for the altered region in Tube A was 325 HV10; the average hardness for the altered region in Tube B was 342 HV10. The average hardness on the casing side of the tubes was 172 and 174 HV10 for Tubes A and B, respectively, both normal for T23. The high hardness values indicate the presence of untempered bainite and martensite, consistent with the observed microstructural features.

Checks on the dimensions and chemical compositions of the two tubes were performed; these were found to agree with the specified values.

Discussion

In both tubes, the cause of the cracking appears to be severe local overheating, which will result in high local residual stresses and a relatively hard, untempered microstructure with reduced ductility and greater susceptibility to cracking mechanisms such as stress corrosion cracking and reheat cracking. The most likely cause of very localized heating to well above the lower critical temperature (A_1) or melting temperature is a welding arc strike, although it is possible that some other electrical arc strike could have occurred during the manufacture of the membrane welded panels, for example, shorting.

Factory paint was found covering the microstructurally altered area in Tube B so that it appears that the overheating occurred in the boiler shop during the manufacturing of the panels. For Tube A it is not certain that the overheating happened in the factory since the factory paint was not present near the cracks, having been removed either by service exposure or during the investigation of the leaks. Overheating in Tube A may have occurred in the factory, during erection, or at some other later time. The lack of significant plastic deformation in the overheated area indicates that overheating did not occur while the tube was pressurized in service.

Because the inner halves of the cracks were oxidized to a similar extent as the tube inner surfaces, initial cracks about halfway through the tube wall appear to have formed either before or shortly after entering service, with these cracks then subsequently propagating through the remainder of the tube wall. The propagation mechanism is not clear; the outer halves of the cracks were separated, and the microstructural features on opposite sides of the cracks did not match, indicating that the crack faces were eroded by fluid flow once the cracks were through-wall, and the inter- or transgranular nature of the crack path in this area could not be determined. However, there was no evidence of gross plastic deformation or creep cavitation found associated with the crack. In this case, it was recommended that the manufacturer of the waterwall panels be consulted to determine the likely source of the overheating and other possible locations where it may have occurred. These areas could be checked for part-through-wall cracks using ultrasonic inspection techniques.

Conclusion

The root cause of the cracks found in these tubes was severe local overheating which led to both a local microstructural region susceptible to reheat and stress corrosion cracking and to high residual stress levels needed to drive the cracking. This case is a good example illustrating the need for higher manufacturing, handling, and quality control standards when working with CSEF steels versus conventional low-alloy boiler steels (e.g., Grades 11, 12, and 22), since Grade 23 is intrinsically more susceptible to failure modes such as reheat cracking and stress corrosion cracking. A local overheating event such as found in this investigation most likely would not have resulted in through-wall cracking for a membrane panel manufactured from a conventional furnace wall tubing alloy such as T12 (1 ¼ Cr – ½ Mo).

Identifying Failure Mechanisms of Typical I-Section Floodwalls

ERIC KJOLSING, Ph.D., PE
ekjolsing@structint.com

DAN PARKER, PE
dparker@structint.com

In 2018, Structural Integrity Associates, Inc. (SI) supported the United States Army Corp of Engineers (USACE) in the structural assessment of the concrete-to-steel connection in typical I-Section flood walls. A representative flood wall section is shown in Figure 1. This effort was part of a broader scope of work in which the USACE is revising their guidance for the design of flood and retaining walls, EM 1110-2-6066. The purpose of the structural assessment was to better understand the mechanics of load transfer from the reinforced concrete section to the embedded sheet pile. Three-dimensional finite element models of the connection were developed employing non-linear constitutive properties for the concrete, structural steel and reinforcement to achieve this goal. A total of nine different I-Wall configurations with varying wall geometry, sheet pile embedment depth, and connection details were analyzed. Hydrostatic load was applied incrementally to simulate the actual load distribution due to a rising water level.

ANACAP, SI's proprietary concrete constitutive model, was used in the analyses to accurately predict the concrete behavior. Among other capabilities, the ANACAP model can capture multi-axial tensile cracking, compressive crushing with strain softening, and crack dependent shear stiffness. Figure 2 shows the evolution of a failure mechanism through the connection in one of the analyses as the hydrostatic load (i.e. water level) is increased. These results, along with additional variational studies, identified the typical failure mechanisms and limiting capacities of the embedded sheet pile connection, as well as providing assessments on the efficacy of retrofit measures and new connection design details.

Please contact Dan Parker, PE if you are interested in learning more about ANACAP or how SI might help you in the evaluation of civil infrastructure.

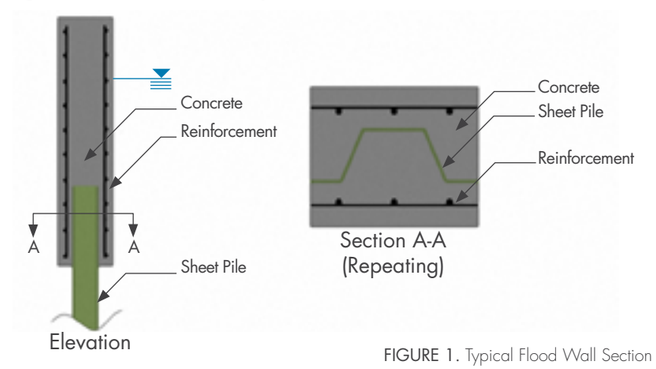

FIGURE 1. Typical Flood Wall Section

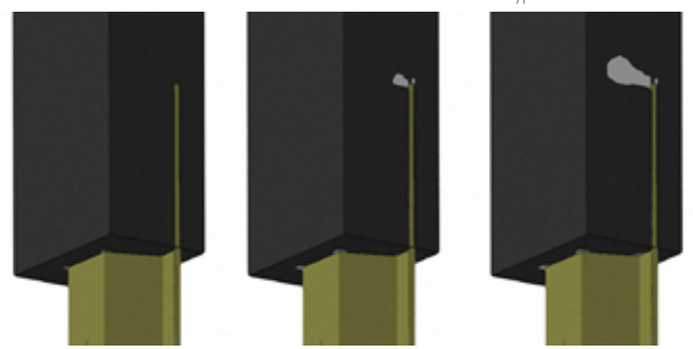

FIGURE 2. Crack Propagation (shown in grey) with Increasing Hydrostatic Load

Evaluation of Reconfiguration and Damage of BWR Spent Fuel During Storage and Transportation Accidents

BILL LYON
blyon@structint.com

Structural Integrity Associates is participating in a Department of Energy (DOE) Integrated Research Projects (IRP) program focused on storage and transportation of used nuclear fuel (UNF). The project, entitled Cask Mis-Loads Evaluation Techniques, was awarded to a university-based research team in 2016 under the DOE Nuclear Fuels Storage and Transportation (NFST) project. The team is led by the University of Houston (U of H) and includes representatives from the University of Illinois at Urbana-Champaign, the University of Southern California, the University of Minnesota, Pacific Northwest National Laboratory, and staff members from the Nuclear Fuel Technology and Critical Structures and Facilities divisions of SI. The primary objectives of NFST are to 1) implement interim storage, 2) improve integration of storage into an overall waste management system, and 3) prepare for large-scale transportation of UNF and high-level waste. The goal of the cask mis-load project is to develop a probabilistically informed methodology, utilizing innovative non-destructive evaluation (NDE) techniques, determining the extent of potential damage or degradation of internal components of UNF canisters/casks during normal conditions of transport (NCT) and hypothetical accident conditions (HAC).

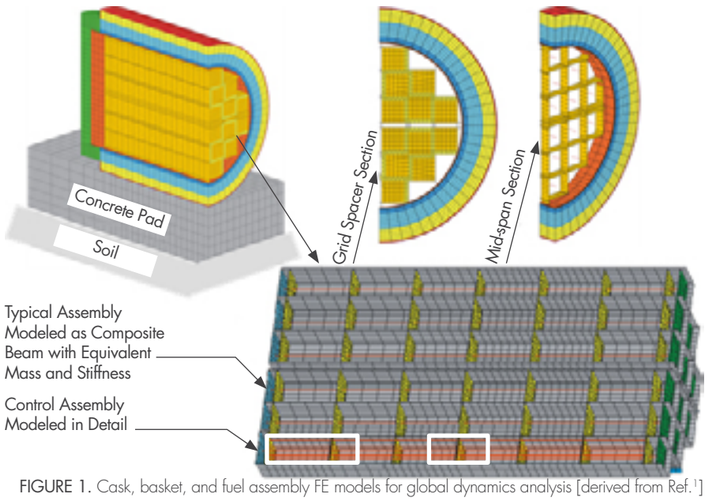

FIGURE 1. Cask, basket, and fuel assembly FE models for global dynamics analysis [derived from Ref.[1]]

An integral part of this methodology uses thermal-mechanical simulations to determine the fuel-assembly/fuel-rod response and subsequent reconfiguration for NCT and HAC. These analyses are comprised of two primary steps 1) global modeling and explicit-dynamics structural analysis, and 2) local fuel performance modeling and failure analysis. The results of these analyses will yield data defining the global forces acting on the fuel rods, spacer grid, and assembly distortions and deformation, and fuel rod failure probability/potential. Our team has conducted extensive work on Pressurized Water Reactor (PWR) fuel during past research sponsored by EPRI [1, 2, 3]. The focus of this new research effort will be high burnup Boiling Water Reactor (BWR) fuel and associated transportation casks.

The four primary objectives for the thermo-mechanical simulation work under the cask mis-load project are the determination of:

- Global forces acting on the components of the fuel assemblies
- Fuel rod, spacer grid, and overall assembly distortions and deformation under the defined conditions
- Failure probability/potential of fuel rods under the defined conditions
- The most likely fuel reconfiguration events

This data will ultimately provide feedback for the calibration and validation process linking the mock-up testing and NDE phases of the overall cask mis-load project methodology.

To date, much work has been completed on the finite element (FE) model analyses needed for the cask level dynamics analyses. This model is based on design information for the Hi-STAR 100 cask, MPS-68 canister, basket, and surrogate GE-14 fuel assembly and rod models (the specific GE-14 design is proprietary). The FE model implementation is based on our prior work using 3D modeling for PWR fuel, assembly, and cask designs. Figure 1 provides several 3D views of prior cask, basket and assembly models developed for PWR fuel types. The BWR-based models are derived along the same path but incorporating the specific design aspects for the components noted above. The surrogate BWR fuel assembly model is integrated into the cask and basket model, as shown in Figure 2. As an example, Figure 3 shows the computed response of the fuel assembly and basket models at the apex of the 9-meter drop analysis.

As noted above, the global forces acting on the components of the fuel assemblies as determined with the dynamics analyses are transformed to determine the force and stresses exerted on individual fuel rods within the assembly.

Continued on next page

Photo by George Joch/courtesy Argonne National Laboratory.

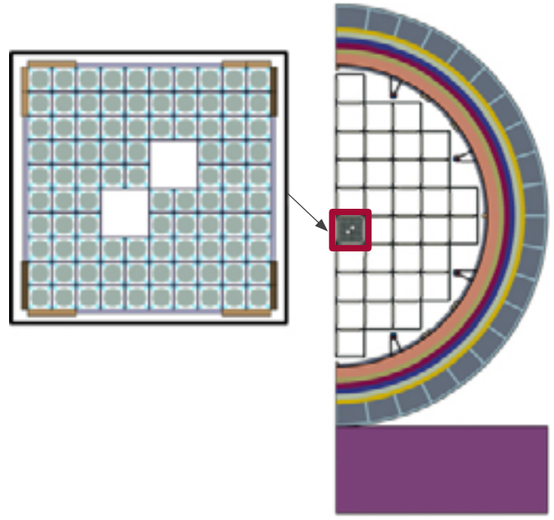

FIGURE 2. Integration of a fuel assembly model into the cask and basket model

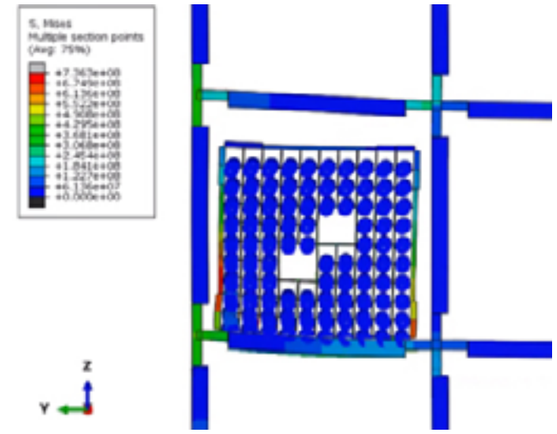

FIGURE 3. Fuel assembly and basket displacement, deformation, and stress computed for the 9-meter drop analysis

Single fuel rod FE model analyses are conducted to evaluate the distribution of stresses and deformation on the cladding. The preliminary results of these analyses are shown in Figure 4 representing the impingement of an external load, for example, at a grid spacer location, on the cladding surface.

Upcoming work will focus on the development of a Zr-2 radial hydride damage model which will be used to relate the effects of the evolution and concentration of radial hydrides during dry storage to the failure probability

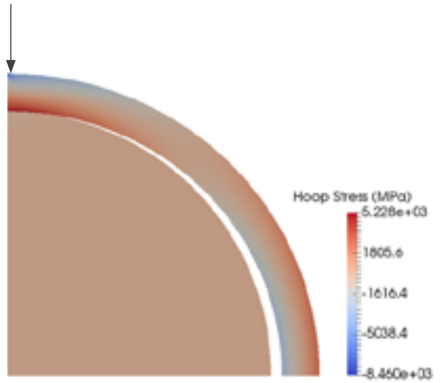

FIGURE 4. Deformation and stress from external impingement on a single fuel rod during the 9-meter drop analysis.

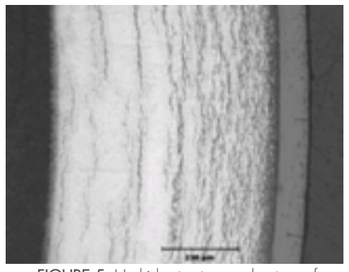

FIGURE 5. Hydride structure and outer surface oxide for high burnup cladding with an average hydrogen concentration of 600 ppm [3]

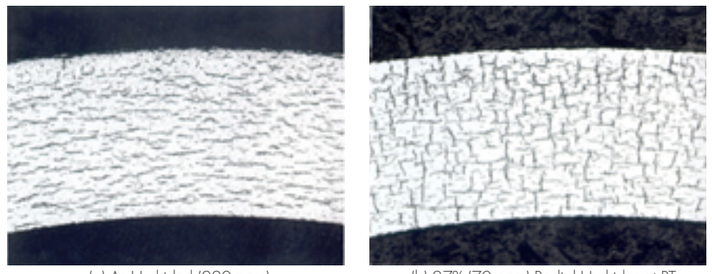

(a) As Hydrided (220 ppm) (b) 27% (70 ppm) Radial Hydrides at RT

FIGURE 6. Hydride structure of cladding samples prepared for mechanical testing: (a) circumferential versus (b) mixed circumferential + radial hydrides [3]

under the stress conditions defined by the global dynamics analyses. Under normal irradiation conditions, hydrides are formed within the cladding material as a result of the diffusion of hydrogen released from the corrosion and oxidation of the exterior of the fuel rod. These hydrides generally form circumferentially in decreasing concentration from the exterior to the interior of the cladding (Figure 5). During the drying process, as spent fuel is prepared for encapsulation in dry storage casks, the orientation of the hydrides can change from circumferential to radial resulting in a mixed hydride structure such as shown in Figure 6 (the cladding material in these samples was artificially charged with hydrogen for testing). Hydride reorientation occurs as a result of the increased cladding stress from the higher internal pressure experienced by the fuel rod as the temperature rises (up to a maximum of 400 °C) during the drying process.

The presence of radial hydrides has a dramatic effect on the mechanical response of the cladding under load and can significantly increase the probability of cladding failure at much lower cladding strains. Ultimately, the Zr-2 radial hydride damage model will be used to inform the local fuel rod analysis and provide a more accurate determination of the probability of fuel rod failure resulting from the local impingement forces experienced during NCT and HAC. This work is new and significant in that it is the first application of this analysis methodology for a BWR fuel design and represents a substantial advancement in the assessment of BWR UNF during normal and hypothetical transportation conditions.

References

[1] Spent Fuel Transportation Applications: Fuel Rod Failure Evaluation under Simulated Cask Side Drop Conditions, 1009929, EPRI, June 2005.

[2] Spent Fuel Transportation Applications: Longitudinal Tearing Resulting from Transportation Accidents – A Probabilistic Treatment, 1013448, EPRI, Final Report, December 2006.

[3] Spent Fuel Transportation Applications – Assessment of Cladding Performance, A Synthesis Report, 1015048 EPRI Technical Report, December 2007.

Turnkey Rapid-Response Plant Support

Disposition of Wall Thinning in Standby Service Water Piping

JASON VAN VELSOR
jvanvelsor@structint.com

ROGER ROYER
rroyer@structint.com

ERIC HOUSTON
ehouston@structint.com

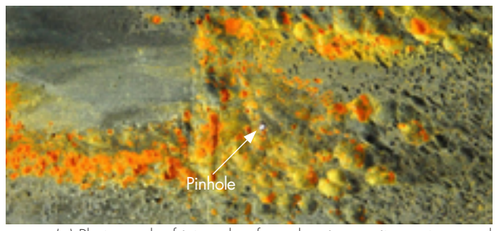

(a) Photograph of internal surface showing cavity wastage and through-wall leak

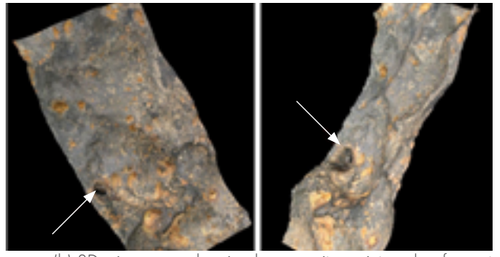

(b) 3D microscopy showing large cavity on internal surface at through-wall location

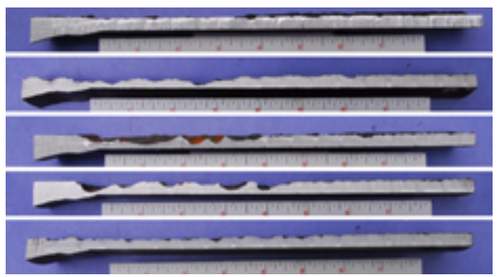

(c) Cross-Section views of destructive testing near leak location

FIGURE 1. Laboratory Examination of Leak Location

Structural Integrity recently had the opportunity to support a client's emergent needs when their Standby Service Water (SSW) piping system experienced a pinhole leak just downstream of a valve. Concerned about other locations in the piping system with similar configurations, the site asked SI to assist with the expedited development of assessment and disposition plans for these other components. In response, SI was able to lean on our core competencies in failure analysis, advanced NDE inspection, and flaw evaluation to develop and deploy a comprehensive solution that met our client's expedited timeline and helped them to mitigate the threat of future unplanned outages. The following sections outline how SI utilized our *in-depth knowledge, cutting-edge technology, and world-class engineering* to meet our client's needs.

Failure Analysis

Following discovery of a pinhole leak in a 10-inch diameter SSW pipe, downstream from a valve, SI's client removed the section of pipe from service and sent the damaged section to SI's Material Science Center where a comprehensive failure analysis was completed. As part of the failure analysis, SI conducted detailed visual examinations, chemical analysis, high-resolution 3D digital microscopy, metallography, and deposit analysis on the received sample. Based on the detailed analyses completed, SI was able to confirm that the observed damage was caused by cavitation that resulted from the turbulent flow and abrupt pressure changes at the throttled upstream valve.

Cavitation happens when the local pressure is reduced to that of the vapor pressure, which commonly occurs in pumps and throttled control valves. At this low pressure, bubbles of water vapor or steam form. The bubbles flow downstream with the water, become unstable, and implode. The bubble

Continued on next page

collapse releases a small but intense shock wave or microjets that break away the protective oxide layer. The newly exposed surface corrodes and the process repeats. Bubble formation and collapse may occur in just a small fraction of a second. Each bubble collapse produces a relatively small amount of damage, with significant damage accumulating during thousands of bubble formation and collapse cycles. Once surface irregularities are formed, bubble formation/attachment will tend to concentrate at damage sites, eventually producing deep, localized attack such as that observed on the pipe section.

The failure analysis completed by SI further determined that the cavitation was occurring intermittently and was likely associated with specific operating conditions of the valve and pipe, suggesting that the cavitation could potentially be minimized through operational changes or controls. The failure analysis process also confirmed that the pipe material had a normal microstructure and that there were no anomalies that contributed to the loss of material.

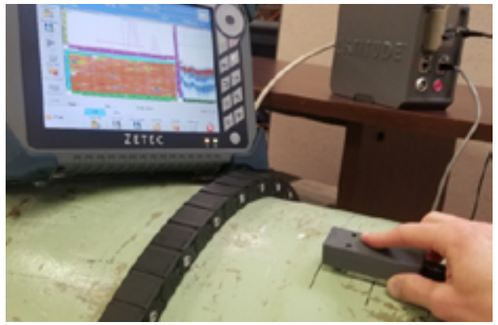

(a) Typical LATITUDE data Collection

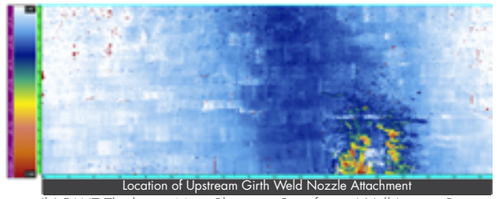

(b) PAUT Thickness Map Showing Significant Wall Loss in Region Near Leak

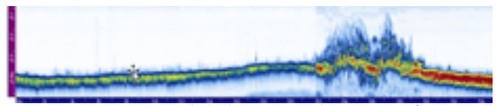

(c) PAUT Cross-Sectional Thickness View Showing Significant Wall Loss in Region Near Leak

FIGURE 2. LATITUDE Images from Laboratory Examination of 10" SSW pipe section.

Advanced NDE

In preparation for the field inspection of the other at-risk components, SI was also tasked with developing an NDE approach for efficient high-resolution wall thickness characterization and demonstrating the approach on the 10-inch sample that was removed from service. Obtaining accurate, high-resolution thickness information was paramount as the data would potentially be used as input for Finite Element Analysis (FEA) if any identified material loss exceeded a critical threshold.

To meet this demanding requirement, SI employed a dual-matrix phased array probe for fast high-resolution coverage and our patent-pending non-mechanized position encoding technology, LATITUDE™ . LATITUDE enables the NDE operator to manipulate the inspection probe by hand, with no mechanical hardware, while still gathering multi-axis encoded data. This approach reduces both the amount and complexity of equipment required on-site and eliminates a significant amount of data post-processing time by removing the need to manually merge individual line scans. This enables the solution to be deployed more quickly and more cost-effectively than other more complicated scanning systems.

The encoded PAUT corrosion mapping approach was demonstrated on the 10-inch diameter sample with the pinhole leak, prior to destructive testing. The results from this examination are shown in Figure 2. Analysis and measurement results from the destructive testing confirmed the accuracy of the developed NDE examination approach.

Engineering Support

In preparation for the examination of the in-service components, SI developed evaluation templates such that detailed evaluations of any identified material loss could be conducted rapidly. The evaluation templates met the structural requirements of the Code of Construction and, therefore, represent a more accurate description of the required section geometry relative to hand calculated t_{min} values. Any inspection findings that meet the requirements of an analysis completed with the prepared templates can be considered acceptable for continued operation until the end of the inspection interval.

If thinning was discovered that was near or below t_{min}, SI was on-call to conduct specific FEA modeling using thickness measurements obtained from NDE examinations and location specific loading. In this situation, finite element models are utilized to calculate the stress field associated with non-uniform pipe thickness obtained from the NDE examinations. Guidance from ASME Section III, NB-3200, Design by Analysis, is taken to determine how component stresses are combined as well as the specific stress allowables. A typical finite element model used in this type of analysis is shown in Figure 3.

A detailed FEA model (developed to easily accept inspection grid data) and calculation template were created for our client as a contingency. If the observed wall thinning profile is found to meet the Code of Construction stress limits, additional uniform wall loss can be applied to determine the amount of allowable thinning. Integration between the NDE and engineering teams, along with the preparation of a template calculation and FEA model, allowed SI to guarantee rapid support. Thus, if an evaluation was required, the analysis results would be available within 24 hours.

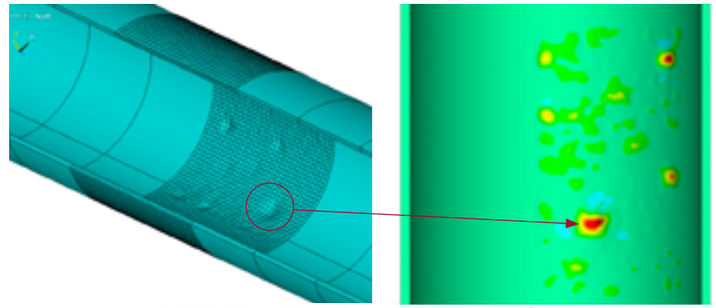

FIGURE 3. Typical Finite Element Model Generated from Encoded PAUT Data

Field Deployment

In addition to performing corrosion mapping on the 10-inch pipe sample that was removed from service, SI deployed a team of two NDE professionals to conduct on-site examinations of one 10-inch and two 18-inch components with similar configurations as the component that had experienced the pinhole leak. On each component, corrosion mapping was completed over a 360° area from the valve flange girth weld, continuing downstream for approximately 12 to 18 inches, to capture the area that was determined to be susceptible to cavitation. Each examination took several hours, including set-up, primary and supplemental data acquisition, and teardown.

Some amount of cavitation damage was identified in each component examined; however, none of the damage exceeded the allowable t_{min} and the FEA modeling contingency was not implemented.

SI provides the individual services described in this article on a regular basis for many of our clients but it is when the SI team gets to collaborate, bringing together our combined areas of expertise, that we are able to maximize the value of the solutions that we provide and to deliver on a tight timeline. For more information about the work summarized here, please contact Eric Houston, ehouston@structint.com.

(a) Extent of Condition Exam Location

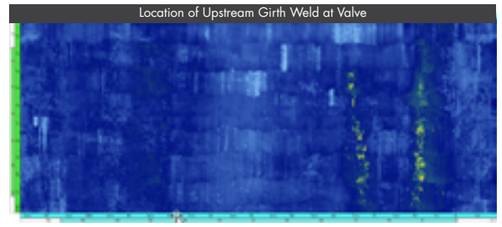

(b) PAUT Thickness Map Showing Minor Wall Loss Downstream of Valve

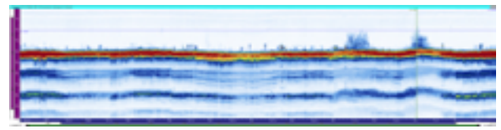

(c) PAUT Cross-Sectional Thickness View

FIGURE 4. LATITUDE Images, Extent of Condition Exam

Multi-discipline Solution for Pressure Vessel Asset Management

DAVID SEGLETES
dsegletes@structint.com

DAN PETERS
dpeters@structint.com

One of the strengths of the Structural Integrity Associates (SI) team lies in the diversity of the skills and capabilities in the organization. Sure, SI can perform inspection, analysis, design, metallurgy, failure investigations, risk assessments, and project management, but one of the real values of working with SI is when all of those aspects are brought together to solve an issue.

FIGURE 1. PT indication in head

Recently, a client approached SI after finding a through-wall flaw in an autoclave at the head-to-shell weld as indicated by a visible dye liquid penetrant examination (Figure 1). The autoclave was one of eight similar vessels used for processing the client's product. Three of the autoclaves are identical in construction to the flawed autoclave and operate with similar process conditions. Remote visual examination by the client indicated that all four autoclaves had similar observations at the inside of the head-to-shell weld, but only one was leaking. The remaining four autoclaves are smaller and are used infrequently. The initial call from the client was for SI to provide emergent support for inspection of the three autoclaves identical to the leaking one to meet production demands. SI responded quickly and examined all four autoclaves using a manual phased array ultra-sonic technique (PAUT) from the exterior of the vessel. The manual PAUT examination provided excellent coverage of the weld region and visualization of the through wall flaw (Figure 2).

The autoclaves are austenitic stainless steel, Type 304 and were constructed from a formed head, two shell sections, and a flanged opening. The sections were welded together using a single "V" weld preparation. The autoclaves are heated using electrical resistance strip heaters affixed to the outside diameter (OD) of the vessel. The autoclaves operate at a temperature of approximately 680°F (360°C) and a pressure of approximately 2690 psig (185 bar).

Ultrasonic Testing

The PAUT technique was selected over conventional ultrasonic testing for the examination of the welds, because it interrogates the full volume of interest using multiple beam angles simultaneously. The objective of the examination was to quantify the current condition of the autoclave vessels. The autoclave with the through-wall flaw was examined, and the flaw extent was mapped (Figure 3). One of the three similar autoclave vessels contained a significant indication (about 50% through the wall) at the head to shell weld with a 360° extent. The other two autoclave vessels contained intermittent flaws, about 30% through the wall. Due to geometric constraints, only the head-to-shell and flange-to-shell welds could be examined using the manual PAUT technique from the autoclave vessel OD. Evaluation of the PAUT data indicated that significant intergranular stress corrosion cracking (IGSCC) to be present in the weld zones.

Metallurgical Testing

In parallel with examining the vessels, SI developed tooling to remove core samples from the vessel with the through-wall flaw (Figure 3). The

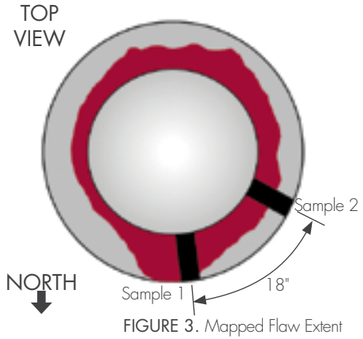

FIGURE 3. Mapped Flaw Extent

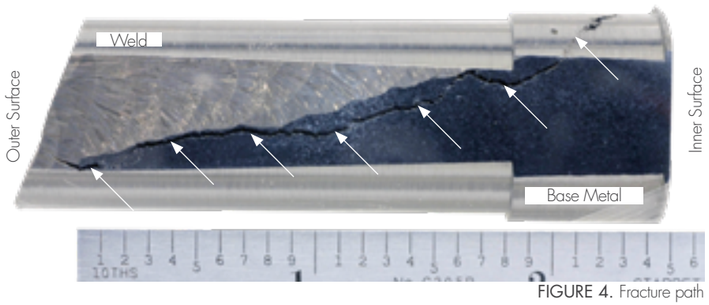

FIGURE 4. Fracture path

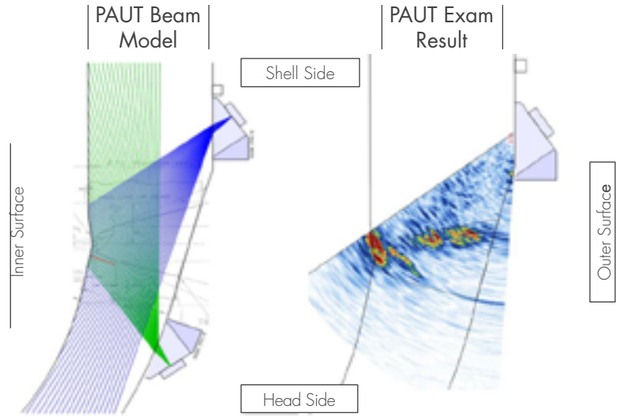

FIGURE 2. Manual PAUT Examination

core samples were submitted to the SI metallurgical services laboratory for assessment of the flaw and determination of cracking mechanism. An over-view of one of the core samples is provided [Figure 4]. The fracture path was adjacent to the weld, in the base metal heat affected zone (HAZ). Under higher magnification, it was observed that the fracture was intergranular and severely branched, to the point that several grains were released during the sample preparation process [Figure 5]. IGSCC of austenitic stainless steel has been reported across multiple industries representing a plethora of environmental conditions. The environmental conditions (high temperature, high purity water) and cracking observed in boiling water reactor (BWR) environments are comparable to the conditions of the flawed autoclave. The removed core

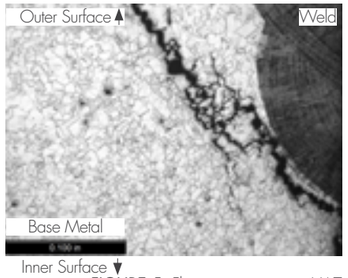

FIGURE 5. Flaw propagation in HAZ

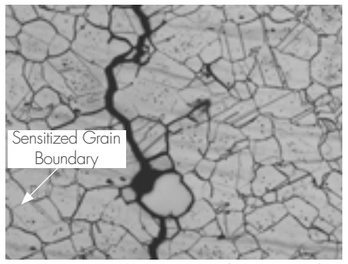

FIGURE 6. Sensitized Grain Boundary

samples were metallurgically etched to reveal any sensitization of the HAZ. Substantial grain boundary sensitization was observed as given by the wide and dark appearance of the grain boundaries (Figure 6). The chemical composition of the base metal was determined as part of this investigation and met the expected composition for type 304SS. The carbon content of the base material was at a level sufficiently low that

Continued on next page

the materials could be considered to be near the upper boundary of what would be regarded as "L" grade materials. The "L" grade variant of type 304SS was introduced to reduce the impact of welding heat on the sensitization of the HAZ.

Additionally, a scanning electron microscope was used to evaluate the crack tip. It detected traces of chlorides and fluorides. Discussion with the client indicated that a potential source could be the service water being used in the vessel.

Fitness-for-Service

Once the extent of the flaws was established in the autoclaves without a through-wall flaw, a fitness for service evaluation was performed per API 579-1/ASME FFS-1 (API 579). API 579 provides industry established guidance in the assessment of pressurized components containing flaws for continued service and is recognized by the National Board Inspection Code.

A life assessment of the vessel was performed utilizing Part 9, fracture mechanics assessment, including SCC: involved cracking. The stresses in the vessel shell were evaluated using a finite element model (Figure 7). The life assessment of the vessel was performed initially using standard crack growth models from API 579 for "crack growth in a light water reactor environment." It was quickly determined that the evaluation was inadequate as it showed that the life of the vessels should be extremely long. The current vessels were installed in the 1980s, thus operating for approximately 40 years. A model for IGSCC from NUREG 0313 Rev 2 was also evaluated based on the findings from the PAUT and metallurgical assessments. This model showed that the entire life of the vessel would be approximately 12 years.

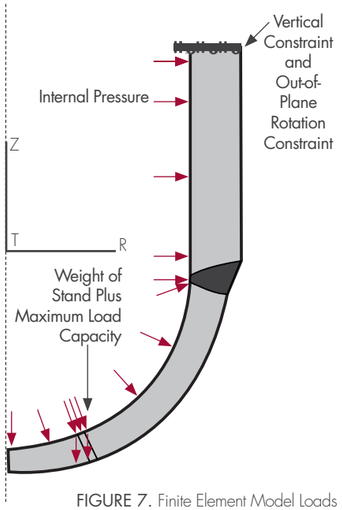

FIGURE 7. Finite Element Model Loads

Discussion with the client was needed to determine which of the crack growth models more closely matched the problem at hand. The initial reaction was that neither one could be correct. However, after some discussion, it was determined that the facility had changed from well water to city water around fifteen years before the failure.

A crack growth assessment based on the IGSCC involvement was then performed using initial flaw sizes, which were the actual size of the flaws detected in the vessel. This analysis determined both the expected rates of crack growth and the size of the flaw, which could result in catastrophic failure of the vessels (Figure 8).

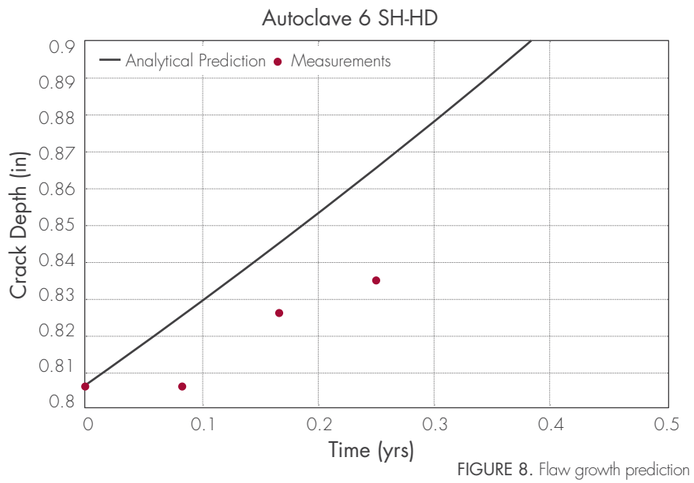

FIGURE 8. Flaw growth prediction

Asset Management Planning

The final part of the story is working on getting the client back online with extended procurement schedules for new equipment. Planning for in-service inspection involves not only leveraging the proper rules and regulations, but also the information and data gathering for a specific unit to ensure that operation with known flaws can be done safely.

The plan was developed using guidance from not only the previous analysis performed but also with guidance from published sources such as the National Board Inspection Code, ASME PCC-3 on Risk-Based Inspection Planning, and Appendix B of ASME Code, Section VIII Division 3 on Requalification of Pressure vessels.

The plan was to determine the remaining life of the vessel from the API 579-1/ASME FFS-1 process discussed previously, including design margins on life, such as would be found in original vessel design codes such as ASME Code, Section VIII. The guidance documents then have the vessels inspected at an interval of 1/10 of the original design life to ensure that the crack growth rates are appropriate. This level of conservatism yielded a monthly inspection program for the vessels. The flaw growth was then tracked to ensure that the original predicted life was conservative (Figure 8).

The monthly inspections were able to be accomplished quickly and efficiently while minimizing downtime by leveraging the SI Internal Vessel Automated Scanner (SIIVAS) (Figure 9). This system allowed for the vessel to be examined quickly and easily in subsequent exams without the removal of external insulation or heaters, and without the need for confined spaced entry permits.

Conclusion

Another example of the value that working with a full-service company such as SI can bring to the table to quickly respond to clients' issues, evaluate difficult failure mechanisms, and establish a long term management program to allow clients to get back online sooner and safely.

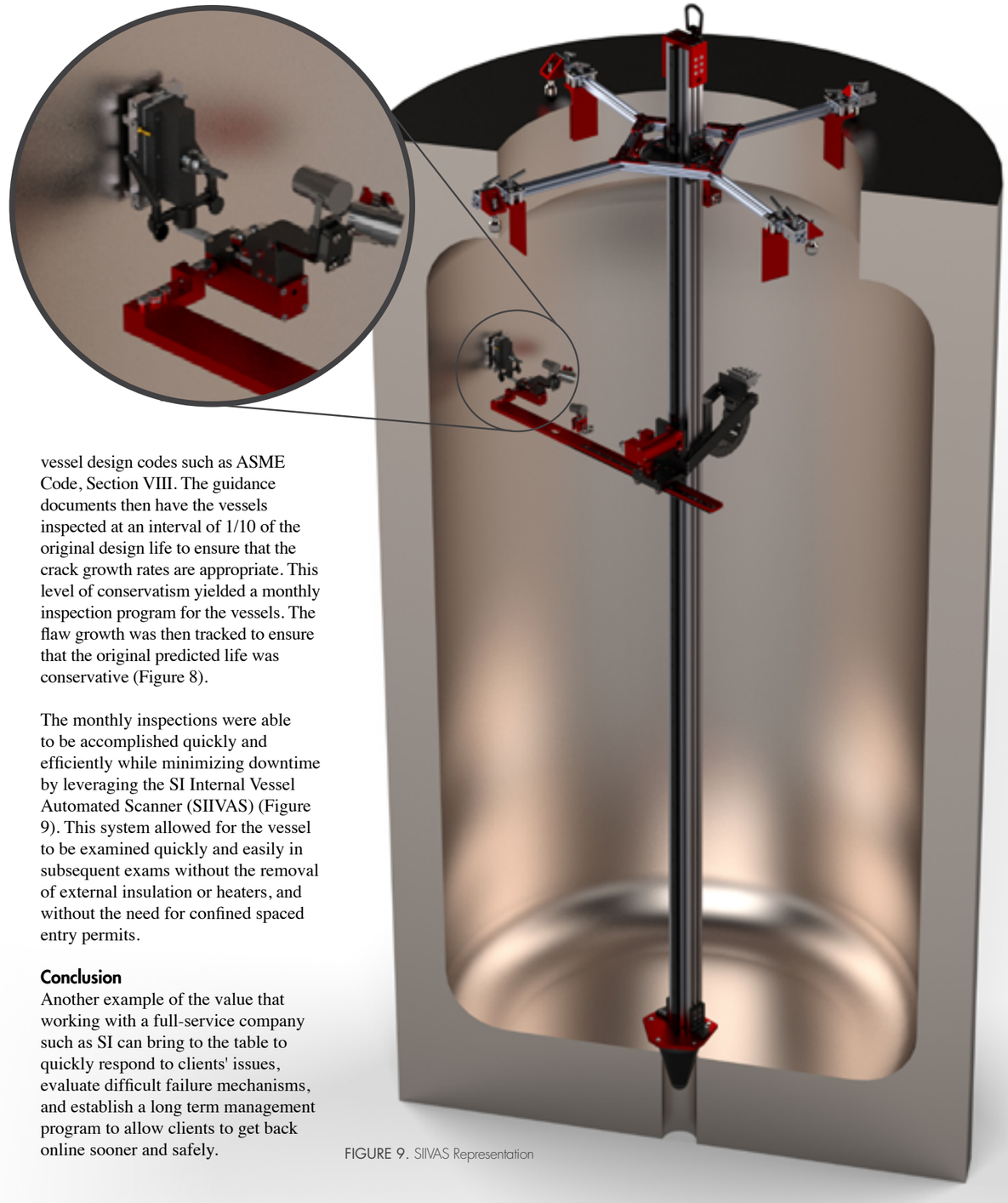

FIGURE 9. SIIVAS Representation

Cross-Weld Creep-Rupture Testing for Seam Weld Life Management

JONNATHAN WARWICK, Ph.D.
jwawickr@structint.com

TERRY TOTEMEIER, Ph.D.
ttotemeier@structint.com

BRIAN CHAMBERS, DUKE ENERGY
brian.chambers@duke-energy.com

Longitudinal seam-welded hot-reheat steam piping operating in the creep regime is a continuing life-management challenge for many older fossil-fired power plants. In response to catastrophic seam-welded piping failures in the 1980's, the Electric Power Research Institute (EPRI) developed a comprehensive inspection protocol to insure continued safe operation of these piping systems [1]. The protocol requires full inspection of seam-welded hot-reheat pipe once a threshold of service exposure (calculated creep life consumption) has been reached, and re-inspection at intervals after the initial inspection depending on the inspection results. Inspection for sub-surface cracking using ultrasonic testing (conventional or advanced) is strongly recommended, in combination with checking for surface cracking using wet fluorescent magnetic particle testing (WFMT). Initial inspection and re-inspection of these piping systems represents a large maintenance cost for utilities, especially as older plants remain in service due to the changing economics of power generation.

SI's inspection protocol for hot-reheat seam-welded piping systems is comprised of a combination of visual, WFMT, and advanced ultrasonic techniques for detection of surface cracking, sub-surface cracking, and incipient creep damage. Ultrasonic inspection is currently performed using time-of-flight-diffraction (TOFD) testing on 100% of the seam weld length and annular phased array (APA) testing at selected locations along the seam weld length. In some cases, linear phased array (LPA) ultrasonic testing may be used in place of TOFD. Both TOFD and LPA have been shown to be able to detect creep damage at the microcracking stage, which is estimated to correspond to at most 85% of the creep-rupture life being consumed. APA has been shown to be able to detect creep damage at the aligned cavitation level, which is estimated to correspond to at most 70% of the creep-rupture life being consumed.

If no damage is found in an inspection, SI's recommended re-inspection interval is defined based on the above-mentioned detection limits, so that a seam-welded pipe that has been inspected using APA with no indications of service damage will have a longer recommended reinspection interval than a seam-welded pipe that was only inspected using TOFD or LPA. However, in some cases, high densities of non-metallic inclusions in the pipe base metal act as ultrasonic reflectors, which mask the presence

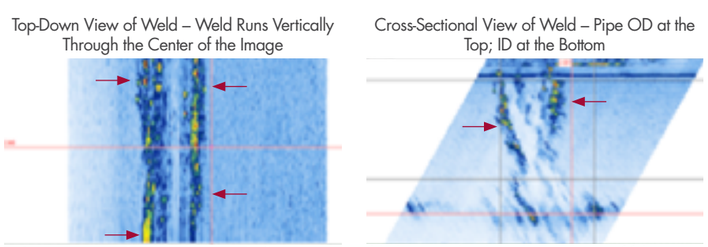

FIGURE 1. APA ultrasonic scan results from a seam-welded pipe with a high concentration of fabrication-type indications along the weld fusion lines (arrowed).

of creep cavities, so that APA cannot definitively determine that service damage is not present. For these cases the recommended reinspection interval will be relatively short, defined on the TOFD or LPA inspection findings alone.

Given the very high cost of inspections (driven mainly by scaffolding and insulation removal costs) and increasingly shorter outage time windows in which to perform them, SI has recently developed and applied a sampling, examination, and creep-rupture testing methodology to generate information and data that can be used to justify longer reinspection intervals for seam-welded pipes in which, due to the presence of high inclusion densities or other fabrication flaws, early-stage creep damage cannot be detected using APA ultrasonic testing. These inclusions and fabrication flaws may even limit the applicability of TOFD or LPA ultrasonic testing. This article presents a typical application example as a case study.

Case Study

The power plant in this example is a supercritical coal-fired unit generating 1100 MW of power. Since starting operation in the early 1970's, the unit has accumulated approximately 300,000 service hours with approximately 500 starts. Sections of the hot-reheat piping system are specified as 36" outer diameter by 1.984" minimum wall thickness ASTM A-155, Class 1 pipe, which is seam-welded 2¼ Cr – 1 Mo material (Grade 22). In a recent APA ultrasonic inspection, several pipe spools in this system were found to have high densities of fabrication-type indications along each weld fusion line and in the cusp region of the double-V groove type welds present. Typical TOFD and APA ultrasonic scans of these areas are shown in Figure 1. Because of these indications, the TOFD detection threshold was used in the re-inspection interval recommendation, which was 27,000 operating hours in this case. The reduced inspection interval was not acceptable to the client due to outage schedules and high cost of inspection.

FIGURE 2. Core removal and pipe plugging process. Core Drilling TOP Pipe Spool with Plug Installed BOTTOM LEFT BOTTOM RIGHT Extracted Core LOWER and Replacement Plug UPPER

Material Sampling and Metallurgical Characterization

Two cylindrical core samples were extracted from the seam weld of the pipe spool which showed the high fabrication flaw density. The three-inch diameter cores were removed and the resulting holes plugged in a single day. In this case a threaded plug with an outer seal weld was used, but a plugged sock-o-let type fitting is another option. Figure 2 shows photos from the core removal process and the plug repair.

The cores were sent to SI's Materials Science Center in Austin, Texas for metallurgical characterization. One of the as-received cores is shown in Figure 3. The location and orientation of the seam weld was marked on outer pipe surface; the weld reinforcement was visible on the oxidized inner pipe surface. The cores

Continued on next page

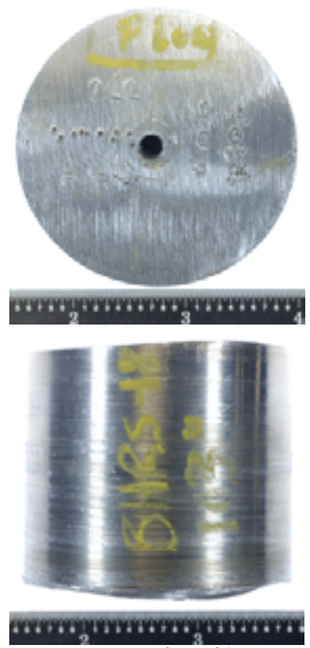

FIGURE 3. Overviews of one of the as-received core samples.

were sectioned transverse to the seam weld and prepared for metallographic examination to confirm the presence of inclusions and/or creep damage in the form of cavitation. Initial sectioning was performed by electro-discharge machining (EDM) to preserve as much material as possible for creep-rupture testing.

Figure 4 shows a macroscopic view of one of the prepared cross-sections; the weld had a double-V geometry typical of hot-reheat seam welds and in agreement with profiles found in ultrasonic tests (Figure 1). Prominent weld heat-affected zones (HAZs) were present in the base metal adjacent to the weld, indicating that the welds had received a subcritical post-weld heat treatment (PWHT) rather than a full renormalize-and-temper PWHT. There was no macro- or micro-cracking observed on either core.

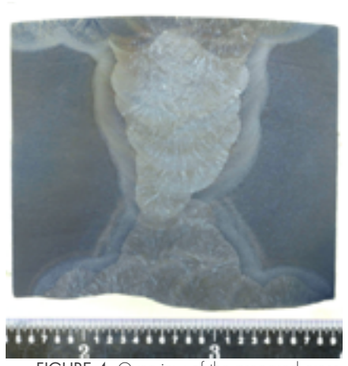

FIGURE 4. Overview of the prepared cross-section through one of the cores. Nital etch.

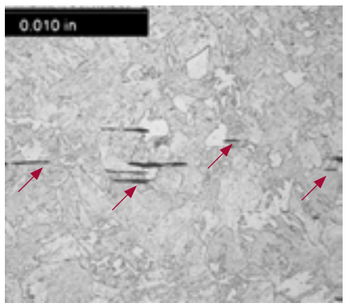

FIGURE 5. Typical base metal microstructure with stringers of non-metallic inclusions present (ARROWED).

Examination at higher magnifications showed that the weld metal, HAZ, and base metal microstructures were normal for the specified Grade 22 material, and that the carbide precipitates were not excessively coarsened or spheroidized. There was no significant creep cavitation visible in either sample, but there were numerous bands of inclusion stringers in the base metals, as shown in Figure 5. The presence of these bands is again consistent with the ultrasonic findings.

The Vickers hardness of the base metal and weld metal were measured and found to be normal for service-exposed Grade 22 material (approximately 170 HV10). The alloy type was checked using handheld x-ray fluorescence spectroscopy (PMI testing); the nominal compositions of the base and weld metals were both consistent with Grade 22 material (2.25Cr-1Mo).

Creep-Rupture Testing

Cross-weld creep-rupture tests were performed on specimens manufactured from the cores. Because the cores were very small it was impossible to machine meaningful specimens directly from them. Instead, rectangular pieces were machined from the cores onto which grip extensions were electron-beam welded. In this way the rectangular core sample pieces became the gauge lengths of the final test specimens. The overall specimen manufacturing process involves etching cross-sections to define the best locations for cross-weld specimens (Figure 6), machining test blanks centered on the cusp of the seam weld where damage typically develops, and then electron-beam welding grip-end pieces (also Grade 22 material) onto the test blanks (Figure 7). There was no PWHT performed after welding, so the microstructural condition of the weld was not altered in the specimen manufacturing process. Figure 8 shows the final machined specimens with the approximate location of the weld fusion lines marked.

Constant-load creep-rupture tests were performed in air at 1150°F (621°C)

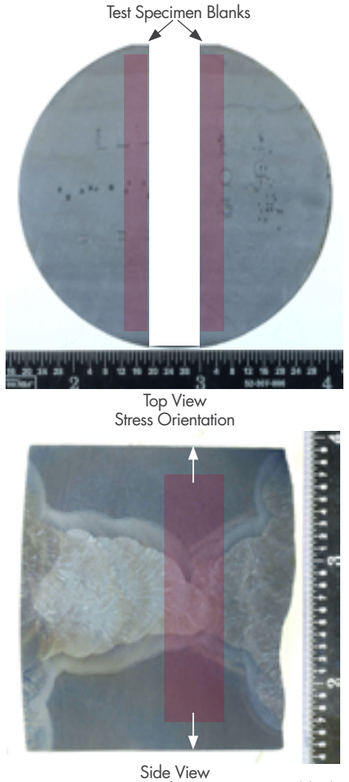

FIGURE 6. Location of creep-rupture test blanks within a core sample.

FIGURE 7. Typical test specimen blank after electron-beam welding of grip ends.

FIGURE 8. Typical cross-weld creep-rupture test specimen after final machining. The approximate locations of the weld fusion lines are marked in the gauge section.

at several stress levels consistent with service loads. Some tests were run to failure, while other tests were terminated after a few months of test time. The test data are compared to the population of base metal and cross-weld literature data for Grade 22 material in Figure 9, which plots the Larson-Miller parameter (LMP) for the tests as a function of stress. The Larson-Miller parameter combines temperature and time in the following form:

$$LMP = T \times [20 + \log(t_r)]$$

where T is the temperature and t_r is the rupture life or test duration. The results for the specimens tested at the three highest stresses are well within the scatterband for new cross-weld material, while the duration of the un-failed test at the lowest stress is approaching the scatterband, indicating that seam welds have very little creep damage, consistent with the microstructural observations of no cavitation, no microstructural coarsening, and no marked hardness decrease.

Overviews of a tested specimen interrupted prior to failure are shown in Figure 10. The specimen was oxidized, as expected; the two ruptured specimens had a ductile morphology with some associated necking. Longitudinal metallographic sections were prepared through these specimens to confirm the location of deformation. Final rupture was in the weld HAZ, consistent with the expected behavior for cross-weld loading of welds that have received a sub-critical PWHT.

FIGURE 10. Overviews of a tested specimen (the test was terminated prior to failure).

Use of Data in Life Management

In this case, because the examination findings and creep-rupture test data indicated that the weld had very little creep damage, it was possible to significantly extend the re-inspection interval for the pipe spool from which the cores were extracted. Although the core sample creep test results are only directly applicable to the pipe spool from which the cores were extracted, the other pipe spools that also showed high base metal inclusion densities were confirmed to have been from the same heat and manufacturing process

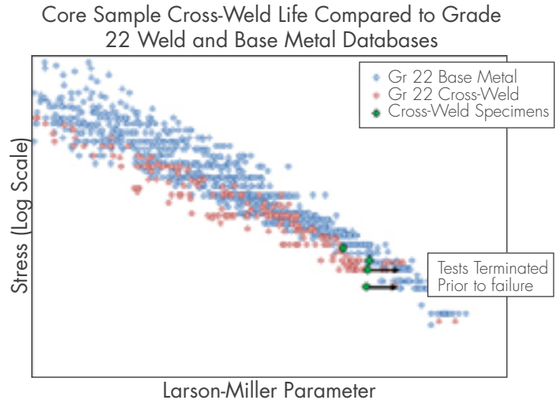

FIGURE 9. Creep-rupture test results for the cross-weld specimen compared to Grade 22 base metal and cross-weld literature data on the basis of Larson-Miller parameter.

(same size, weld process), therefore the inspection interval was also extended for those spools.

It is important to recognize that the creep test results cannot generally be directly applied to confidently predict the remaining life of the pipe. The issues with using cross-weld creep rupture data in predicting remaining lives of seam-welded components have been described in Refs. [2] and [3]. A cross-weld test specimen extracted from a seam weld and loaded in uniaxial tension clearly does not fully represent the overall stress state for the full weld in the pressurized pipe, and there are additional complications created by using accelerated conditions (temperature and/or stress) in the creep-rupture test. However, as noted in Ref. [2], uniaxial cross-weld tests tend to underestimate remaining lives, so the results are expected to be conservative. Ref. [3] notes the additional complicating factors of weld metal to base metal strength mismatch; there also can be global stress-concentrating features associated with the seam weld such as pipe ovality and weld peaking angle. Hence cross-weld creep-rupture test results must be carefully considered in conjunction with other inspection findings, operating history and current operating conditions, and other possible pipe loads. These factors should all be included in a comprehensive seam-weld life assessment.

Conclusions

This example shows how examination and testing of core samples removed from "un-inspectable" (from an advanced ultrasonics perspective) seam-welded piping can greatly increase the confidence in the condition of the seam weld, and therefore provide an engineering-justified extended re-inspection interval, at a relatively modest cost relative to that of the overall inspection. Beyond seam welds, this core sample creep test methodology can also be used to characterize other discrepant material conditions, such as low hardness regions in Grade 91, or can be used to obtain creep data specific to a particular service-exposed material to obtain more accurate remaining life assessments.

References

[1] EPRI, *Guidelines for the Evaluation of Seam-Welded High-Energy Piping, Fourth Edition*, EPRI Report 1004329, 2003.

[2] Viswanathan, R. and J. Foulds, "Accelerated Stress Rupture Testing for Creep Life Prediction—Its Value and Limitations." *Journal of Pressure Vessel Technology*, 1998. 120(5): p. 105-115.

[3] Segle, P., et al., "Some Issues in Life Assessment of Longitudinal Seam Welds Based on Creep Tests with Cross-Weld Specimens." *International Journal of Pressure Vessels and Piping*, 1996. 66: p. 199-222.

Baffle-Former Bolt Management: Cost/Benefit Studies

TIM GRIESBACH
tgriesbach@structint.com

CHRIS LOHSE, P.E.
clohse@structint.com

For the past several years baffle-former bolt (BFB) cracking in pressurized water reactors has become a significant concern for of PWR plants. In 2016, three similar Westinghouse designed plants (Indian Point 2, Salem 1, and D. C. Cook Unit 2) experienced significant numbers of cracked BFBs, attributed to irradiation-assisted stress corrosion cracking (IASCC). These plants had common characteristics that included the 4-loop plant design, downflow configuration, and Type 347 stainless steel bolting material. BFB cracking is not an entirely new phenomenon as it was initially detected in the French PWR fleet in the 1990s. However, the extent of cracking found in some of the US plants has greatly exceeded prior cracking. Extensive industry programs have identified and categorized by tier group the most susceptible plants, and the EPRI Materials Research Program (MRP) has published guidance regarding baffle-former bolt UT inspections for PWR plants for detection of degraded and cracked bolts in the baffle-former assembly (MRP-2017-009).

A typical arrangement of the baffle-former assembly showing the BFBs and other bolt types is shown in Figure 1. There are between 700 – 1100 baffle-former bolts (depending on design) that hold the baffle plates in place for structural support. While the baffle-former assembly is a highly redundant structure, a significant number of the bolts must remain intact to assure functionality of the baffle-former assembly during a design basis event such as a loss-of-coolant accident (LOCA) or seismic activity.

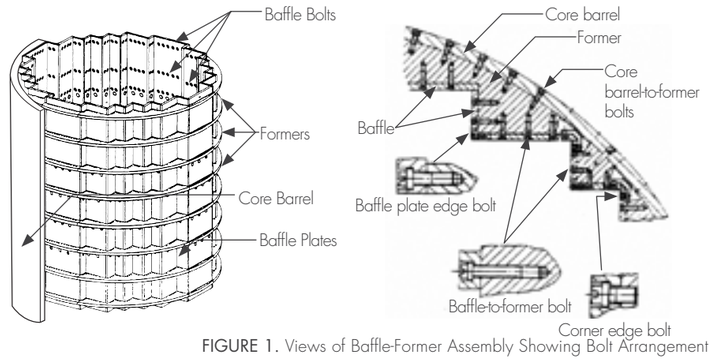

FIGURE 1. Views of Baffle-Former Assembly Showing Bolt Arrangement

The baffle-former assembly provides core support and directs coolant flow through and around the core. The susceptibility to BFB cracking depends on several external factors that influence crack initiation (i.e., fluence and temperature) and design or operating conditions that contribute to tensile stresses in the bolts. The factors that load the bolts are bolt preload, the differential pressure across the baffle-former plates, thermal expansion of the assembly, stress relaxation, and void swelling. Differential pressure loading across the baffle plates increases the stress in the bolts and is more significant for plants operating in the downflow configuration than upflow configuration. The difference between downflow and upflow configuration for the coolant flow is shown in Figure 2.

Managing BFB cracking has become a significant concern for these susceptible plants because of the uncertainty and cost of mitigation measures. Many options are being considered. However, it is difficult to understand the value of each option. As other options become available, how can they be compared to the traditional approaches for BFB management? SI uses a decision management tool for analysis of run/repair/replace decisions. This tool is well-suited to the evaluation of decisions requiring cost and uncertainty and incorporates the probability of failure model results with the costs associated with each alternative strategy.

Several actions may be considered as options for managing BFB cracking once a plant is identified as being susceptible:

1. Inspect and only replace bolts as needed
2. Perform upflow conversion and inspect/replace as needed
3. Perform proactive bolt replacement (partial pattern or full bolt replacement)
4. Upflow conversion and proactive bolt replacement

To evaluate the optimal strategies and implement these options(s), it is crucial to first determine the likelihood (or probability) of future bolt failures, consider changes that could occur by implementing one or more mitigation measures, and compare the projected costs and outcomes associated with the various strategies. Then, by performing variations of plant-specific cost/benefit analysis and making these comparisons, informed decisions can be made when considering the different combinations of technical objectives and economic trade-offs.

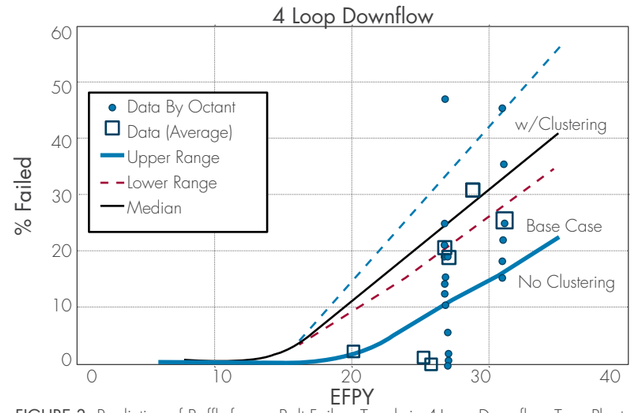

FIGURE 3. Prediction of Baffle-former Bolt Failure Trends in 4-Loop Downflow Type Plants

The cost/benefit approach for BFBs is as follows:
First, the projection of BFB cracking is required to understand the level of failures expected for each option. The industry previously projected the number of BFB failures for various plant designs to help determine the inspection interval. SI participated in helping develop those guidelines using an in-house bolt failure prediction model. For this prediction model, a bolting failure is considered based on IASCC susceptibility and the time or effective fluence to cause crack initiation. As shown in Figure 3, once cracking initiates, the spreading of failed bolts can occur more rapidly, as demonstrated by the upward trend in % failed bolts. The results are presented as a probability of failure (i.e., number or pct. of failed bolts) as a function of fluence accumulation, which is plotted in Figure 3 as a function of effective full power years (EFPY). The probabilistic prediction model is benchmarked with the measured failure trends for the 4-loop downflow type plants. These trend lines of BFB failure predictions are used as input when considering the various options to mitigate BFB failures.

As discussed previously, there are many options that utilities can consider to address BFB failures. These options include: do nothing and replace what is cracked, preemptively replace bolts, combine an upflow conversion with preemptive bolt replacement. To compare these options, the cost and impact for the utility are essential parameters.

The alternative analysis cost/benefit study includes a financial model that considers the discounted cash flows and expected outcomes for each of the alternatives evaluated, compared to the base case. The costs and timing of implementing the various mitigation options take into account the future cash flows and estimated cost savings (per year) expected.

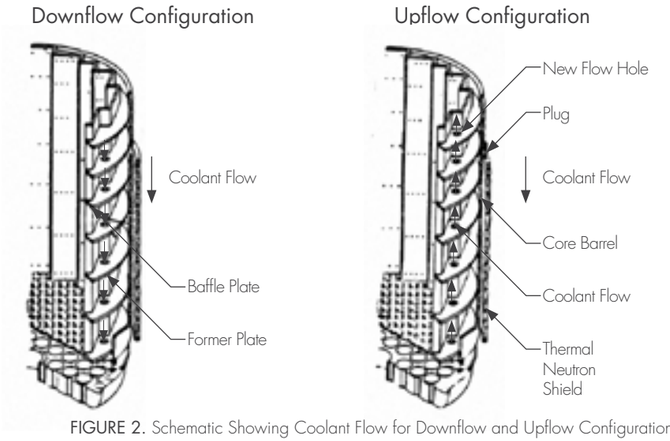

FIGURE 2. Schematic Showing Coolant Flow for Downflow and Upflow Configuration

Continued on next page

Each option for managing BFB cracking includes several variables:

- What is the actual cost of my option?
  - Equipment rental fees and cost of tooling
  - Inspection costs (some options may be able to defer future inspections)
  - Unplanned outage extension
  - Planned outage extension
  - Upflow conversion cost (and other potential benefits after conversion)
  - Possible change in bolt replacement rate – Current bolt replacement tools have only achieved ~10 bolts per day replacement rates. What happens with a faster production rate?
- How does this choice affect future failure probability of bolts?
  - Replaced bolts are less likely to fail
  - Upflow conversion can make bolts less susceptible
  - Inspecting only (do nothing) will not change the bolt degradation trend
- Cost of money now vs. in the future (i.e., discount rate)

Each of these options is evaluated to determine the "value" of implementing an alternative strategy compared to several other options. Each of these options or strategy is examined in terms of the probability of expected outcome related to BFB failures and their relative expected lifetime costs in terms of a planned (net present) value, or NPV. These results can be used to help make decisions on the best option

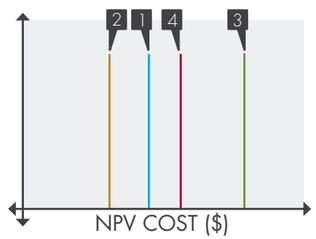

FIGURE 4. Sample NPV Cost for Various Options

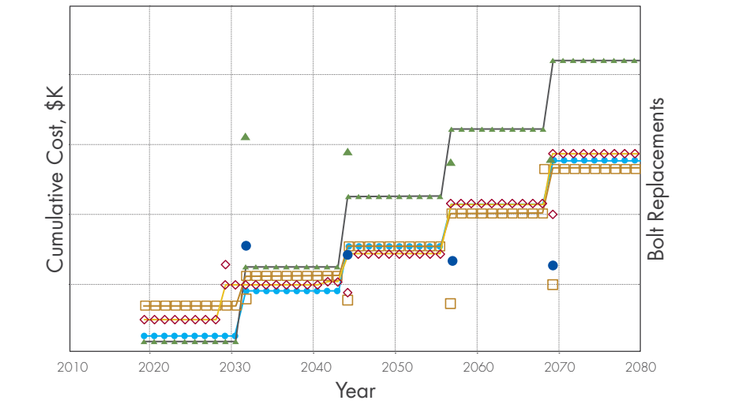

FIGURE 5. Overall Costs and Number of Bolts Replaced

to manage baffle bolt degradation using the best estimate costs and expected value results; the resulting strategies can be ranked by the relative NPV cost, as illustrated in Figure 4.

Figure 5 shows a more detailed description of the various options over the remaining time horizon of the operating plant.

The multiple options, as shown here, are considered for a cost comparison. In these sample scenarios, the proactive bolt replacement with no upflow conversion is significantly more expensive than the other options. After about 2058, option 2 (upflow conversion and replace bolts as needed) is the least costly option. At different times, the relative rankings of the different options are shown to change. For example, the Upflow Conversion options are more expensive early in life when the conversion costs are incurred, but those options recoup that investment over time as failure rates and numbers of bolts to be replaced are reduced over time.

Once the costs and expected values of the various options are determined, SI works with the utility to identify the alternative(s) that best fit the performance objectives and cost (or cash flow) objectives for planning purposes. The results are presented in terms of time horizons for implementation of the planning options and management decisions, recognizing that the analytical models can be refined later using actual inspection results and real-time information and related operating experience for each of the various strategies.

BFB cracking has been shown to cause significant outage impacts to utilities of these susceptible plants. Understanding the options and managing the issue can help utilities save money in the long run and eliminate surprises. For more information on how SI could help in your planning, please contact Tim Griesbach or Chris Lohse.

In-line Inspection Performance Validation Pipe Experiment

JACOB ARROYO
jarroyo@structint.com

You've just completed the first in-line inspection (ILI) of a new pipeline asset. The ILI tool results are in, and there are no required repairs! However, how sure are we of the accuracy of the results? Could the tool have under-called some of the reported anomalies? Are there any regulatory requirements beyond the "response criteria" mentioned in CFR 192 and 195 for operators of hazardous transmission pipelines? These are the problems that ILI verification is trying to solve.

Traditionally, validations can be done using costly excavations of anomalies found by the tool. In cases where those anomalies need to be repaired, this approach is effective, and the validation does not require any further excavations. For some ILI inspections, the tool does not call any anomalies that need to be repaired. The traditional approach, in this case, has been to excavate sub-critical anomalies just for validation. In such cases, an ILI validation spool can be a valuable asset. ILI validation spools can be designed to quantify the uncertainty of the full spectrum of anomaly types without additional excavations, thus freeing up valuable resources to be allocated elsewhere to improve safety, minimizing the exposure risk of excavating pipeline assets while under full operating pressure.

Continued on next page

ILI Validation Spool vs Validating Anomalies

Validating an ILI inspection by excavating anomalies the tool called raises several problems. For one thing, the NDE methods used to characterize some anomalies have their level of uncertainty. Secondly, it is difficult to excavate enough anomalies to cover the full spectrum of anomalies the inspection is looking for if all that is available to validate the tool results is "pitting" anomaly types; the performance may not be within the stated specifications for "pinhole" anomalies. Finally, excavating a small number of anomalies only provides a low level of confidence from a statistical perspective.

Validation spools offer an alternate approach. A validation spool is a spool of pipe with artificial anomalies that can be dropped in and out of the active system. This spool can be designed to validate the full spectrum of anomaly types the ILI tool may encounter within the inspection. The data that the tool collects on these known anomalies can then demonstrate to stakeholders the actual performance of the inspection. Validation spools do not suffer from the issues of variety, quantity, and uncertainty that plague the anomaly validation approach.

Engineering and Design Case Study

Structural Integrity (SI) was recently contracted to design a validation spool for a major pipeline operator. The scope of the project was to design a pipe spool five feet in length that could be installed as part of the inspection activities before the tool launch date.

SI used the guidance provided in API 1163 2nd edition to engineer the ILI validation spool. Table 1 is an example of what the stated specifications ILI companies will deliver with their inspections. The dimensional classes are found within API 1163 and shown in Figure 1.

POD	Pitting	General	Pinhole	Circumferential Slotting	Circumferential Grooving	Axial Slotting	Axial Grooving
90%	±10%	±10%	±25%	±15%	±15%	±20%	±25%

TABLE 1. Example Uncertainty Specifications from ILI Companies

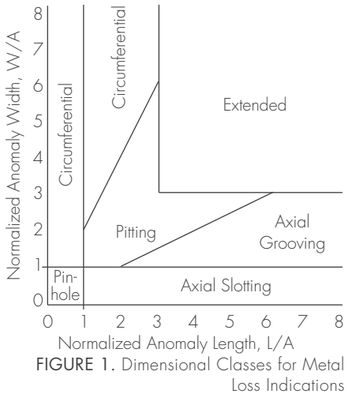

FIGURE 1. Dimensional Classes for Metal Loss Indications

Fifteen manufactured flaws were used to validate the inspection results in this case - three to five times more anomalies than the typical operator would excavate to validate an ILI run. The manufactured flaws for this project were designed to meet an ANSI 600 class system and Maximum Operating Pressure (MOP) of 1480. All 15 anomalies were manufactured with a tolerance of ±0.001 inch, using a proprietary manufacturing process.

One of the challenges of this approach is manufacturing defects that are representative of actual degradation in a pipeline. Using a naïve approach such as a grinder may produce anomalies with the desired length and depth, but to the ILI tool such anomalies may look different from real-world anomalies. One could use a cutout with real-world anomalies, but it may be challenging to acquire pipe that has enough actual degradation to test the full spectrum of anomaly types.

To address these concerns, SI partnered with FlawTech to simulate corrosion flaws representative of real-world corrosion. The defects were manufactured to specified dimensions while closely representing actual corrosion degradation of the pipeline asset. The figures below provide some examples of the metal loss defects manufactured for this project.

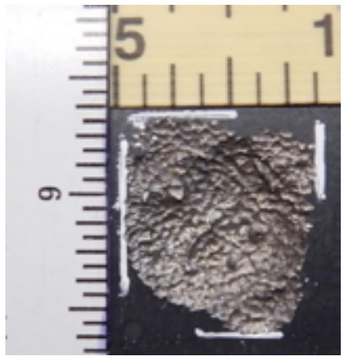

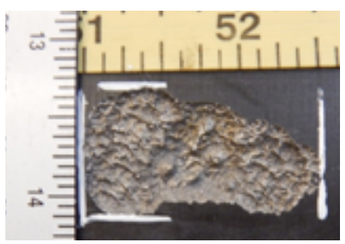

CONCLUSIONS

Pipeline operators can recognize the significant value in having a calibrated test spool to quickly and effectively validate ILI performance. Validation spools offer several advantages over traditional validation approaches, and improvements in technology are reducing their drawbacks. In particular, the variety, quantity, and measurement accuracy of manufactured anomalies can be far superior to traditional approaches. Furthermore, a validation spool reduces the safety risk associated with excavating on an operational asset. SI believes that adoption of validation spools will help the industry in achieving compliance, better qualifying inspection tools, and improving pipeline safety.

Application of Probabilistic Flaw Tolerance Evaluation

Optimizing NDE Inspection Requirements

CHRISTOPHER LOHSE
clohse@structint.com

There have been several industry initiatives to support optimization of examination requirements for various items/components (both Class 1 and Class 2 components) in lieu of the requirements in the ASME Code, Section XI. The ultimate objective of these initiatives is to optimize the examination requirements (through examination frequency reduction, examination scope reduction, or both) while maintaining safe and reliable plant operation. There are various examples of examination optimization for both boiling water reactors (BWRs) and pressurized water reactors (PWRs). Each of these technical bases for examination optimization relies on a combination of items. The prior technical bases have relied on: (1) operating experience and prior examination results as well as (2) some form of deterministic and/or probabilistic fracture mechanics. For BWRs, the two main technical bases that are used are BWRVIP-05 and BWRVIP-108. These technical bases provide the justification for scope reduction for RPV circumferential welds,

Continued on next page

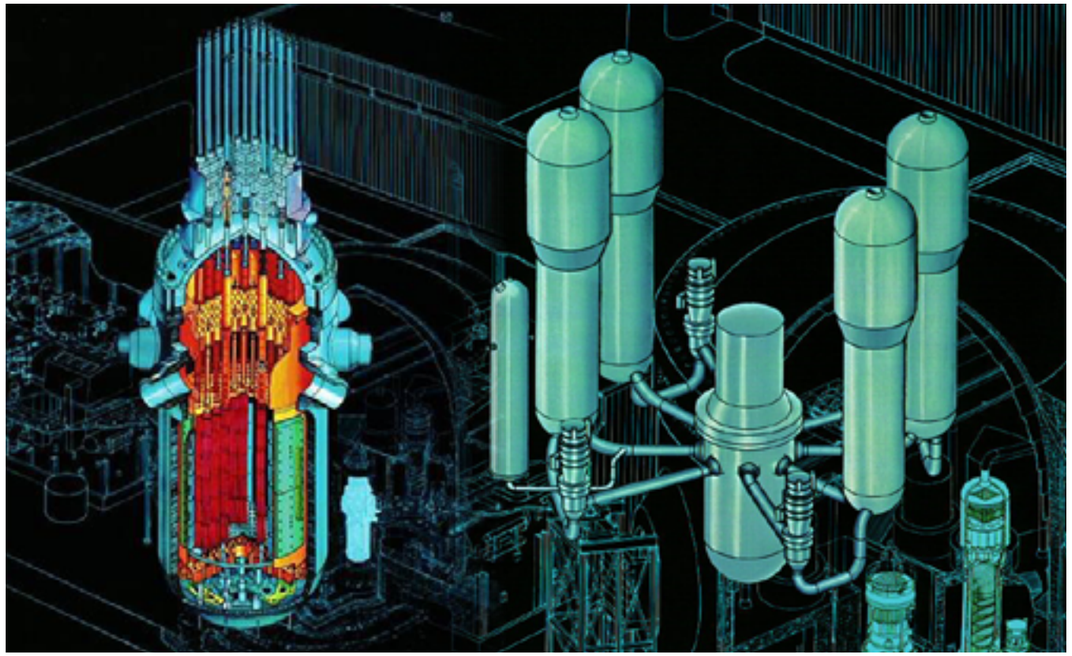

nozzle-to-shell welds, and nozzle inner radius sections. For PWRs, the main technical basis for RPV welds is WCAP-16168. These technical bases are for the RPV welds of BWRs and PWRs which represent just a small subset of the examinations required by the ASME Code, Section XI. Therefore, the industry is evaluating whether technical bases can be optimized for other components requiring examinations.

Recently, Structural Integrity (SI) and the Electric Power Research Institute (EPRI) worked on developing technical bases for other ASME Code, Section XI components. The first of these components are PWR main steam and feedwater nozzle-to-shell welds and nozzle inner radius examinations. These are Section XI Item Nos. C2.21, C2.32, and C2.22. This technical basis work included a review of the inspection history for these items, selection of representative main steam and feedwater nozzle configurations for evaluation, evaluation of potential degradation mechanisms, and flaw tolerance evaluations consisting of probabilistic and deterministic fracture mechanics analyses.

As with all inspection optimization technical bases, a survey of inspection results was performed. The survey of results for the three ASME Code items of interest was performed. These results are contained in EPRI Report No. 3002012965. Out of a total of 727 examinations identified for the plants that responded, only one examination identified an indication that exceeded the acceptance criteria of the ASME Code, Section XI. This one examination identified a flaw during a surface examination of the nozzle-to-shell weld. Since it was a surface examination, the indication was removed by light grinding. No other issues or indications were identified in the survey results. As the survey results showed a very limited number of indications that exceeded the acceptance criteria, these items warrant an evaluation of optimized examination requirements.

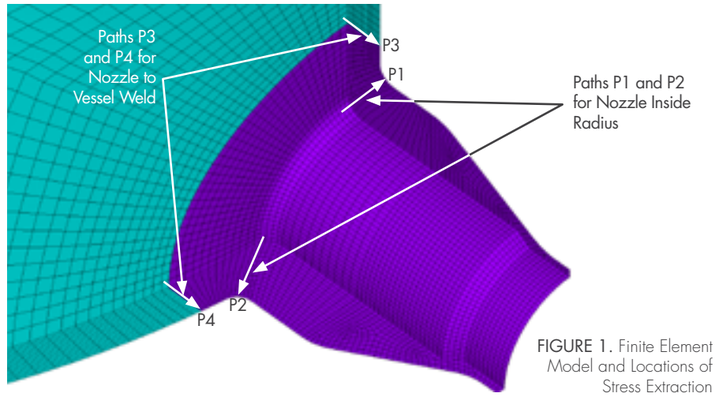

FIGURE 1. Finite Element Model and Locations of Stress Extraction

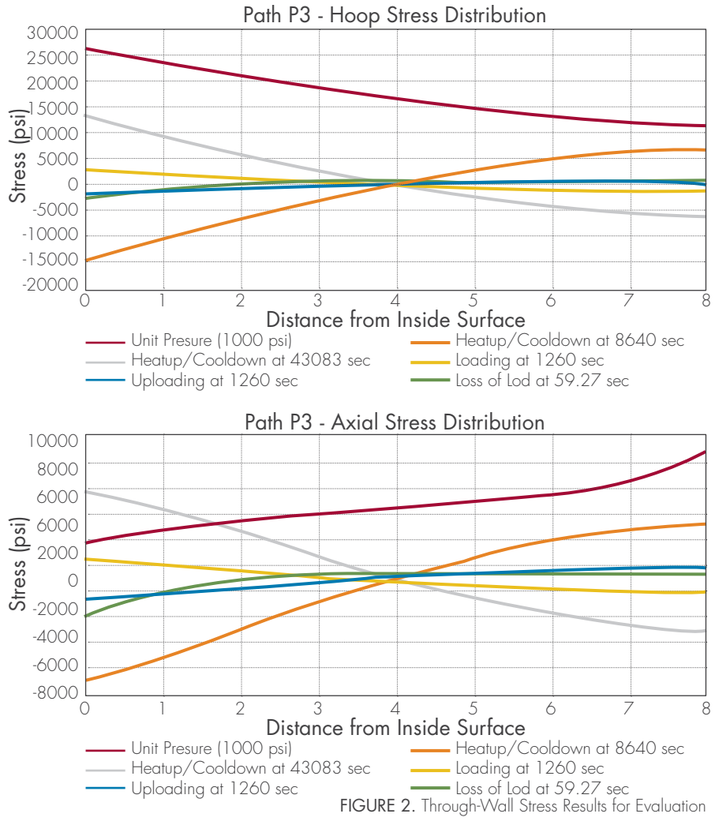

FIGURE 2. Through-Wall Stress Results for Evaluation

To perform the flaw tolerance evaluation, SI developed and performed several stress analyses. Figure 1 shows a finite element model of the feedwater nozzle and the paths where stresses were extracted.

Figure 2 shows hoop and axial stresses for the various transients and loading conditions analyzed.

The stress results were used in a probabilistic fracture mechanics (PFM) evaluation to determine the probability of leakage and failure for the various inspection scenarios. The goal in the PFM evaluation was to demonstrate that the probability of failure is less than the NRC requirement of 1×10-6 failures per year. The evaluation used a SI-developed software called "PROMISE (PRobabilistic OptiMization of InSpEction)". The software uses a Monte Carlo probabilistic analysis technique with the overall technical approach shown in Figure 3. The PFM analysis includes many factors that are treated as random variables, such as:

- Crack distribution (length and depth)
- Fracture Toughness
- Inspection Coverage
- Examinations Performed (PSI and ISI with defined intervals)
- Probability of Detection for Examinations
- Applied Stresses (operating loads, transients, and residual)

Sensitivity studies were performed to identify the random variables that have the most impact on the calculated probabilities. Sensitivity to the probability of rupture, probability of leakage, or both, were evaluated. The evaluation also varied inputs to demonstrate that this technical basis was applicable to a range of plant designs.

The evaluation looked at various inspection scenarios for the main steam and feedwater nozzles. The various scenarios looked at the preservice inspection (PSI) for all cases and then various options of 10, 20, and 30-year intervals. The results of these evaluations are shown in Figure 4. Based on the results, several various inspection scenarios would meet the safety goal of less than 1×10^{-6} failures per year.

The full discussion of the work performed for the main steam and feedwater nozzles is contained in EPRI Report No. 3002014590 and is available for download at EPRI.com. The report provides a list of requirements that must be met to be considered bounded by the evaluation. If bounded, the technical basis can be used by plants to support plant specific relief requests to justify alternative examination strategies for their main steam and feedwater nozzle welds. For information on this specific topic or the flaw tolerance approach please contact D.J. Shim (dshim@structint.com) or Chris Lohse (clohse@structint.com).

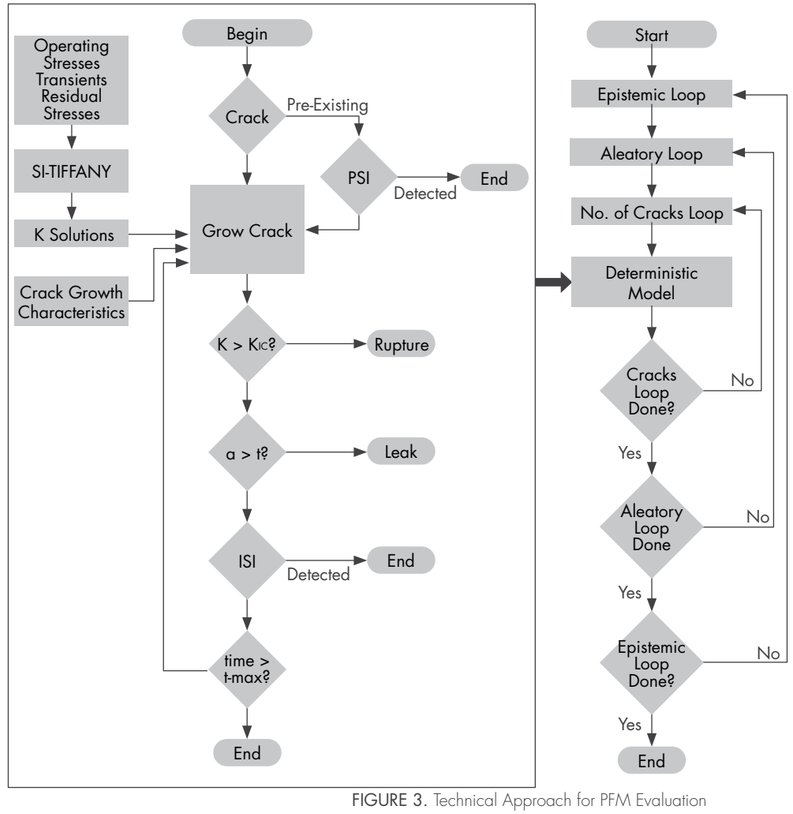

FIGURE 3. Technical Approach for PFM Evaluation

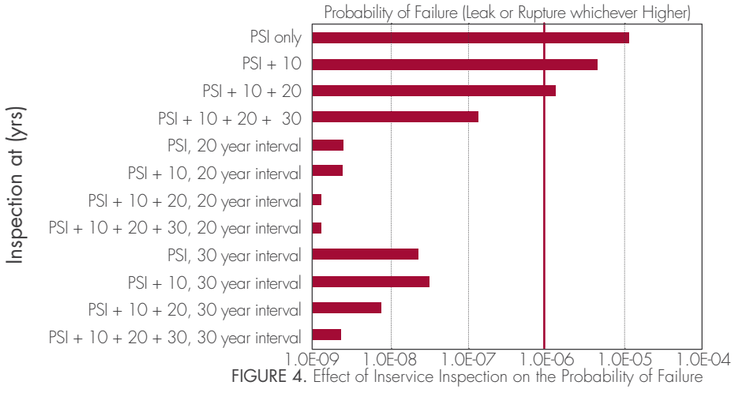

FIGURE 4. Effect of Inservice Inspection on the Probability of Failure

Structural Integrity Associates, Inc.®
11515 Vanstory Drive Suite 125
Huntersville, NC 28078

1-877-4SI-POWER www.structint.com

DON'T JUST SEE THE PROBLEM, VISUALIZE THE SOLUTION

Visual Mode Shapes & Motion Amplification with IRIS MTM

Imagine a camera and software tool showing mode shapes and motion amplification, bringing the phrase 'seeing is believing' to the interpretation of vibration characteristics and responses. Captured video results provide a 'picture worth a thousand words' when communicating the complex vibration phenomena to both technical and non-technical audiences. Simultaneously monitor all points of your process and machinery, without impact to your flow of business.

The IRIS M platform allows the user to visually accomplish in 1-2 hours what can take days or even weeks to perform in other software platforms – animation of mode shapes with frequencies between 0-100 Hz.

We use RDI Technologies, IRIS M™ for Motion Amplification. Interested in learning more about our motion amplification service? Follow this link: www.structint.com/IRISM

STRUCTURAL INTEGRITY ASSOCIATES ANNOUNCES ACQUISITION OF MATERIALS TECHNOLOGY CORPORATION

Specialty creep testing for welded or ex-service samples requiring unique specimen designs and complex machining.

Materials Technology Corporation was founded by Howard Voorhees in 1963 and has been instrumental in developing creep data underpinning alloy development. Data generated by the group also provides valuable insight into life assessment of power generation and petrochemical plants. Materials Technology Corporation is also renowned for the quality creep testing of complex alloys and welded samples.

Structural Integrity has long relied on creep data generated by the team, and is proud to be able to continue and grow this unique competence. Structural Integrity will continue the legacy, providing independent creep testing services, as well as integrated life assessment solutions that incorporate creep testing.

For more information, go to:

www.structint.com/news-and-views-46